Implications of Neutrinoless Double Beta Decay

Thesis submitted for the award of the degree

of

Doctor of Philosophy

in

Applied Physics

by

Vivek Kumar Nautiyal
Enrolment No.: 053/14

Under the Supervision of
Dr. Ramesh Chandra

Department of Applied Physics
School for Physical Sciences
Babasaheb Bhimrao Ambedkar University, Lucknow
U.P., (India) – 226025
2020

DEDICATED

TO

MY

FAMILY

DECLARATION

I declare that the thesis titled "**Implications of Neutrinoless Double Beta Decay**" has been prepared by me under the supervision of **Dr. Ramesh Chandra**, Assistant Professor, Department of Applied Physics, School for Physical Sciences, Babasaheb Bhimrao Ambedkar University, Lucknow. No part of this thesis has formed the basis for the award of any degree, diploma or fellowship previously. Further, I declare that the material embodied in the present work is based on original research work and the indebtedness to others has been duly acknowledged at relevant places. This is also declared that the thesis is essentially free from all kinds of plagiarism.

Nautiyal 05/02/2020

(Vivek Kumar Nautiyal)

Department of Applied Physics

School for Physical Sciences

Babasaheb Bhimrao Ambedkar University

Vidya Vihar, Raebareli Road

Lucknow, (U.P.), India- 226025

Date: 05/02/2020

Place: Lucknow

CERTIFICATE

This is to certify that the thesis titled "**Implications of Neutrinoless Double Beta Decay**" submitted by **Mr. Vivek Kumar Nautiyal** is an original research work and has not been previously submitted in part or full for the award of any other degree or diploma to this or any other university or institutions.

The thesis submitted to Babasaheb Bhimrao Ambedkar University, Lucknow satisfies all the requirements as stipulated in the *Doctor of Philosophy (Ph.D.) Regulations – 1999 as amended in 2008/2010/2013* and it is fit for submission and evaluation for the award of the degree of Doctor of Philosophy of the University.

05-02-2020

Date: 05/02/2020

Supervisor

05/02/2020

Head of the Department

ACKNOWLEDGEMENT

First and foremost, I would like to thank the Almighty for His continuous showers of blessings throughout my research work without which it would not have been possible to begin this task. Thank you God for this day on which the research work stands successfully compiled in this thesis.

I feel obliged to take this opportunity to express my heartfelt reverences towards my supervisor and mentor Dr. Ramesh Chandra, Assistant Professor, for his invaluable guidance, vision, sincerity and motivation that kept me deeply inspired during whole course of research work. Besides guiding and encouraging me throughout this task, he was always there providing scholarly inputs and clarifying my doubts. Even the most stupid queries were met with amicable and positive disposition and with great sense of humor.

Next I would like to express my deep sense of gratitude towards my family. My father Shri Vijay Kumar Nautiyal and Mother Smt. Rekha Nautiyal have been constant torch bearers for me constantly encouraging and providing all necessary guidance, support and inspiration towards acquiring new skills. Support of my elder brother Mr. Vipin Nautiyal, without them it would have not been such a smooth task. I am highly indebted to all my family members, they helped me glide smoothly during times of despair.

I would like to pay my high gratitude towards Prof. P. K. Rath, Lucknow University who continuously provided valuable suggestions and concise comments on given state of research work without which it would have been an impossible task.

I would like to express my gratitude to Prof. B. C. Yadav, Head of the Department, for his patient guidance, enthusiastic encouragement and useful critiques of this research work. His advice and assistance kept my progress on schedule and helped raise the bar to this satisfactory level.

I am highly grateful to the help and support provided by faculties of the department: Prof. Devesh Kumar, Dr. K. B. Thapa, Dr. Devendra Singh and Dr. A. K. Yadav for helping me improve this task. They were always available for fruitful discussions culminating into successful results. I feel extremely enlightened by the company of their thought provoking deliberations.

I would like to mention the help provided in my research work by Mrs. Nilima Das who were ever willing to lend helping hand even during odd hours. I would also like to thank Dr. Yash Kaur Singh, Dr. Ruchi Mishra and Mr. Ratindra Gautam for the help provided during course of Ph.D. research and manuscript preparation. I thank one and all who have directly or indirectly helped me or inspired me towards achievement of my goal.

Finally I would like to appreciate support and facilities extended by staff at Library and Computer Center of the Department as well as the University for aiding in literature survey and other requirements.

Nautiyal

(Vivek Kumar Nautiyal)

ABSTRACT

The confirmation of neutrino oscillation -one of most captivating topics of Neutrino Physics- suggests that neutrinos are massive, and consequently, two possibilities, namely Dirac or Majorana nature of these particles arise. However, the actual mass of neutrinos can not be extracted from the oscillation data, which provide only mass-squared differences. The absolute mass scale of neutrinos and the nature of neutrinos are open challenges to physicsts. The study of tritium single β decay and $\beta\beta$ decay together are capable to meet the above mentioned challenges. The neutrinoless double beta ($0\nu\beta^-\beta^-$) decay is the only potentially viable way to answer the question whether neutrinos are of Dirac or Majorana nature. The experimental observation of $0\nu\beta^-\beta^-$ decay will immediately imply the Majorana nature of neutrinos.

The $0\nu\beta^-\beta^-$ decay has not been experimentally observed hitherto, and only limits on half-lives of $0\nu\beta^-\beta^-$ decay are available. These half-life limits permit to extract limits on various effective lepton number violating parameters. One has to understand the mechanism of nuclear transition and evaluate the corresponding nuclear transition matrix elements (NTMEs) with high reliability in order to get accurate effective lepton number violating parameters. The $2\nu\beta^-\beta^-$ and $0\nu\beta^-\beta^-$ decays involve the same set of initial and final nuclear wave functions. The usual strategy is to first calculate NTMEs $M_{2\nu}$ for $2\nu\beta^-\beta^-$ decay. The $2\nu\beta^-\beta^-$ decay has been observed in eleven nuclei out of 35 possible candidates. The half-life of $2\nu\beta^-\beta^-$ decay is a product of accurately known phase space factor and NTME. One can extract $M_{2\nu}$ from the observed half-lives of $2\nu\beta^-\beta^-$ decay. A comparison between the theoretically calculated and experimentally extracted $M_{2\nu}$ provides a cross-check on the reliability of different nuclear models. In the present work, the $2\nu\beta^-\beta^-$ decay as well as the $0\nu\beta^-\beta^-$ decay have been studied.

PREFACE

The present thesis is on the study of $0\nu\beta^-\beta^-$ decay of ^{94,96}Zr, ^{100}Mo, ^{110}Pd, ^{128,130}Te and ^{150}Nd nuclei for the $0^+ \rightarrow 0^+$ transition. In the absence of experimental observation of $0\nu\beta^-\beta^-$ decay, the nuclear models predict the half-lives assuming certain value for the neutrino mass or extract limits on various effective gauge parameters from the experimentally observed limits on half-lives $T^{0\nu}_{1/2}$.

Nuclear models employed so far for calculating NTMEs can be broadly classified in to shell model and its variants, quasiparticle random phase approximations (QRPA) and its extensions and alternative models. The shell model is the best choice for the calculation of NTMEs. However, its application is limited only to *pf* shell nuclei, the study of which requires a large number of basis states. In heavier nuclei, it is difficult to perform a reliable shell model calculations without severe truncation. The QRPA and its extensions are the commonly used models for the calculation of NTMEs. The QRPA calculations can be performed in large model spaces and this is the advantage over the shell model approach. Nevertheless, the extreme sensitivity of NTMEs to the strength of particle-particle interaction does not allow a reliable prediction of $2\nu\beta^-\beta^-$ decay rates. Moreover, the QRPA solutions collapse within the physical range of particle-particle strength parameter g_{pp}. Many extensions of the QRPA have been proposed to cure these problems, but none of them are free from ambiguities. The small predictive power of the QRPA is the main motivation to look for alternative models. In the present work, we calculate NTMEs of $2\nu\beta^-\beta^-$ as well as $0\nu\beta^-\beta^-$ decay in Projected Hartree-Fock-Bogoliubov (PHFB) model using pairing plus quadrupole-quadrupole plus hexadecapole-hexadecapole ($PQQHH$) type of effective two-body interaction. The validity of PHFB model is tested by calculating a number of spectroscopic properties as well as NTMEs $M_{2\nu}$ and comparing them with the experimental data. The present thesis contains following five chapters.

In Chapter 1, the literature survey on work done so far to study the $2\nu\beta^-\beta^-$ as well as $0\nu\beta^-\beta^-$ decay has been presented.

In Chapter 2, we present the theoretical formalism to calculate the nuclear spectroscopic properties, specifically, the yrast spectra, reduced $B(E2{:}0^+ \rightarrow 2^+)$ transition probabilities, deformation parameter β_2 and g-factors $g(2^+)$. The calculated spectroscopic properties of ^{94,96}Zr, ^{94,96,100}Mo, ^{100,104}Ru, ^{104,110}Pd, ^{110}Cd, ^{128,130}Te, ^{128,130}Xe, ^{150}Nd and ^{150}Sm nuclei are compared with the observed experimental data.

In Chapter 3, we calculate NTMEs $M_{2\nu}$ and half-lives $T^{2\nu}_{1/2}$ of $2\nu\beta^-\beta^-$ decay of ^{94,96}Zr, ^{100}Mo, ^{104}Ru, ^{110}Pd, ^{128,130}Te and ^{150}Nd nuclei for the $0^+ \rightarrow 0^+$ transition. We also examine the effect of deformation on NTMEs $M_{2\nu}$.

In Chapter 4, we study the $0\nu\beta^-\beta^-$ decay of ^{94,96}Zr, ^{100}Mo, ^{104}Ru, ^{110}Pd, ^{128,130}Te and ^{150}Nd nuclei for the $0^+ \rightarrow 0^+$ transition within mass mechanism. We calculate the required NTMEs and extract limits on the effective light as well as heavy Majorana neutrino mass $\langle m_\nu \rangle$ and $\langle M_N \rangle$, respectively. We also investigate the role of deformation on NTMEs of $0\nu\beta^-\beta^-$ decay. In addition, we also estimate the uncertainties associated with NTMEs.

Finally, we conclude with Chapter 5 in which the most important aspects of nuclear structure in the context of PHFB model are discussed. We also suggest a number of necessary improvements to be incorporated in the PHFB model for a more reliable study of $\beta^-\beta^-$ decay in general and $0\nu\beta^-\beta^-$ decay in particular.

LIST OF TABLES

Table 2.8: Comparison of calculated and experimentally observed g factors $g(2^+)$ [Raghavan (1989)] of ^{94,96}Zr, ^{94,96,100}Mo, ^{100,104}Ru, ^{104,110}Pd, ^{110}Cd, ^{128,130}Te, ^{128,130} Xe, ^{150}Nd and ^{150}Sm nuclei. The $g(2^+)$ has been calculated in units of nuclear magneton for$g_l^\pi = 1.0$, $g_l^\nu = 0.0$ and $g_s^\pi = g_s^\nu = 0.50$. '*' value taken from [Speidel *et al.* (2002)].

Table 3.1: Experimental half lives $T^{2\nu}_{1/2}$ of $2\nu\beta^-\beta^-$ decay of A = 48, 76, 82, 94, 96, 100, 110, 116, 128, 130, 136, 150, 238 and 244 nuclei for the $0^+ \rightarrow 0^+$ transition. †denotes all modes.

Table 3.2: Theoretically calculated NTMEs $M_{2\nu}$ within the PHFB model with four different parametrizations and their average value $\overline{M}_{2\nu}$ along with experimental values [Barabash (2010)].

Table 3.3: Theoretically calculated NTME $M_{2\nu}$ and half-life $T^{2\nu}_{1/2}$ of $2\nu\beta^-\beta^-$ in different nuclear models for the $0^+ \rightarrow 0^+$ transition of ^{94,96}Zr, ^{100}Mo, ^{104}Ru, ^{110}Pd, ^{128,130}Te and ^{150}Nd nuclei. The numbers corresponding to (a) and (b) are calculated for $g_A = 1.2701$ and 1.0 respectively. "*" denotes present calculation.

Table 4.1: Decomposition of NTMEs $M^{(0\nu)}$ calculated in (a) $PQQ1$, (b) $PQQHH1$, (c) $PQQ2$ and (d) $PQQHH2$ parametrizations for the $0\nu\beta^-\beta^-$decay of ^{100}Mo nuclei due to the exchange of light Majorana neutrinos.

Table 4.2: Decomposition of NTMEs $M^{(0N)}$ calculated in (a) $PQQ1$, (b) $PQQHH1$, (c) $PQQ2$ and (d) $PQQHH2$ parametrizations for the $0\nu\beta^-\beta^-$decay of ^{100}Mo nuclei due to the exchange of heavy Majorana neutrinos.

Table 4.3: Calculated NTMEs $M^{(0\nu)}$ with (a) $PQQ1$, (b) $PQQHH1$, (c) $PQQ2$ and (d) $PQQHH2$ parametrizations for the $0\nu\beta^-\beta^-$ decay of ^{94,96}Zr, ^{100}Mo, ^{104}Ru, ^{110}Pd, ^{128,130}Te, ^{150}Nd isotopes due to the exchange of light Majorana neutrinos.

Table 4.4: Calculated NTMEs $M^{(0N)}$ with (a) $PQQ1$, (b) $PQQHH1$, (c) $PQQ2$ and (d) $PQQHH2$ parametrizations for the $0\nu\beta^-\beta^-$ decay of ^{94,96}Zr, ^{100}Mo, ^{104}Ru, ^{110}Pd, ^{128,130}Te,

^{150}Nd isotopes due to the exchange of heavy Majorana neutrinos.

Table 4.5: Comparison of NTMEs due to light neutrino exchange $M^{(0\nu)}$ in different nuclear models.

Table 4.6: Comparison of NTMEs $M^{(0N)}$ due to heavy neutrino exchange in different nuclear models.

Table 4.7: Changes (in %) of the NTMEs $M^{(I)}$ $(I = 0\nu, 0N)$ due to exchange of light and heavy Majorana neutrinos, for the $0\nu\beta^-\beta^-$ decay with the inclusion of FNS and F+SRC ((i) F+SRC1, (ii) F+SRC2, (iii) F+SRC3) for the four different parametrizations of the effective two-body interaction.

Table 4.8: Experimental Half-life $T^{(0\nu)}_{1/2}$ and Phase space factor G_{01} [Stoica *et al.* (2013)] for the $0\nu\beta^-\beta^-$ decay of ^{94,96}Zr, ^{100}Mo, ^{110}Pd, ^{128,130}Te and ^{150}Nd isotopes.

Table 4.9: Average NTMEs $\overline{M}^{(I)}$ $(I = 0\nu, 0N)$ and uncertainities $\Delta\overline{M}^{(I)}$ along with effective neutrino mass $\langle m_\nu \rangle$ (in eV), $\langle M_N \rangle$ (in GeV), predicted half-lives $T^{(0\nu)}_{1/2}$ (for light neutrino exchage at $\langle m_\nu \rangle = 50$ meV) and nuclear sensitivities $\xi^{(I)}$ for the $0\nu\beta^-\beta^-$ decay of ^{94,96}Zr, ^{100}Mo, ^{110}Pd, ^{128,130}Te and ^{150}Nd isotopes.

Table 4.10: Deformation ratios $D^{(I)}$ $(I = 0\nu, 0N)$ of $0\nu\beta^-\beta^-$ decay of ^{94,96}Zr, ^{100}Mo, ^{104}Ru, ^{110}Pd, ^{128,130}Te and ^{150}Nd isotopes for the PQQ1 parametrization.

LIST OF FIGURES

TABLES OF CONTENTS

Chapter 1

Introduction

The discovery of radioactivity by Henri Becquerel in 1896 opened a new dimension in the field of nuclear physics. Alpha, beta and gamma rays are the relics of radioactive decays, and their emissions are governed via strong, weak and electromagnetic interactions respectively. The energy spectrum of alpha and gamma decays are discrete in nature due to the emission of a single particle. In 1914, James Chadwick reported the continuous energy spectrum of beta radiation. In order to explain this continuous spectrum, Wolfgang Pauli proposed the emission of a chargeless and massless fermion along with beta particle and called it "neutron" [W. Pauli (1930)]. On 4^{th} December 1930, Pauli wrote a letter to nuclear physicsts who were going to meet a few days later in Tübingen, Germany, "*Dear Radioactive Ladies and Gentlemen, As the bearer of these lines, to whom I graciously ask you to listen, ... I have hit upon a desperate remedy to save the "exchange theorem" of statistics and the law of conservation of energy. Namely, the possibility that in the nuclei there could exist electrically neutral particles, which I will call neutrons, that have spin 1/2 and obey the exclusion principle and that further differ from light quanta in that they*

do not travel with the velocity of light. The mass of the neutrons should be of the same order of magnitude as the electron mass and in any event not larger than 0.01 proton mass. - The continuous beta spectrum would then make sense with the assumption that in beta decay, in addition to the electron, a neutron is emitted such that the sum of the energies of neutron and electron is constant.....". In 1932, J. Chadwick discovered the particle that today we call "neutron" in the nuclear reaction

$$^4\mathrm{He} + ^9\mathrm{Be} \rightarrow ^{12}\mathrm{C} + n \tag{1.1}$$

After the discovery of neutron, the particle proposed by Pauli was called *neutrino* (little neutron) by Enrico Fermi, who gave the first successful theory of β decay in 1934.

The Sun and reactors are the rich sources of neutrinos. In 1946, Bruno Pontecorvo suggested the first radiochemical method of experimental detection of neutrinos on the observation of the following reaction:

$$\nu + ^{37}\mathrm{Cl} \;\rightarrow\; e^- + ^{37}\mathrm{Ar} \tag{1.2}$$

The experimental detection of antineutrino was done by F. Reines and C. W. Cowan in an inverse beta reaction

$$\overline{\nu} + p \;\rightarrow\; e^+ + n$$

at Savannah River experiment during 1954-1956 [Cowan *et al.* (1956)]. On June 14, 1956, Reines and Cowan sent a telegram to Pauli at Zurich University: "*We are happy to inform you that we have definitely detected neutrinos from fission fragments by observing inverse beta decay of protons. Observed cross section agrees well with expected six times ten to minus forty-four square centimeters.*" In 1957, Davis experiment gave the first

indication of the distinction between a neutrino and antineutrino because of the ^{37}Ar was not generated in the reaction

$$\overline{\nu} + {}^{37}\,\mathrm{Cl} \;\rightarrow\; e^{-} + {}^{37}\,\mathrm{Ar} \tag{1.4}$$

which provided a compulsion to assign a lepton number.

In 1956, T. D. Lee and C. N. Yang proposed that parity (P) might not be conserved in weak interaction in order to resolve the $\tau - \theta$ puzzle. Mrs. Wu and co-workers of the National Bureau of Standards in 1957 carried out an experiment and verified the hypothesis of Lee and Yang [Wu *et al.* (1957)].The experiment seemed also to indicate that the charge-symmetry (C) was violated. In 1957, Landau, Lee, Yang and Salam proposed the theory of massless two component neutrino in which neutrino has definite helicity. In the same year, the helicity was determined experimentally by M. Goldhaber, L. Grodzins and A. W. Sunyar [Goldhaber *et al.* (1958)]. In 1962, the data of Brookhaven neutrino experiment [Danby *et al.* (1962)] established that there exist another type of neutrino called as muon neutrino (ν_μ) for which Leon M. Lederman, M. Schwartz and J. Steinberger were awarded the Nobel Prize in 1988. In 1975, Stanford Linear Accelerator discovered tau (τ) particle. Like other lepton family members *i.e.* electron and muon, it was natural to expect tau-neutrino (ν_τ) associated with tau lepton. In 2000, the first direct detection of the ν_τ was established by the DONUT experiment at Fermilab.

The weak interaction has very astonishing properties. It is different from the other three interactions in one very fundamental way *i.e.* the parity is not conserved by the former. The force carriers of weak interaction are $W^{\pm}$ and Z^0 bosons. The six leptons and six quarks are classified into three independent doublets:

	$1^{st}\ family$	$2^{nd}\ family$	$3^{rd}\ family$
Lepton doublets	$\begin{bmatrix} e^- \\ \nu_e \end{bmatrix}$	$\begin{bmatrix} \mu^- \\ \nu_\mu \end{bmatrix}$	$\begin{bmatrix} \tau^- \\ \nu_\tau \end{bmatrix}$
Quark doublets	$\begin{bmatrix} u \\ d \end{bmatrix}$	$\begin{bmatrix} c \\ s \end{bmatrix}$	$\begin{bmatrix} t \\ b \end{bmatrix}$

Due to the lepton flavor conservation these doublets, namely (e^-, ν_e), (μ^-, ν_μ) and (τ^-, ν_τ) do not mix with each others. Quark sector is different than lepton sector because of the mixing among them known as CKM (Cabibbo-Kobayashi-Maskawa) mixing.

The Standard model (SM) of electroweak interactions was formulated by S. Weinberg [Weinberg (1967)] and A. Salam [Salam (1969)] in 1967, which is based on an SU(2)×U(1) gauge symmetry proposed by S. L. Glashow in 1961 [Glashow (1961)]. The SM predicted the existence of weak neutral currents and the Z^0 boson. This Standard model also includes the Higgs mechanism, based on the symmetry breaking which was proposed by P. W. Higgs (1964*a*), (1964*b*), (1966), F. Englert and R. Brout (1964), Guralnik *et al.* (1964) and Kibble (1967) that allows the massless gauge bosons. The theory of SM proposed by Weinberg and Salam was not normalized. In 1971, G. 't Hooft and M.J.G. Veltman [Hooft (1971a), (1971b), Hooft and Veltman (1972)] made the theory renormalizable. The discovery of neutral current neutrino interactions in Gargamelle experiment at CERN [Hasert *et al.* (1973a), (1973b), (1974)], testified at Fermilab [Benvenuti (1974)]. The

observation of the neutral weak current and the discovery of $W^{\pm}$ and Z^0 bosons [Arnison *et al.* (1983), Bagnaia *et al.* (1983)] contributed spectacularly to the success of SM. The theory of SM is so potent that in principle, all the events of microscopic particles can be understood in an elementary and unified way. However, neutrinos should have zero mass according to the SM. On the other hand, quantum theory requires that neutrinos must have mass to change flavor which has been confirmed in neutrino oscillation experiments. Since neutrinos do have mass, there are two possibilities, namely Dirac and Majorana nature of neutrinos. Therefore, the mass as well as nature of neutrinos is not completely known till date, and neutrinos are the most enigmatic particles in the fermionic sector.

1.1 Neutrino Mass

Weyl predicated the two component spinor theory for a massless neutrino. Unlike weyl 2-component, massive neutrino has 4-component spinor. If two of them are same then it has possibility that neutrino has 2-component spinor but with mass.

1.1.1 Dirac and Majorana neutrino masses

Dirac was the first person who gave the theory of antiparticles in order to explain the negative energy problem. Unlike positron (e^+), antiparticle of a electron, neutral pion (π^0) has its own antiparticle whereas neutral kaon (K^0) has distinct antiparticle. Both pion and kaon are composed of quarks and antiquarks. In order to resolve the discrepancy E. Majorana (1937) gave the concept of particle which is its own antiparticle called as Majorana particle. Since, the neutrino interacts via weak interaction and weak interaction

does not follow the conservation of charge conjugation C, hence, the Majorana neutrino can not be an eigenstate of C alone.

In order to understand the difference between Majorana and Dirac neutrino, first we have to assume that there exist a left handed massive neutrino ν_L. If CPT invariance is valid then there exists a right handed antineutrino $\overline{\nu}_R$. Since the speed of massive particles is less than the speed of light, there is always a choice to select the frame of reference which moves faster than the reference frame in which ν_L exists. Thus, the Lorentz transformation alters the direction of the momentum and keeps its spin unaltered and ν_L turns into right handed ν_R which may or may not be same as $\overline{\nu}_R$. If ν_R is not same, then ν_R has its own particle $\overline{\nu}_L$. Thus, there exist four states (quadruplet state) at a time known as Dirac neutrino ν^D, as shown in Figure 1.1(a). On the other side, if ν_R is the same particle as ν_L then, there exist only one pair of state as shown in Figure 1.1(b). This pair of state is known as Majorana neutrino ν^M.

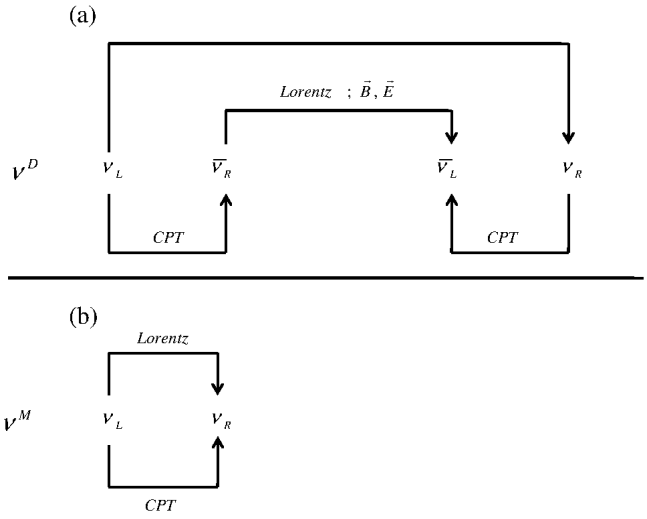

Figure 1.1: (a) Dirac neutrino ν^D. (b) Majorana neutrino ν^M.

Diagonalization of mass term : The mass of neutrinos is calculated by the mass term of the Lagrangian. This mass term must be Lorentz invariant and Hermitian. This requirement restricts the possible mass terms to two groups: $\overline{\psi}\psi$ and $\overline{\psi}^C\psi^C$ as well as $\overline{\psi}\psi^C$and its Hermitian conjugate $\overline{\psi}^C\psi$. The Dirac field Lagrangian has the form

$$L_D = -\frac{1}{2}\int d^4x \ \left(\overline{\psi}\gamma_\mu\partial_\mu\psi + \overline{\psi}m_D\psi\right) \tag{1.5}$$

The first part of Eq. (1.5) is the kinetic term and mass term is in the second part. This Lagrangian is invariant under the global phase transformation

$$\psi \rightarrow e^{i\alpha}\psi \ ; \ \psi^C \rightarrow e^{-i\alpha}\psi^C \tag{1.6}$$

where $\overline{\psi}\psi^C$and $\overline{\psi}^C\psi$ is an another Lorentz invariant mass term (Majorana mass term) that is not invariant under this phase transformation. Consequently, the Dirac mass term is associated with the conserved lepton number while the Majorana mass term violates the lepton number conservation. The most general Lorentz invariant and Hermitian Lagrangian has the form

$$-2L_M = \frac{1}{2}\left(\overline{\psi}m_D\psi + \overline{\psi}^C m_D\psi^C + \overline{\psi}m_M\psi^C + \overline{\psi}^C m_M^*\psi\right) \tag{1.7}$$

where $m_M = m_1 + im_2$, The matrix form of Eq. (1.7) has to be

$$-2L_M = \frac{1}{2}\left(\overline{\psi}, \overline{\psi}^C\right)\begin{pmatrix} m_D & m_M \\ m_M^* & m_D \end{pmatrix}\begin{pmatrix}\psi \\ \psi^C\end{pmatrix} \tag{1.8}$$

On the diagonalization of the matrix in Eq. (1.8), we obtain definite mass as well as two eigenvalues *i.e.* $m_D \pm |m_M|$, and two eigenvectors which are given as

$$\begin{pmatrix}\varphi_+\\ \varphi_-\end{pmatrix} = \frac{1}{\sqrt{2}}\begin{pmatrix} e^{-i\theta}\psi + e^{i\theta}\psi^C \\ -e^{-i\theta}\psi + e^{i\theta}\psi^C \end{pmatrix} \tag{1.9}$$

where, $\tan 2\theta = m_2/m_1$. These eigenvectors are the eigenstates of charge conjugation with distinct eigenvalues *i.e.* $m_D \pm |m_M|$. Hence, these eigenvectors are Majorana fields. If $m_M = 0$ in Eq. (1.7), then the mass matrix, as given in Eq.(1.8), is already diagonal with the eigenvalue m_D. Therefore, in this case the eigenvectors are not the eigenstate of C and termed as Dirac particle. The Dirac particles have different particle and antiparticle state. These are also not a CP conjugation egienstate and hence, Dirac particles exhibits magnetic as well as electric dipole moments. On the other hand, Majorana particles do not have magnetic and electric dipole moments because these have eigenstates of CP.

On consideration of chiral projections of ψ, $\overline{\psi}_L\psi_R$ and $\overline{\psi}_R\psi_L$ represent the Dirac mass term while $\overline{\psi}_L(\psi^C)_R$ etc., represent the Majorana mass term. The above mentioned both type of mass terms violates the chirality. As we know, γ_5 are the 4×4 Dirac matrices. Therefore, the mass matrix as well as the parameters in Eq. (1.8) must be doubles given as

$$-2L_M = \frac{1}{2}\left(\overline{\psi}_R, (\overline{\psi}^C)_R, \overline{\psi}_L, (\overline{\psi}^C)_L\right)\begin{pmatrix} 0 & M \\ & \\ & \\ M^\dagger & 0 \end{pmatrix}\begin{pmatrix} \psi_R \\ (\psi^C)_R \\ \psi_L \\ (\psi^C)_L \end{pmatrix} \tag{1.10}$$

and M is a 2×2 matrix and contains three parameters m_D, m_1, m_2. These parameters are related with M as

$$M \approxeq m_D I + m_1 \sigma_x + m_2 \sigma_y \tag{1.2}$$

where σ_x, σ_y are the Pauli spin matrices. The eigen values of Eq. (1.10) is given by

$$\lambda_{\pm} = \frac{1}{2}\left\{(m_R + m_L) \pm \left[(m_R - m_L)^2 + 4m_D^2\right]^{\frac{1}{2}}\right\} \tag{1.11}$$

with $m_R = m_1 + |m_2|$ and $m_L = m_1 - |m_2|$.

1.1.2 Neutrino Oscillation

In case of neutrino, the most general mass term is [Gribov and Pontecorvo (1969)]

$$-L_M \;=\; m_{\nu_e\nu_e}\overline{\nu}_e\nu_e \;+ m_{\nu_\mu\nu_\mu}\overline{\nu}_\mu\nu_\mu \;+\; m_{\nu_e\nu_\mu}(\overline{\nu}_e\nu_\mu \;+ \overline{\nu}_\mu\nu_e) \tag{1.12}$$

Above equation can be diagonalize by putting

$$\begin{aligned} \nu_e &= \cos\theta\ \nu_1 + \sin\theta\ \nu_2 \\ \nu_\mu &= -\sin\theta\ \nu_1 + \cos\theta\ \nu_2 \end{aligned} \tag{1.13}$$

where ν_1 and ν_2 are the Dirac particles having definite masses m_1 and m_2, respectively and they are not eigenstates of charge conjugation CP and the eigenvalues of Eq. (1.12) are

$$m_{1,2} \;=\; \frac{1}{2}\left\{m_{\nu_e\nu_e} \;+\; m_{\nu_\mu\nu_\mu} \;\pm\; [(m_{\nu_e\nu_e} \;-\; m_{\nu_\mu\nu_\mu})^2 \;+\; 4m^2_{\nu_e\nu_\mu}]^{\frac{1}{2}}\right\} \tag{1.14}$$

and θ can be calculated as

$$\tan 2\theta \;=\; 2m_{\nu_e\nu_e} \;/\; (m_{\nu_\mu\nu_\mu} \;-\; m_{\nu_e\nu_e}) \tag{1.15}$$

In case of negative eigenvalues, the field $\gamma_5\nu_2$ should be used. The time evolution of the particles ν_1 and ν_2 is given as

$$|\nu_1(t)\rangle \ = e^{-iE_1t} \ |\nu_1(0)\rangle \ ; \quad |\nu_2(t)\rangle \ = e^{-iE_2t} \ |\nu_2(0)\rangle \tag{1.16}$$

where $E_i \ = \ (p^2 + m_i^2)^{\frac{1}{2}}$ is the neutrino energy. Here, we have assumed that the propagation of these particles are without interactions. Electron neutrino ν_e has been created at $t = 0$ and it will evolve in time then the state at time t is

$$\begin{aligned} |\nu_e(t)\rangle \ &= \ \cos\theta \ e^{-iE_1t} \ |\nu_1(0)\rangle \ + \ \sin\theta \ e^{-iE_2t} \ |\nu_2(0)\rangle \\ &= \ \left(\cos^2\theta \ e^{-iE_1t} \ + \ \sin^2\theta \ e^{-iE_2t} \ \right) \ |\nu_e(0)\rangle \\ &\quad + \ \cos\theta \ \sin\theta \ \left(e^{-iE_2t} \ - \ e^{-iE_1t} \ \right) \ |\nu_\mu(0)\rangle \end{aligned} \tag{1.17}$$

At time t it is in the state $|\nu_\mu\rangle$. Now the probability of electron neutrino, initialy at time $t = 0$, is in the state $|\nu_\mu\rangle$ at time t, is given by the absolute square of the amplitude of $|\nu_\mu(0)\rangle$ in Eq. (1.17), *i.e.*,

$$P(\nu_e \to \nu_\mu) \ = \ |\langle\nu_\mu|\nu_e(t)\rangle|^2 \ = \ \frac{1}{2} \ \sin^2\theta \ \left(1 - \cos \ \frac{m_2^2 - m_1^2}{2p}t\right) \tag{1.18}$$

The above expression describes the neutrino flavor oscillation. The probability $P(\nu_e \to \nu_e)$ of electron neutrino ν_e which is initially at $t = 0$ is still in the state ν_e at latter time t is given by the absolute square of the amplitude of $|\nu_e(0)\rangle$ in Eq. (1.17) *i.e.* $|\langle\nu_e(0)|\nu_e(t)\rangle|^2$ and the total probability is always one

$$P(\nu_e \to \nu_e) \ + \ P(\nu_e \to \nu_\mu) \ = 1 \tag{1.19}$$

1.1.3 Experimental aspects of Neutrino oscillations

There are two aspects for the experimental determination of neutrino masses. The experimental aspect of neutrino oscillations initiated in 1970 by R. Davis *et al.* through the observation of solar neutrinos in the Homestake solar neutrino observatory. They were found the observed rate of solar neutrinos much smaller than the predicted rate by the Standard Solar Model (SSM). This inconsistency was known as solar neutrino puzzle. In order to understand the above-mentioned inconsistency, B. Pontecorvo gave the concept of neutrino oscillation before the Davis experiment started. Kamiokande was the second experiment that was performed to detected the solar neutrinos was also measured the rate smaller than the predicted rate by the SSM. In the nineties GALLEX and SAGE (radiochemical experiment) gave a significant contribution to the flux, through the detection from all the reactions like pp, CNO cycles etc., which approximately measured the half of the predicted rates.

Upto the nineties no such reactor and accelerator based experiments were found the indications of neutrino oscillation. In 1998 the experimental detection of neutrino oscillations came forward with the observation of up-down asymmetry in atmospheric neutrino muon events through the detection of cherenkov radiation in Super Kamiokande. In 2002 SNO experiments gave the indication of vanishing of solar neutrino ν_e through the observation of the CC and NC reactions. In 2004 the KamLAND reactor neutrino experiment was observed the distortion in $\overline{\nu}_e$ spectrum. The accelerator long-baseline K2K and MINOS experiments were confirmed the results of neutrino oscillations obtained from the atmospheric Super-Kamiokande experiment. Neutrino oscillations were not found in the

CHOOZ and Palo Verde reactor experiments. The MiniBooNE experiment doesn't confirm accelerator short-baseline LSND indication. The result provided by LSND needs an existence of sterile neutrinos. All these experiments provides the large data to support the neutrino having masses and mixing among the ν_e, ν_μ and ν_τ neutrinos.

Solar neutrino experiment

Thermonuclear pp and CNO cycles are the sources of the generation of solar electron neutrinos. The temperature at the centre of the sun is 15×10^6 K. This temperature favours the dominance of pp cycle over the CNO cycle. Significantly heavier stars have much higher temperature than the sun are favorable for CNO cycle. The contribution of CNO cycle in the generation of energy of the sun is about 1%. First deuterium is produced in pp reactions

$$p + p \rightarrow d + e^+ + \nu_e \qquad p + e^- + p \rightarrow d + \nu_e \tag{1.20}$$

In Eq. (1.20), deuterium produced from pp reaction gives an major contribution about 99.71%, while pep reaction has only 0.23% contribution. Deuterium and proton make the ^{3}He

$$p + d \rightarrow^3 He + \gamma \tag{1.21}$$

This ^{3}He is disappears as follows

$$\begin{aligned} {}^3He +{}^3 He &\rightarrow^4 He + p + p \qquad (84.82\%) \\ {}^3He + p &\rightarrow^4 He + e^+ + \nu_e \qquad (\text{about } 10^{-5}\%) \\ {}^3He +{}^4 He &\rightarrow^7 Be + \gamma \qquad (15.08\%) \end{aligned} \tag{1.22}$$

The ^{7}Be produced in the third reaction (Eq. (1.22)) ultimately produces the ^{4}He nuclei

$$^7Be + e^- \rightarrow ^7 Li + \nu_e \qquad ^7Li + p \rightarrow ^4 He + ^4 He \tag{1.23}$$

$$^7Be + p \rightarrow ^8 B + \gamma \qquad ^8B \rightarrow ^8 Be^* + e^+ + \nu_e \qquad ^8Be^* \rightarrow ^4 He + ^4 He \tag{1.24}$$

These produced positrons annihilate with the electrons produces the sun's energy and neutrino by the reaction

$$4p + 2e^- \rightarrow ^4 He + 2\nu_e + Q \tag{1.25}$$

where

$$Q = 4m_p + 2m_e - m_{^4He} \approx 26.73 \text{ MeV} \tag{1.26}$$

The sun energy ($\frac{1}{2}Q \approx 13.36$ MeV) are released with the emission of one neutrino. The energy are released in the form of photons ($\sim$98%) and neutrinos ($\sim$2%). Consider E is the energy of neutrino. The emission of such neutrinos is accompanied by the production of luminous energy equal to $\frac{1}{2}Q - E$. If $\varphi_r(E)$ is the flux on the earth of neutrinos from the source r ($r = pp, ^7Be, ^8B, \ldots$) we have the following relation

$$\int \sum_r \left(\frac{1}{2}Q - E\right) \varphi_r(E)\, dE = \frac{\mathcal{L}}{4\pi R^2} \tag{1.28}$$

where $\mathcal{L}$ is the luminosity of the sun and R is the sun-earth distance. Eq. (1.28) is known as Luminosity relation. We have assumed the fact that neutrinos were produced 8 min before the detection. While, photon takes about 10^5 years to reach from center to the surface of the sun. Now, luminosity relation has the form

$$\sum_r \left(\frac{Q}{2} - \overline{E}_r\right) \varphi_r = \frac{\mathcal{L}}{4\pi R^2} \tag{1.29}$$

$$\overline{E}_r = \frac{1}{\varphi_r} \int E\, \varphi_r(E)\, dE \tag{1.30}$$

$\overline{E}_r$ is the average neutrino energy and $\varphi_r = \int \varphi_r(E)\, dE$ is the total flux of the neutrinos. From the analysis of flux data predicted by SSM, we can neglect the second term of the Eq. (1.29). The expression for the total flux has the form

$$\varphi = \sum_r \varphi_r \simeq \frac{\mathcal{L}}{2\pi R^2 Q}$$

Taking into account that $\mathcal{L} = 2.40 \times 10^{39}$ MeV s^{-1} and $R = 1.496 \times 10^{13}$ cm we can find

$$\varphi \simeq 6.4 \times 10^{10}\ cm^{-2} s^{-1}$$

Homestake Chlorine Solar Neutrino Experiment Homestake was the first experiment carried out by R. Davis [Davis *et al.* (1968)], in which solar electron neutrinos, were detected. For this R. Davis got the Nobel prize in 2002. In the Davis experiment radiochemical Cl-Ar method, given by B. Pontecorvo in 1946, was used. Solar electron neutrinos were detected via the observation of the reaction.

$$\nu_e + {}^{37}\mathrm{Cl} \rightarrow e^- + {}^{37}\mathrm{Ar} \tag{1.31}$$

Energy threshold set for this reaction is equal to 0.814 MeV. The ^{37}Ar atoms are radioactive and they decay via electron-capture with emission of Auger electrons. The half-life of the decay is 34.8 days. In this experiment, 615 tons of liquid perchloroethylene (C_2Cl_4) were used as an detector. This experiment was carried out in the Homestake mine (USA) at depth of 1480m for minimizing the cosmic ray background. Taken the two-months exposure time, radioactive ^{37}Ar atoms produced in the reaction (1.31) were extracted and the signal of auger electron was detected by putting the ^{37}Ar atoms in the low background proportional counter. The energy threshold is larger for the Cl-Ar reaction (1.31)

in comparison with pp neutrinos. After 108 runs, the measured event rate between 1970 to 1994 are found to be

$$R_{Cl} = (2.56 \pm 0.16 \pm 0.16) \text{ SNU}$$

while on the consideration of no neutrino oscillation the rate predicted by Standard Solar Model (SSM)

$$R_{SSM} = (8.1 \pm 1.3) \text{ SNU}$$

Radiochemical GALLEX-GNO and SAGE Experiments Radiochemical GALLEX-GNO [Anselmann *et al.* (1994), Altmann *et al.* (2005)] and SAGE [Abdurashitov *et al.* (1994)] experiments were designed to detect the solar neutrinos as well as the low energy neutrinos from pp reaction. The observed neutrinos came from the reaction.

$$\nu_e + {}^{71}\text{Ga} \rightarrow e^- + {}^{71}\text{Ge} \tag{1.32}$$

Threshold set for this reaction is equal to 0.233 MeV. The half life of ^{71}Ge is equal to 11.43 days. 100 tons of water solution of gallium chloride were used as an detector in GALLEX-GNO experiment while in the SAGE experiment 50 tons of ^{71}Ga in form of liquid. In order to minimize the background, former experiment was carried out in underground Gran Sasso Laboratory (Italy) and the later one in the Baksan Neutrino Observatory. They have taken 123 GALLEX and GNO exposure runs, one exposure run is about 4 weeks, between the year 1991-2003. Whereas, In the SAGE experiment they have taken 92 runs during 1990-2001 and They got the event rate is

$$R_{Ga} = (67.5 \pm 5.1) \text{ SNU} \qquad \text{(GALLEX-GNO)}$$

$$R_{Ga} = \left(70.8^{+5.3}_{-5.2}\right) \text{ SNU} \qquad \text{(SAGE)}$$

Kamiokande and Super-Kamiokande Solar Neutrino Experiments They were used a 2,140 ton water Cherenkov as detector. This Kamiokande experiment [Renshaw *et al.* (2014)] was done in the Kamioka mine (Japan) at a depth of about 1,000 m. Recoil electrons from the elastic neutrino-electron scattering were used to detect the solar neutrinos.

$$\nu_x + e \rightarrow \nu_x + e \qquad (x = e, \mu, \tau) \tag{1.33}$$

They had used 1000 photomultipliers of diameter 50 cm as detector to detect the cherenkov radiation in water which is produced by electron neutrinos came from the process (1.33). They have found the total flux of high energy ^{8}B neutrinos from this experiment is

$$\varphi_\nu^K = (2.80 \pm 0.19 \pm 0.33)\,.10^6\ cm^{-2}s^{-1}$$

This experiment was run from year 1987 to 1995. In 1996 they were used a 50 kiloton water Cherenkov as detector and hence named as Super-Kamiokande (SK). The first phase of SK (SK-I) initiated in 1996 and completed in 2001 while the second phase (SK-II) initiated in December 2002 and completed in October 2005. In this phase 11,000 photomultipliers were used. The total flux from both of the phases are found to be

$$\begin{aligned} \varphi_\nu^{SK-I} &= (2.35 \pm 0.02 \pm 0.08)\,.10^6\ cm^{-2}s^{-1} \\ \varphi_\nu^{SK-II} &= (2.38 \pm 0.05 \pm 0.16)\,.10^6\ cm^{-2}s^{-1} \end{aligned}$$

SNO Solar Neutrino Experiment The rate predicted by Standard Solar Model (SSM) were larger than the rate obtained from the Homestake, GALLEX-GNO, SAGE, Kamiokande and Super-Kamiokande experiments. This experiment [Ahmad *et al.* (2002)] was carried out in the Creighton mine (Sudbury, Canada) at a depth of 2092 m. They

used 1,000 tons of D_2O contained in acrylic vessel as detector along with 9,456 photomultipliers of diameter 20 cm to detect the cherenkov radiation. In this experiment, the detection of solar neutrinos was done through three processes given as.

$$\begin{aligned} \nu_e + d &\rightarrow e^- + p + p && \text{CC process} \\ \nu_x + d &\rightarrow \nu_x + p + n \quad (x = e, \mu, \tau) && \text{NC process} \\ \nu_x + e &\rightarrow \nu_x + e && \text{ES process} \end{aligned} \tag{1.34}$$

The total fluxes of neutrinos are found to be

$$\begin{aligned} \varphi_{\nu_e}^{CC} &= \left(1.68 \pm 0.06^{+0.08}_{-0.09}\right) .10^6 \ cm^{-2}s^{-1} \\ \varphi_{\nu_{e,\mu,\tau}}^{NC} &= \left(4.94 \pm 0.21^{+0.38}_{-0.34}\right) .10^6 \ cm^{-2}s^{-1} \\ \varphi_{\nu}^{ES} &= (2.35 \pm 0.22 \pm 0.15) .10^6 \ cm^{-2}s^{-1} \end{aligned}$$

Borexino Solar Neutrino Experiment In 2007 Borexino solar neutrino experiment [Bellini *et al.* (2014)] has started. The detector of this experiment is a scintillator with a mass of 278 tons in a nylon vessel. In order to detect the scintillation light the inner surface of the detector contains 2212 photomultipliers. ^{7}Be neutrinos with energy 0.862 MeV are observed in real time. After the run of 192 days, the interaction rate of ^{7}Be obtained is $R_{Borexino} = (49 \pm 3 \pm 4)$ counts/(day 100 ton). Considering no neutrino transitions and the flux of the ^{7}Be neutrinos is given by the SSM ($\varphi(^7Be) = (5.08 \pm 0.25)\cdot 10^9 cm^{-2}s^{-1}$), we get the rate $R_{SSM} = (74 \pm 4)$ counts/(day 100 ton).

Super-Kamiokande Atmospheric Neutrino Experiment

Neutrino having energy from 100 MeV to 10 TeV are detected in this atmospheric neutrino experiment [Fukuda *et al.* (1998)]. Interaction of neutrinos and antineutrinos with the nuclei in the detector produced an electron and muons which is used for the detection of neutrinos having energies ranges from 100 MeV to 10 GeV through the observation of the reaction:

$$\nu_l(\overline{\nu}_l) + N \rightarrow l^-(l^+) + X \qquad l = (e, \mu) \tag{1.35}$$

Pions and kaons are produced by the interaction of cosmic ray with nuclei of the atmosphere and the subsequent decay of the pions, kaons and muons generated atmospheric neutrinos. The observation of atmospheric neutrinos follow the reactions

$$\begin{aligned} \pi^+ &\rightarrow \mu^+ + \nu_\mu \qquad \mu^+ \rightarrow e^+ + \nu_e + \overline{\nu}_\mu \\ \pi^- &\rightarrow \mu^- + \overline{\nu}_\mu \qquad \mu^- \rightarrow e^- + \overline{\nu}_e + \nu_\mu \end{aligned} \tag{1.36}$$

The differentiability between electrons and muons generated in Eq. (1.35) is important for the investigation of flavor neutrino oscillations. Detection of Cherenkov radiation is the indication of leptons in this experiment. Cherenkov ring for electrons is totally different from muons. Instead of muon, Cherenkov ring for electrons have more diffuse light. The ratio r of the $(\nu_\mu + \overline{\nu}_\mu)$ and $(\nu_e + \overline{\nu}_e)$ fluxes gives the indication of flavor neutrino oscillations. Double ratio $R = \frac{r_{means}}{r_{MC}}$ (r_{means} is the measured and r_{MC} is the predicted $\frac{\mu}{e}$ ratios) from the SK-I run was found the value in the sub-GeV region

$$R_{sub-\mathrm{GeV}} = 0.658 \pm 0.016 \pm 0.035$$

In the multi-Gev region

$$R_{multi-\mathrm{GeV}} = 0.658 \pm 0.016 \pm 0.035$$

KamLAND Reactor Neutrino Experiment

KamLAND experiment [Eguchi *et al.* (2003)] produced the results of reactor $\overline{\nu}_e$. This experiment was carried out in Japan (Kamioka mine). One kilo-ton of high purity liquid scintillator is used as detector that is contained in nylon ballon of diameter 13 m which is further suspended in buffer oil. Both are contained in stainless steel vessel of diameter 18 m. Inside the inner surface of the vessel, 1,879 photomultiplier tubes were mounted while 225 phototubes were mounted outside the vessel. Electron antineutrinos generated from the 55 Japanese reactors are detected in the KamLAND experiment through the observation of the reaction.

$$\overline{\nu}_e + p \rightarrow e^+ + n \tag{1.38}$$

Eq. (1.38) is a famous inverse beta decay.

CHOOZ Reactor Neutrino Experiment 5 tons of Gd liquid scintillator contained in an acrylic vessel used as detector in this experiment [Apollonio *et al.* 2003],. The antineutrinos were detected through the observation of the reaction (1.38). Further, γ signal produced by the positron annihilation and a delayed signal from the capture of the neutron by Gd (in this process γ's with a total energy of 8 MeV are produced) were recorded in coincidence. In this experiment, 3,600 antineutrino events were recorded from April 1997 to July 1998. The ratio R of the total number of detected $\overline{\nu}_e$ events to the

expected events was found

$$R = 1.01 \pm 2.8\%$$

Long-Baseline Accelerator Neutrino Experiments

K2K Accelerator Neutrino Experiment K2K [Ahn *et al.* (2006)] and MINOS [Adamson *et al.* (2008)] experiments are used to study the mass squared difference of atmospheric neutrinos Δm^2_{23}. These experiments are the long-baseline accelerator experiments. The oscillation length of a neutrino having energy 1 GeV and $\Delta m^2_{23} \simeq 2.5 \times 10^{-3}$ eV^2 is

$$L_{23} \simeq 2.5 \frac{E}{\Delta m^2_{23}}\ m \simeq\ 10^3\ km \tag{1.39}$$

K2K was the first long baseline experiment. In this experiment KEK accelerator (Japan) and Super Kamiokande are used as source of neutrinos and detector respectively. The distance between these two is 250 km. Neutrino beam (97.3% of ν_μ, 1.3% of ν_e and 1.4% of $\overline{\nu}_\mu$) was generated by the successive decay of secondary particles that was produced by the bombardment of protons having energy of 12 GeV from the KEK accelerator to the aluminum target. The survival probability of the two neutrinos is given by.

$$P(\nu_\mu \rightarrow \nu_\mu)\ = 1 - \sin^2 2\theta_{23}\ \sin^2\left(1.27\ \Delta m^2_{23} \frac{L}{E}\right) \tag{1.40}$$

where L is the distance between the source and detector, E is the neutrino energy and Δm^2_{23} is the neutrino mass squared difference in eV^2. K2K experiment was design to searched for the vanishing of muon neutrinos. The reduction in total flux and distortion of neutrino spectrum are the indication of the disappearance of muon neutrino. Analysis from the data produced in K2K experiment, the range of Δm^2_{23} for $\sin^2 2\theta_{23} = 1$ was

found.

$$1.9 < \Delta m^2_{23} < 3.5 \times 10^{-3}\text{eV}^2 \qquad 90\%\ \text{CL}$$

MINOS Accelerator Neutrino Experiment In the MINOS experiment [Adamson *et al.* (2008)] the Fermilab Main Injector facility used as source and Sudan mine at a distance of 735 km as detector respectively. Neutrino beam (92% of ν_μ, 1.2% of ν_e, 0.1% of $\overline{\nu}_e$ and 5.8% of $\overline{\nu}_\mu$) was generated by the successive decay of pions and kaons that was produced by the bombardment of protons having energy of 120 GeV from the Main injector to the graphite target. Muon neutrinos are detected in the MINOS experiment through the observation of the process

$$\nu_\mu + Fe \rightarrow \mu^- + X$$

MINOS experiment measured the muon neutrino survival probability as a function of the neutrino energy. The survival probability of two neutrinos is given by Eq. (1.40). During the period of May 2005 to July 2007, 848 muon events were observed in this experiment. The analysis of two neutrino data of MINOS gave the values for the neutrino oscillation parameters are

$$\Delta m^2_{23} = (2.43 \pm 0.13)\ 10^{-3}\ \text{eV}^2, \qquad \sin^2 2\theta_{12} > 0.90\ (90\%\ \text{CL})$$

MiniBooNE Accelerator Neutrino Experiment In the MiniBooNE experiment [Ray (2007)], the distance between source and detector was 540 m. Neutrino beam was generated by the successive decay of pions and kaons that was produced by the bombardment of protons having energy of 8 GeV from the Fermilab Booster facility to the beryllium target. A spherical tank with an inner radius of 610 cm filled with 800 tons of

pure mineral oil used as detector. Charged particles were detected through the observation of directional Cherenkov radiation and isotropic scintillation light. 380 candidates for CC quasielastic events

$$\nu_e + n \rightarrow e^- + p$$

were observed.

1.2 Double Beta decay

The nuclear $\beta\beta$ decay, which is a rare and remarkable second order process of weak interaction in nature, is expected to proceed through two different modes, namely two neutrino double beta ($2\nu\beta\beta$) decay and neutrinoless double beta ($0\nu\beta\beta$) decay. Historically, the first signature of nuclear $\beta\beta$ decay offered by nature was that some even Z-even N nuclei otherwise candidates for β decay could still be found in the earth's crust, billions of years after they should have become extinct through radioactive disintegrations. Werner Heisenberg postulated that due to a pairing force between like nucleons, these even-even nuclei are more bound than the neighboring odd-A nuclei and, hence, stable against β decays. In case of ^{100}Mo and ^{100}Tc , the former being lighter than the latter, is stable against β^- decay. However, this stability argument is not a complete solution. The $\beta^-\beta^-$ decay should indeed take place from ^{100}Mo to ^{100}Ru, as the former is heavier than the latter, although single β^- decay from ^{100}Mo to ^{100}Tc is forbidden energetically. The half-life of $2\nu\beta^-\beta^-$ decay was calculated by Maria Goepert-Mayer (1935) at the suggestion of Eugene P. Wigner and the half-life was greater than 10^{17} years, which is exceedingly slow even on the geological time scale. Thus, the rarity of $\beta\beta$ decay would account for the

original puzzle of why some unstable even-even isotopes are still around. The $2\nu\beta\beta$ decay can be classified into the following four categories on the basis of electron or positron emission.

$$\begin{aligned}
&(i) \quad {}^{A}_{z}X \rightarrow^{A}_{Z+2} Y + 2e^- + 2\overline{\nu}_e && \text{(double elctron emission)} \\
&(ii) \quad {}^{A}_{Z}X \rightarrow^{A}_{Z-2} Y + 2e^+ + 2\nu_e && \text{(double positron emission)} \\
&(iii) \quad e^- + {}^{A}_{Z}X \rightarrow^{A}_{Z-2} Y + e^+ + 2\nu_e && \text{(electron capture-positron emission)} \\
&(iv) \quad 2e^- + {}^{A}_{Z}X \rightarrow^{A}_{Z-2} Y + 2\nu_e && \text{(double electron capture)}
\end{aligned} \tag{1.3}$$

In 1939, W. Furry conjectured that if neutrino is a Majorana particle [Majorana (1937) and Racah (1937)], the neutrinoless double beta ($0\nu\beta^-\beta^-$) decay could take place. This process takes place as follows

$$ {}^{A}_{Z}X \rightarrow^{A}_{Z+2} Y + 2e^- \tag{1.4}$$

and the estimated half-life of a nucleus in the $0\nu\beta^-\beta^-$ decay mode was of the order of 10^{11} years [Furry (1939)]. In $0\nu\beta\beta$ decay, there is no corresponding requirement for neutrinos, although the conservation of energy and momentum required the emission of neutrinos in single β decay. The energy and momentum could be conserved in this decay mode, releasing two electrons or positrons only. Thus, the $2\nu\beta\beta$ and $0\nu\beta\beta$ decay modes are competing processes. There are also four $0\nu\beta\beta$ decay modes depending on whether electron or positron is emitted.

$$\begin{aligned}
&(i) \quad {}^{A}_{z}X \rightarrow^{A}_{Z+2} Y + 2e^- && \text{(double electron emission)} \\
&(ii) \quad {}^{A}_{Z}X \rightarrow^{A}_{Z-2} Y + 2e^+ && \text{(double positron emission)} \\
&(iii) \quad e^- + {}^{A}_{Z}X \rightarrow^{A}_{Z-2} Y + e^+ && \text{(electron capture-positron emission)} \\
&(iv) \quad 2e^- + {}^{A}_{Z}X \rightarrow^{A}_{Z-2} Y^* && \text{(double electron capture)}
\end{aligned} \tag{1.5}$$

There are 35 possible candidates undergoing $\beta^-\beta^-$ decay. In Table 1.1, we have given a list of them along with Q-value, natural abundance and β_2 parameter.

The first theoretical investigation of $\beta\beta$ decay [Zeldovich *et al.* (1954), Primakoff (1952) and Rosen and Primakoff (1959)] suggested that the 0ν $\beta^-\beta^-$ process enjoy a phase space advantage by a factor of 10^8 over the 2ν $\beta^-\beta^-$ decay. This result was quite inspiring for the experimentalists, as a lifetime of the order of 10^{15} years was within the reach of the then experimental capabilities. In the early 1950's, a series of geochemical, radiochemical and counter experiments established a limit on the total half-lives of ${}^A_ZX \rightarrow {}^A_{Z+2}Y$ that far exceeded the values for the 0ν $\beta^-\beta^-$ decay process. These results strongly suggested that the electron neutrino was a Dirac particle and prompted to introduce a lepton number L to distinguish the neutrino from its antiparticle. Thus lepton number L was introduced as

$$L = \begin{cases} 1 & for \quad e^-,\, \nu_e \\ -1 & for \quad e^+, \overline{\nu}_e \end{cases} \tag{1.6}$$

The assumption that lepton numbers are additive and total lepton number is conserved allows 2ν $\beta^-\beta^-$ decay but forbids the 0ν $\beta^-\beta^-$ decay.

With the discovery that the weak interaction violates the conservation of parity maximally, it became apparent that the Dirac or Majorana character of the electron neutrino was still in question. This can be explained as follows. In the β^- decay

$$n \rightarrow p + e^- + \overline{\nu}_{eR} \tag{1.7}$$

$$\nu_{eL} + n \rightarrow p + e^- \tag{1.8}$$

the $\overline{\nu}_e$ is right-handed and ν_e is left-handed . Thus, even if neutrino is a massless Majorana particle

$$
\begin{aligned}
2n &\rightarrow n + p + e^- + \overline{\nu}_{eR} \\
&= n + p + e^- + \nu_{eR} \\
&\nrightarrow 2p + 2e^-
\end{aligned} \tag{1.9}
$$

because the first neutrino has the wrong helicity for absorption on a neutron. Hence, the absence of $0\nu\beta^-\beta^-$ decay implies neither a Dirac electron neutrino nor a conserved lepton number L.

Following 1957, there was a marked decline in interest for the study of $\beta\beta$ decay. The requirement that both lepton number conservation and the γ_5-invariance of the weak current had to be violated for the $0\nu\beta^-\beta^-$ decay to occur discouraged experimental searches. Later on, it was conjectured theoretically that 0ν $\beta\beta$ decay is expected to proceed mainly via the small admixtures of right handed currents in the predominantly left handed Lagrangian [Primakoff and Rosen (1961), (1969)] and consequently, the experimental activity was resumed in the 1960's.

1.3 Nuclear structure aspect of $\beta^-\beta^-$ decay

The nuclear $\beta\beta$ decay in general and $0\nu\beta^-\beta^-$ decay in particular is a convenient tool to test physics beyond the SM. With the development of modern gauge theories at the beginning of 1970's, Doi *et al.* [(1981), (1982), (1983), (1985)] suggested that the study of $0\nu\beta^-\beta^-$ decay rate has the following important ramifications vis-a-vis constraints on parameters of various gauge field theories beyond the SM, namely (i) lepton number

conservation, (ii) mass and charge conjugation properties of electron neutrino and (iii) possible right handed admixtures in the weak leptonic current.

The $0\nu\beta^-\beta^-$ decay has not been observed so far. Hence, the models predict the half-lives assuming certain value for the neutrino mass or conversely extract various gauge parameters from the observed half-life limits of the $0\nu\beta^-\beta^-$ decay. The reliability of predictions can be judged a priori only from the success of a nuclear model in explaining various observed physical properties of nuclei. The common practice is to calculate the $M_{2\nu}$ to start with, and compare them with the experimentally observed value as the two decay modes involve the same set of initial and final nuclear wave functions. However, the structure of operators are completely different for $2\nu\beta^-\beta^-$ and $0\nu\beta^-\beta^-$ decay. In the case of the former, the 1^+ states play an important role and in the case of the latter, all possible states contribute due to the appearance of neutrino potential in nuclear transition operators.

The $2\nu\beta^-\beta^-$ decay is a second order process of weak interaction and conserves the lepton number exactly. Hence, it is allowed in the SM. The inverse half-life of the $2\nu\beta^-\beta^-$ decay for the $0^+ \rightarrow 0^+$ transition is given by

$$\left[T^{2\nu}_{1/2}(0^+ \rightarrow 0^+)\right]^{-1} = G_{2\nu} \left|M_{2\nu}\right|^2 \tag{1.10}$$

where the integrated kinematical factor $G_{2\nu}$ can be calculated with good accuracy and the nuclear transition matrix element (NTME) $M_{2\nu}$ is nuclear model dependent. The half-life of $2\nu\beta^-\beta^-$ decay for the $0^+ \rightarrow 0^+$ transition has been already measured for 11 nuclei, namely ^{48}Ca, ^{76}Ge, ^{82}Se, ^{96}Zr, ^{100}Mo, ^{116}Cd, ^{128,130}Te, ^{136}Xe, ^{150}Nd and ^{238}U, out of 35 possible candidates (Table 1.2). Hence, the values of NTMEs $M_{2\nu}$ can be extracted

directly. Consequently, the validity of different models employed for nuclear structure calculations can be tested by calculating $M_{2\nu}$.

Over the past few years, several nuclear models have been employed to calculate the $2\nu\beta^-\beta^-$ and $0\nu\beta^-\beta^-$ decay rates in two-nucleon (2n) mechanism. They can be broadly classified into three types, namely shell model and its variants, quasiparticle random phase approximation (QRPA) and its extensions and alternative models. The details about these models have been discussed by Suhonen *et al.* (1998) and Faessler *et al.* (1998). For the sake of completeness, we briefly discuss below the relative applicability, success and failure of various models used so far to study the $\beta\beta$ decay process.

1.3.1 Shell model and its variants

The shell model is the best choice for the calculation of the $M_{2\nu}$. Haxton *et al.* (1984) and Vergados (1976) have studied the $\beta\beta$ decay of ^{76}Ge, ^{82}Se and ^{128,130}Te nuclei in weak coupling limit. The large scale shell model calculations by Skouras *et al.* (1983), Zhao *et al.* [(1990), (1993)] and Strassbourg-Madrid collaboration [(1990), (1995)] are more promising in nature. The calculations by Caurier *et al.* are more realistic in nature in which the $M_{2\nu}$ of ^{82}Se is calculated exactly and those of ^{76}Ge and ^{136}Xe are dealt in a nearly exact manner [Caurier *et al.* (1996)]. The conventional shell model and Monte-Carlo shell model (MCSM) [Koonin *et al.* (1997) and Radha *et al.* (1996)] have been tested against each other for the case of ^{48}Ca in complete pf-shell and ^{76}Ge in upper fpg-shell and the agreement is interestingly good. It is expected that the MCSM could be a good alternative to conventional shell model calculations in near future. The NTMEs $M^{(0\nu)}$ of $0\nu\beta^-\beta^-$ decay of ^{128,130}Te are calculated by Haxton *et al.* (1984) and Caurier *et al.* (1999) in

weak coupling shell model (WCSM). Sen'kov and Horoi (2014) have investigated a novel method for accurate calculation of $M^{(0\nu)}$ for ^{76}Ge. The NTMEs $M^{(0\nu)}$ of ^{48}Ca, ^{76}Ge, ^{82}Se, ^{124}Sn, ^{128,130}Te and ^{136}Xe have been calculated in interacting shell model (ISM) by Caurier *et al.* (2008) and Menéndez *et al.* (2008). Recently Menéndez *et al.* (2018) have calculated NTMEs due to light Majorana neutrino exchange $M^{(0\nu)}$ as well as heavy Majorana neutrino exchange $M^{(0N)}$ for $0\nu\beta^-\beta^-$ of ^{48}Ca, ^{76}Ge, ^{82}Se, ^{124}Sn, ^{130}Te and ^{136}Xe nuclei in shell model.

1.3.2 QRPA and their extensions

The QRPA has been used to study various excitations in even Z-even N nuclei [Baranger (1960)]. This formalism has been applied to study the role of proton-neutron modes in the Gamow-Teller beta decay [Halbleib *et al.* (1967)]. Vogel and Zirnbauer were the first to provide an understanding of the observed suppression of $M_{2\nu}$ in the QRPA model [Vogel and Zirnbauer (1986)]. It was observed that the quenching of $M_{2\nu}$ can be achieved by a proper inclusion of ground state correlations through the particle-particle interaction in the S=1, T=0 channel and the calculated half-lives are in close agreement with all the experimental data.

The QRPA frequently overestimates the ground state correlations as a result of an increase in the strength of attractive p-n interaction leading to the collapse of QRPA solutions. The physical value of this force is usually close to the point at which the QRPA solutions collapse. To cure the strong suppression of $M_{2\nu}$, several extensions of QRPA have been proposed. The most important extensions are full QRPA [Cheoun *et al.* (1993), (1995)], renormalized QRPA (RQRPA) or full RQRPA [Toivanen *et al.* (1995),

(1997), Schwieger *et al.* (1996), (1997)], higher QRPA [Raduta *et al.* (1991), Stoica *et al.* (1993), (1994), (1995) and (1996), Sambataro *et al.* (1997)], MCM [Suhonen *et al.* (1993), Civitarese *et al.* (1994)] and particle number projection [Civitarese *et al.* (1990) and (1991), Krmpotic *et al.* (1993), Suhonen (1993), Suhonen *et al.* (1992)]. However, none of the above methods is free from ambiguities [Faessler (1999)]. Altogether QRPA and their various extensions with the ability to adjust one free parameter are able to explain the observed $2\nu\beta^-\beta^-$ decay rate.

In case of $0\nu\beta^-\beta^-$ decay, the NTMEs $M^{(0\nu)}$ are calculated in QRPA [Engel *et al.* (1988), Muto *et al.* (1989), Tomoda (1991), Pantis *et al.* (1994), (1996), Suhonen *et al.* (1994), (2002), Barbero *et al.* (1999), Civitarese *et al.* (2003)] and its extensions, namely SRPA [Stoica *et al.* (2001), RQRPA [Simkovic *et al.* (1997), Faessler *et al.* (1998), Simkovic *et al.* (2001), Stoica *et al.* (2001)], pnQRPA [Civitarese and Suhonen (2009), Hyvarinen and Suhonen (2015)], QRPA with isospin restoration [Simkovic *et al.* (2013)], deformed QRPA [Fang *et al.* (2010), (2011), Faessler *et al.* (2012), Mustonen *et al.* (2013)] and deformed QRPA with isospin restoration [Fang *et al.* (2018)]. The NTMEs $M^{(0N)}$ have been calculated only in QRPA [Tomoda (1991), Hirsch *et al.* (1996) and Pantis *et al.* (1996)], pnQRPA [Hyvarinen and Suhonen (2015)] and RQRPA [Simkovic *et al.* (2010)].

1.3.3 Alternative models

The shell model and the QRPA model besides having their own limitations fail to fulfil the Ikeda sum rule. The small predictive power of QRPA and their extensions is the main motivation for us to seek an alternative description which might result in a more reliable approach for the study of nuclear $\beta\beta$ decay processes. Under alternative models,

the operator expansion method (OEM) [Ching *et al.* (1989), Simkovic (1989), Engel *et al.* (1992), Wu *et al.* (1991) and (1992), Hirsch *et al.* (1993), Muto (1993), Simkovic (1998)], the broken SU(4) symmetry [Bernabeu *et al.* (1990), Vladimirov *et al.* (1992), Moe and Vogel (1994) and Rumyantsev *et al.* (1995)], group theoretical studies in SU(2) [Hirsch *et al.* (1996)], SO(5) [Hirsch *et al.* (1997)], O(8) [Engel *et al.* (1997)] and the pseudo SU(3) [Hirsch *et al.* (1994), (1995)], two-vacua RPA (TVRPA) [Simkovic *et al.* (1994) and Teneva *et al.* (1995)], the single state dominance hypothesis (SSDH) [Ejiri *et al.* (1996), Civitarese *et al.* (1998) and (1999)], energy density functional (EDF) theory [Rodríguez *et al.* (2010), Vaquero *et al.* (2013)], interacting boson model (IBM) [Barea and Iachello (2009), Barea *et al.* (2012)], IBM2 [Iachello *et al.* (2011), Barea *et al.* (2013)], IBM2 with isospin restoration [Barea *et al.* (2015)], covariant density functional theory (CDFT) [Yao *et al.* (2015), Song *et al.* (2017)], and Projected Hartree-Fock-Bogoliubov (PHFB) method [Tomoda *et al.* (1985) and (1986)] have their own problems.

1.4 Experimental search for $\beta^-\beta^-$ decay

The experimental aspects of $0\nu\beta^-\beta^-$ decay has been reviewed over the years to update its experimental status [Barabash *et al.* (2018), Dell'Oro *et al.* (2015) and references there in]. In Table 1.2, we have compiled all the experimentally measured half-life limits of $0\nu\beta^-\beta^-$decay for the $0^+ \rightarrow 0^+$ transition. As discussed earlier that $0\nu\beta^-\beta^-$ decay has not been experimentally observed till date and aim of all the present experimental activities is to observe this particular decay mode. A few of the promising experimental projects running world wide are discussed in the below.

The Cryogenic Underground Observatory for Rare Events (CUORE) consist of one tower (CUORE-0) which containing a 52 TeO_2 crystals of total mass 39 kg. The obtained sensitivity of ^{130}Te in 2015 after 2 year of data collection is $T^{0\nu}_{1/2} > 2.7 \times 10^{24}$ yr (90% C.L.). Combined with the data of prototype Cuoricino it is $T^{0\nu}_{1/2} > 4 \times 10^{24}$ yr (90% C.L.) [Artusa *et al.* (2014a)]. Meanwhile, CUORE detector array has been completed by putting tower of 19 CUORE-0 with a total mass of 988 kg. After cooling down and commissioning, data acquisition is scheduled to start in the first quarter of 2017 [Domizio (2016)]. The designed sensitivity after a 5 year run will be $T^{0\nu}_{1/2} > 9.5 \times 10^{25}$ yr (90% C.L.) [Artusa *et al.* (2014b)]. The energy resolution is good for Ge diode which is about 0.2%. Thus, the GERmanium Detector Array (GERDA) used a high purity germanium detectors which are enriched in ^{76}Ge at (86-88)%. The efficiencies of the detectors are again high that is 62-66%. Between the year 2011 to 2013 the Phase I of GERDA was initiated and GERDA obtained a half-life limit of ^{76}Ge is $T^{0\nu}_{1/2} > 2.1 \times 10^{25}$ yr (90% C.L.) [Agostini *et al.* (2013)]. In December 2015, the Phase II was initiated and obtained a half-life limit of $T^{0\nu}_{1/2} > 5.4 \times 10^{25}$ yr (90% C.L.) [Agostini *et al.* (2017)]. In Phase I (2011-2012) of the KamLAND-Zen (KAmioka Liquid Scintillator Anti-Neutrino Detector) experiment, xenon enriched in ^{136}Xe at 91% was used. This experiment deduced a half-life limit of $T^{0\nu}_{1/2} > 1.9 \times 10^{25}$ yr (90% C.L.) for ^{136}Xe with an exposure of 89.5 kg.yr [Gando *et al.* (2013)]. In the Phase II (2013-2016) 504 kg.yr of data were collected. This led to a half-life limit of $T^{0\nu}_{1/2} > 9.2 \times 10^{25}$ yr (90% C.L.). By combining both results, the $T^{0\nu}_{1/2}$ limit becomes $> 1.1 \times 10^{26}$ yr (90% C.L.) [Gando *et al.* (2016)]. These are the best limits achieved in the field so far. The Enriched Xenon Observatory (EXO) experiment uses a liquid xenon (LXe) enriched in ^{136}Xe at 81% as source. Phase I (2011-2014) of EXO-200

reached a high detector efficiency of 85% and based on 100 kg.yr of collected data, a half-life limit $T^{0\nu}_{1/2} > 1.1 \times 10^{25}$ yr (90% C.L.) was deduced for ^{136}Xe while in phase II (first quarter of 2016), they reached to the energy resolution of 3%. The goal sensitivity after a 3 yr run will be $T^{0\nu}_{1/2} > 5.7 \times 10^{26}$ yr (90% C.L.) [Yen (2016)]. The SuperNEMO demonstrator is based on the design principles of the NEMO-3 tracking calorimeter. In 2016, two calorimeter walls were installed, commissioning of the trackers is planned in the 1st quarter of 2017 [Waters (2016)]. 7 kg of ^{82}Se are planned to be used, but also other isotopes will be considered. If successful, 20 demonstrator modules might be installed afterwards in the framework of SuperNEMO. The goal sensitivity after a 5 yr operation would be $T^{0\nu}_{1/2} > 1 \times 10^{26}$ yr (90% C.L.). Other experiments and R&D projects are in the pipeline.

1.5 Objective of the thesis

In $\beta\beta$ decay, the total angular momentum of four s-wave leptons can be 0, 1 or 2 and is equal to the total angular momentum transferred from the nucleus. The lowest 1^+ state in the final nucleus of any $\beta\beta$ decay candidate lies much higher than the first excited 2^+ state, hence the $0^+ \rightarrow 1^+$ transition are much less probable than the $0^+ \rightarrow 0^+$ and the $0^+ \rightarrow 2^+$ transition. The $0^+ \rightarrow 2^+$ transition is not observed experimentally so far. Hence, our aim is to study the $0\nu\beta^-\beta^-$ decay processes for the $0^+ \rightarrow 0^+$ transition. The $0\nu\beta^-\beta^-$ decay is possible in a number of gauge field theoretical models violating the conservation of the lepton number L. Further, there are different mechanisms inducing the $0\nu\beta^-\beta^-$ decay even in a particular gauge theoretical model. The consideration of all these aspects

will be interesting only after the experimental observation of $0\nu\beta^-\beta^-$ decay. Presently, we restrict our study to the occurrence of $0\nu\beta^-\beta^-$ decay in left-right symmetric GUT and extract limits on the effective mass of light as well as heavy Majorana neutrinos from the observed limits on the half-lives $T^{0\nu}_{1/2}$ of $0\nu\beta^-\beta^-$ decay.

All the nuclei undergoing $\beta\beta$ decay are even-even type, in which the pairing degrees of freedom play an important role. Moreover, it has been already conjectured that the deformation can play a crucial role in case of 2ν $\beta\beta$ decay of ^{100}Mo and ^{150}Nd [Suhonen *et al.* (1994), Griffiths *et al.* (1992)]. Hence, it is desirable to have a model which incorporates the pairing and deformation degrees of freedom on equal footing in its formalism. For this purpose, the PHFB model is one of the most natural choices. There exists an inverse correlation between the Gamow-Teller strength and quadrupole moment [Aurbeck *et al.* (1993), Troltenier *et al.* (1996)]. It is well known that the pairing part of the two body interaction is responsible for the reduction of collectivity where as the quadrupole-quadrupole (QQ) interaction enhances the collectivity in the nuclear intrinsic wave functions. In other words, the pairing interaction is responsible for the sphericity of the nucleus where as the QQ interaction makes the nucleus deformed. Hence, to examine the explicit role of deformation degrees of freedom vis-à-vis the suppression, the pairing plus quadrupole-quadrupole interaction (PQQ) [Baranger *et al.* (1968)] will be the most appropriate choice.

The PHFB model in conjunction with PQQ interaction has been applied successfully to calculate the $2\nu\beta^-\beta^-$ decay of nuclei along with spectroscopic properties in the mass range $A = 90 - 150$ and it has been shown that the deformations of the intrinsic ground states play a crucial role in reproducing a realistic $M_{2\nu}$ [Dixit *et al.* (2002), Chandra *et*

al. (2005), Singh *et al.* (2007)]. The $0^+ \rightarrow 2^+$ transition of $2\nu\beta^-\beta^-$ decay has also been studied in the same PHFB model [Chaturvedi *et al.* (2003), Singh *et al.* (2005), Singh *et al.* (2017)]. Using a pairing plus multipole type of effective two-body interaction, the $0\nu\beta^-\beta^-$ decay [Chandra *et al.* (2009), Rath *et al.* (2010), Rath *et al.* (2013)], in mass mechanism [Chaturvedi *et al.* (2008)], due to exchange of heavy Majorana neutrino [Rath *et al.* (2012)], Majoron accompanied $0\nu\beta^-\beta^-$ decay [Rath *et al.* (2013), (2016)] and $0\nu\beta^-\beta^-$ decay involving light Majorana neutrino mass and right-handed current [Singh *et al.* (2019)] have been also successfully studied in the PHFB model. The above works show the wide applicability of the PHFB model. In the above work the single particle energies used were same for all the nuclei involved in the study of $\beta^-\beta^-$ decay which were taken from Vergados *et al.* (1971). The success of PHFB model in the study of $\beta^-\beta^-$ decay has motivated us to apply the PHFB model by using the single particle energies derived from the Woods-Saxon potential as most of the present nuclear models are using Woods-Saxon single particle energies.

To be specific, our aim is to study $0\nu\beta^-\beta^-$ decay for the $0^+ \rightarrow 0^+$ transition in the mass range $A = 90 - 150$ for some potential candidates namely for ^{94,96}Zr, ^{100}Mo, ^{110}Pd, ^{128,130}Te and ^{150}Nd not in isolation but together with other observed nuclear phenomena in the PHFB formalism using the single particle energies derived from the Woods-Saxon potential. The ^{116}Sn and ^{136}Xe are the other two $\beta\beta$ emitters occurring in the sdgh shell in which $2\nu\beta^-\beta^-$ decay is already observed. We have not attempted to study the $0\nu\beta^-\beta^-$ decay of ^{116}Sn and ^{136}Xe as these nuclei can not be properly treated in the PHFB model. In Chapter 2, we have calculated the yrast spectra, reduced transition probabilities $B(E2{:}0^+ \rightarrow 2^+)$, deformation parameters β_2 and the gyromagnetic factors

$g(2^+)$ of ^{94,96}Zr, ^{94,96,100}Mo, ^{100,104}Ru, ^{104,110}Pd, ^{110}Cd, ^{128,130}Te, ^{128,130}Xe, ^{150}Nd and ^{150}Sm participating in the $0\nu\beta^-\beta^-$ decay and compared with the available experimental data as a test of the reliability of the wave functions. Subsequently, the PHFB wave functions are employed to study $2\nu\beta^-\beta^-$ decay of the above mentioned nuclei for the $0^+ \rightarrow 0^+$ transition and compared the theoretically calculated NTMEs $M_{2\nu}$ with the experimental values as a further test of reliability in Chapter 3. In Chapter 4, we have studied the $0\nu\beta^-\beta^-$ decay of above nuclei for the $0^+ \rightarrow 0^+$ transition and extracted the limits on light and heavy neutrino masses. Further, the role of deformation on NTMEs $M^{(0\nu)}$ and $M^{(0N)}$ is studied. A brief discussion on uncertainty in NTMEs is also presented. We discuss a number of necessary improvements to be incorporated in the PHFB model for a more reliable study of the $\beta\beta$ decay in Chapter 5.

Table 1.1: List of 35 naturally occuring $\beta^-\beta^-$ emitters along with $Q_{\beta\beta}$ for the $0^+ \rightarrow 0^+$ transition, natural abundance of the parent isotope (P) [Wapstra and Audi (1985), Lederer and Shirley (1978)] and deformation parameter β_2 [Raman *et al.* (2001)].

Nuclear	$Q_{\beta\beta}$	$P(\%)$	β_2	
Transition	(keV)		Parent	Daughter
$^{46}_{20}$Ca$\rightarrow^{46}_{22}$Ti	987.0±4.0	0.0035	0.153±0.005	0.317±0.008
$^{48}_{20}$Ca$\rightarrow^{48}_{22}$Ti	**4271.0±4.0**	0.187	0.106±0.018	0.269±0.007
$^{70}_{30}$Zn$\rightarrow^{70}_{32}$Ge	1001.0±3.0	0.62	0.228±0.010	0.2245±0.0026
$^{76}_{32}$Ge$\rightarrow^{76}_{34}$Se	**2039.6±0.9**	7.8	0.2623±0.0039	0.3090±0.0033
$^{80}_{34}$Se$\rightarrow^{80}_{36}$Kr	130.0±9.0	**49.8**	0.2318±0.0027	0.265±0.008
$^{82}_{34}$Se$\rightarrow^{82}_{36}$Kr	**2995.0±6.0**	9.2	0.1934±0.0027	0.2021±0.0045
$^{86}_{36}$Kr$\rightarrow^{86}_{38}$Sr	1256.0±5.0	17.3	0.145±0.006	0.140±0.008
$^{94}_{40}$Zr$\rightarrow^{94}_{42}$Mo	1145.3±2.5	17.4	0.090±0.010	0.1509±0.0015
$^{96}_{40}$Zr$\rightarrow^{96}_{42}$Mo	**3350.0±3.0**	2.8	0.080±0.017	0.1720±0.0016
$^{98}_{42}$Mo$\rightarrow^{98}_{44}$Ru	112.0±7.0	**24.1**	0.1683±0.0028	0.1947±0.0030
$^{100}_{42}$Mo$\rightarrow^{100}_{44}$Ru	**3034.0±6.0**	9.6	0.2309±0.0022	0.2148±0.0011
$^{104}_{44}$Ru$\rightarrow^{104}_{46}$Pd	1299.0±4.0	18.7	0.2707±0.0020	0.209±0.007
$^{110}_{46}$Pd$\rightarrow^{110}_{48}$Cd	**2013.0±19.0**	11.8	0.257±0.006	0.1770±0.0039
$^{114}_{48}$Cd$\rightarrow^{114}_{50}$Sn	534.0±4.0	**28.7**	0.1903±0.0035	0.121±0.013
$^{116}_{48}$Cd$\rightarrow^{116}_{50}$Sn	**2802.0±4.0**	7.5	0.1906±0.0034	0.1118±0.0016
$^{122}_{50}$Sn$\rightarrow^{122}_{52}$Te	364.0±4.0	4.56	0.1036±0.0011	0.1847±0.0008
$^{124}_{50}$Sn$\rightarrow^{124}_{52}$Te	**2288.1±1.6**	5.64	0.0953±0.0011	0.1695±0.0009

Table 1.1 continued

Nuclear Transition	$Q_{\beta\beta}$ (keV)	P(%)	β_2	
			Parent	Daughter
$^{128}_{52}$Te→$^{128}_{54}$Xe	868.0±4.0	**31.7**	0.1363±0.0011	0.1836±0.0049
$^{130}_{52}$Te→$^{130}_{54}$Xe	**2533.0±4.0**	**34.5**	0.1184±0.0014	0.169±0.007
$^{134}_{54}$Xe→$^{134}_{56}$Ba	847.0±10.0	10.4	0.119±0.011	0.1609±0.0009
$^{136}_{54}$Xe→$^{136}_{56}$Ba	**2479.0±8.0**	8.9	0.122±0.010	0.1258±0.0012
$^{142}_{58}$Ce→$^{142}_{60}$Nd	1417.6±2.5	11.1	0.1277±0.0008	0.0917±0.0010
$^{146}_{60}$Nd→$^{146}_{62}$Sm	56.0±5.0	17.2	0.1524±0.0025	-
$^{148}_{60}$Nd→$^{148}_{62}$Sm	1928.3±1.9	5.7	0.2013±0.0037	0.1423±0.0030
$^{150}_{60}$Nd→$^{150}_{62}$Sm	**3367.1±2.2**	5.6	0.2853±0.0021	0.1931±0.0021
$^{154}_{62}$Sm→$^{154}_{64}$Gd	1251.9±1.5	**22.6**	0.3410±0.0020	0.3120±0.0028
$^{160}_{64}$Gd→$^{160}_{66}$Dy	1729.5±1.4	**21.8**	0.3534±0.0020	0.3387±0.0036
$^{170}_{68}$Er→$^{170}_{70}$Yb	653.9±1.6	14.9	0.3363±0.0029	0.3258±0.0037
$^{176}_{70}$Yb→$^{176}_{72}$Hf	1078.8±2.7	12.6	0.305±0.005	0.2953±0.0028
$^{186}_{74}$W→$^{186}_{76}$Os	490.3±2.2	**28.6**	0.2257±0.0039	0.2000±0.0034
$^{192}_{76}$Os→$^{192}_{78}$Pt	417.0±4.0	**41.0**	0.1667±0.0012	0.1532±0.0016
$^{198}_{78}$Pt→$^{198}_{80}$Hg	1048.0±4.0	7.2	0.1141±0.0006	0.1065±0.0006
$^{204}_{80}$Hg→$^{204}_{82}$Pb	416.5±1.9	6.9	0.0686±0.0006	0.0412±0.0005
$^{232}_{90}$Th→$^{232}_{92}$U	858.0±6.0	**100**	0.2608±0.0014	0.264±0.013
$^{238}_{92}$U→$^{238}_{94}$Pu	1145.8±1.7	**99.275**	0.2863±0.0024	0.2861±0.0019

Table 1.2: Experimental half-life limits $T^{0\nu}_{1/2}$ of $0\nu\beta^-\beta^-$ decay of A = 48, 76, 82, 94, 96, 98, 100, 116, 128, 130, 136, 150 and 238 nuclei for the $0^+ \rightarrow 0^+$ transition.

Transition	$T^{0\nu}_{1/2}$ (yr)	C.L.(%)	Project	Reference
^{48}Ca→^{48}Ti	>1.3 × 10^{22}	90	NEMO 3	[Barabash *et al.*(2011)]
	>2.7×10^{22}	90	GSS+GSE+RCNS	[Umehara *et al.* (2008)]
	≥1.4×10^{22}	90	ELEGANT VI	[Ogawa *et al.* (2004)]
	>1.5×10^{21}	90	TGV	[Brudanin *et al.* (2000)]
	>9.5×10^{21}	76	HEP Beijing	[You *et al.* (1991)]
	>2.0×10^{21}	80		[Bardin *et al.* (1970)]
^{76}Ge→^{76}Se	>9.0×10^{25}	90	GERDA-II	[Agostini *et al.* (2019)]
	>8.0×10^{25}	90	GERDA	[Agostini *et al.* (2018)]
	>1.9×10^{25}	90	MAJORANA	[Aalseth *et al.* (2018)]
	>3.0×10^{25}	90	GERDA	[Agostini *et al.* (2013)]
	>1.57×10^{25}	90	IGEX	[Aalseth *et al.* (2002)]
	>1.9×10^{25}	90	HM	[Klapdor *et al.* (2001)]
	>1.6×10^{25}	90	IGEX	[Gonzalez *et al.* (2000)]
	>1.6×10^{25}	90	HM	[Baudis *et al.* (1999)]
	>1.2×10^{25}	90	MPIH+KIAE	[Morales (1999)]
	>1.1×10^{25}	90	HM	[Baudis *et al.* (1997)]
	>7.4×10^{24}	90	HM	[Gunther *et al.* (1997)]
	>5.6×10^{24}	90	HM	[Balysh *et al.* (1995)]
	>1.4×10^{24}	90	HM	[Balysh *et al.* (1992)]
	>2.5×10^{23}	68	UC+LBL	[Caldwell *et al.* (1986)]
	>1.0×10^{23}	68	PNL+USC	[Avignone *et al.* (1985)]
	>2.0×10^{22}	68		[Forster *et al.* (1984)]
	>1.2×10^{23}	68		[Bellotti *et al.* (1984)]
	>3.0×10^{22}	68		[Simpson *et al.* (1984)]
	>4.0×10^{21}	68		[Leccia *et al.* (1983)]

Table 1.2 continued

Transition	$T^{0\nu}_{1/2}$ (yr)	C.L.(%)	Project	Reference
^{82}Se$\rightarrow^{82}$Kr	$>2.4\times10^{24}$	90	CUPID-0	[Azzolini *et al.* (2018)]
	$>1.0\times10^{23}$	90	NEMO 3	[Arnold *et al.* (2005)]
	$>1.9\times10^{23}$	90	NEMO 3	[Lalanne (2005)]
	$\geq9.5\times10^{21}$	90	NEMO 2	[Arnold *et al.* (1998)]
	$>5.0\times10^{21}$	90	NEMO 2	[Barabash *et al.* (1998)]
	$>2.7\times10^{22}$	68	UC Irvine	[Elliott *et al.* (1992)]
	$>1.8\times10^{22}$			[Moe *et al.* (1988)]
^{94}Zr$\rightarrow^{94}$Mo	$>1.9\times10^{19}$	90	NEMO 2	[Arnold *et al.* (1999)]
^{96}Zr$\rightarrow^{96}$Mo	$>9.2\times10^{21}$	90	NEMO 3	[Barabash *et al.* (2011)]
	$>9.2\times10^{21}$	90	NEMO 3	[Argyriades *et al.* (2010)]
	$>1.0\times10^{21}$	90	NEMO 2	[Arnold *et al.* (1999)]
	$>8.0\times10^{20}$	90	NEMO 2	[Barabash *et al.* (1998)]
^{98}Mo$\rightarrow^{98}$Ru	$>1.0\times10^{14}$			[Fremlin *et al.* (1952)]
^{100}Mo$\rightarrow^{100}$Ru	$>1.1\times10^{24}$	90	NEMO 3	[Arnold *et al.* (2015)]
	$>4.6\times10^{23}$	90	NEMO 3	[Arnold *et al.* (2005)]
	$>3.5\times10^{23}$	90	NEMO 3	[Lalanne (2005)]
	$>5.5\times10^{22}$	90	ELEGANT V	[Ejiri *et al.* (2001)]
	$>4.9\times10^{21}$	90	ITEP+INFN	[Ashitkov *et al.* (2001)]
	$>2.2\times10^{22}$	90	ELEGANT V	[Kudomi *et al.* (2000)]
	$>2.3\times10^{21}$	90	ITEP+INFN	[Ashitkov *et al.* (1999)]
	$>5.2\times10^{22}$	68	ELEGANT V	[Kudomi *et al.* (1998)]
	$>2.2\times10^{22}$	68	LBL+UNM	[Garnjost *et al.* (1997)]
	$>1.23\times10^{23}$	90	UC Irvine	[De Silva *et al.* (1997]
	$>5.2\times10^{22}$	68	ELEGANT V	[Ejiri *et al.* (1996)]

Table 1.2 continued

Transition	$T^{0\nu}_{1/2}$ (yr)	C.L.(%)	Project	Reference
	$>6.4\times10^{21}$	90	NEMO 2	[Dassie *et al.* (1995)]
	$>4.4\times10^{22}$	68	LBL+UNM	[Garnjost *et al.* (1993)]
	$>4.7\times10^{21}$	68	ELEGANT V	[Ejiri *et al.* (1991)]
	$>7.1\times10^{20}$	68	INS Baksan	[Vasilev *et al.* (1990)]
	$>4.0\times10^{21}$	68	LBL+UNM	[Garnjost *et al.* (1989)]
	$>1.0\times10^{19}$	68	UC Irvine	[Elliott *et al.* (1987)]
^{116}Cd$\rightarrow^{116}$Sn	$>7.0\times10^{22}$	90	INR+INFN	[Danevich *et al.* (2000)]
	$>3.2\times10^{22}$	90	INR+INFN	[Danevich *et al.* (1999)]
	$>5.0\times10^{21}$	90	NEMO 2	[Arnold *et al.* (1996)]
	$>2.9\times10^{22}$	90	INR	[Danevich *et al.* (1995)]
	$>2.9\times10^{21}$	90	Osaka	[Ejiri *et al.* (1995)]
	$>5.4\times10^{21}$	68		[Kume *et al.* (1994)]
	$>2.6\times10^{18}$	90	ITEP+INFN	[Pipke *et al.* (1994)]
^{128}Te$\rightarrow^{128}$Xe	$>1.1\times10^{23}$	90	INFN+LNGS	[Arnaboldi *et al.* (2003)]
	$>8.6\times10^{22}$	90	INFN+LNGS	[Allessandrello *et al.* (2000)]
	$>7.7\times10^{24}$		Geochemical	[Bernatowicz *et al.* (1993)]
^{130}Te$\rightarrow^{130}$Xe	$>1.5\times10^{25}$	90	CUORE	[Alduino *et al.* (2018)]
	$>4.0\times10^{24}$	90	CUORE-0	[Alduino *et al.* (2016)]
	$>7.0\times10^{20}$	90	NEMO 3	[Arnold *et al.*(2015)]
	$>1.8\times10^{24}$	90	CUORICINO	[Arnaboldi *et al.* (2005)]
	$>5.5\times10^{23}$	90	CUORICINO	[Arnaboldi *et al.* (2004)]
	$>2.1\times10^{23}$	90	INFN+LNGS	[Arnaboldi *et al.* (2003)]
	$>1.4\times10^{23}$	90	INFN+LNGS	[Allessandrello *et al.* (2000)]
	$>7.7\times10^{22}$	90	Milano	[Morales (1999)]
	$>5.6\times10^{22}$	90	INFN+LNGS	[Allessandrello *et al.* (1998)]

Table 1.2 continued

Transition	$T^{0\nu}_{1/2}$ (yr)	C.L.(%)	Project	Reference
^{136}Xe$\rightarrow^{136}$Ba	$>2.1\times10^{23}$	90	PANDAX-II	[Kaixiang *et al.* (2019)]
	$>1.8\times10^{25}$	90	EXO-200	[Albert *et al.* (2018)]
	$>1.07\times10^{26}$	90	KamLAND-Zen	[Gando *et al.* (2016)]
	$>1.1\times10^{25}$		EXO-200	[Albert *et al.* (2014)]
	$>1.6\times10^{25}$	90	EXO	[Auger *et al.* (2012)]
	$>2.6\times10^{24}$	90	KamLAND-Zen	[Gando *et al.* (2012)]
	$>1.2\times10^{24}$	90	INFN	[Bernabei *et al.* (2002)]
	$>4.4\times10^{23}$	90	Caltech+PSI+UN	[Luescher *et al.* (1998)]
	$>4.2\times10^{23}$		Gotthard tunnel	[Busto *et al.* (1996)]
	$>2.6\times10^{23}$	90	Gotthard tunnel	[Vuilleumier *et al.* (1993)]
	$>3.0\times10^{21}$	68	ITEP+INR	[Barabash *et al.* (1989)]
	$>1.0\times10^{21}$	90	Milano+INFN	[Alessandrello *et al.* (1988)]
	$>2.0\times10^{21}$	68		[Barabanov *et al.* (1986)]
^{150}Nd$\rightarrow^{150}$Sm	$>2.0\times10^{22}$	90	NEMO-3	[Arnold *et al.* (2016)]
	$>1.8\times10^{22}$	90	NEMO 3	[Barabash *et al.*(2011)]
	$>1.8\times10^{22}$	90	NEMO-3	[Argyriades *et al.* (2009)]
	$>1.2\times10^{21}$	90	UC Irvine	[De Silva *et al.* (1997]
	$>2.1\times10^{20}$	90	ITEP +INR	[Artemiev *et al.* (1995)]
	$>2.1\times10^{21}$			[Moe *et al.* (1994)]
	$>1.7\times10^{21}$		INR	[Klimenko *et al.* (1986)]
^{238}U$\rightarrow^{238}$Pu	$>1.0\times10^{12}$	68	INR	[Tretyak *et al.* (2005)]

Chapter 2

Spectroscopic properties of some nuclei in mass range $A = 90 - 150$ participating in $\beta^-\beta^-$ decay

The $2\nu\beta^-\beta^-$ as well as $0\nu\beta^-\beta^-$ decay of potential nuclei in the mass range $A = 90 - 150$ have been already studied successfully in the PHFB model using four different parametrizations of pairing plus mutipolar effective two-body interaction. The study of single beta decay rates and the distribution of Gamow-Teller strength has implications in the understanding of the role of the isoscalar part of the proton-neutron interaction. However, it is not possible to study these processes in the present version of the PHFB model. This is a serious draw back in the present formalism of the PHFB model. We will attempt to remove this draw back in the future studies.

Our aim is to calculate the NTMEs for $0\nu\beta^-\beta^-$ decay of ^{94,96}Zr, ^{100}Mo, ^{104}Ru, ^{110}Pd, ^{128,130}Te and ^{150}Nd isotopes for the $0^+ \rightarrow 0^+$ transition. Prior to the calculation of

NTMEs, we test the reliability of wave functions by calculating the spectroscopic properties, namely sub-shell occupation numbers, yrast spectra, reduced $B(E2{:}0^+ \rightarrow 2^+)$ transition probabilities, deformation parameter β_2 and g-factors $g(2^+)$ of the nuclei in mass range $A = 90 - 150$ participating in $\beta^-\beta^-$ decay and comparing them with the available experimental results. In the present study, we use the single particle energies for all parent and daugther nuclei participating in $\beta^-\beta^-$ decay derived from Woods-Saxon potential.

The present chapter is organized in the following Sections. In Section 2.1, a brief outline of the PHFB model has been given. A detailed derivation of the HFB method has been given by Baranger (1963), Villars (1966) and Goodman (1979). The formalism to calculate the spectroscopic properties has been presented in Section 2.2. We have compared the calculated sub-shell occupation numbers, yrast spectra and electromagnetic properties with available experimental data for ^{94,96}Zr, ^{94,96,100}Mo, ^{100,104}Ru, ^{104,110}Pd, ^{110}Cd, ^{128,130}Te, ^{128,130}Xe, ^{150}Nd and ^{150}Sm nuclei in Section 2.3. Finally, the conclusions are given in Section 2.4.

2.1 The PHFB model

In the PHFB calculation, the HFB intrinsic state $|\Phi_K\rangle$ is obtained through a self-consistent solutions of the HFB Hamiltonian [Baranger (1963), Villars (1966) and Goodman (1979)]. Subsequently, states with good angular momentum **J** are projected out from the axially symmetric HFB intrinsic state $|\Phi_K\rangle$ using the standard technique given by Onishi and Yosida (1966).

2.1.1 HFB theory

The nuclear many-body Hamiltonian for non-relativistic point nucleons neglecting three and many-nucleon forces is given by

$$H = \sum_{\alpha\beta} \langle \alpha | \ T \ | \beta \rangle a^{\dagger}_{\alpha} a_{\beta} + \frac{1}{4} \sum_{\alpha\beta\gamma\delta} \langle \alpha\beta | \ V \ | \gamma\delta \rangle a^{\dagger}_{\alpha} a^{\dagger}_{\beta} a_{\delta} a_{\gamma} \tag{2.1}$$

The HFB equations are obtained by equating to zero the off diagonal bilinear quasiparticle part of the transformed Hamiltonian after making a canonical transformation from a_{α}'s to quasi-fermions q_{α}'s. The general Bogoliubov transformations are considered to define the quasiparticle creation and destruction operators in terms of particle creation and destruction operators.

$$q^{\dagger}_{\alpha} = \sum_{\beta} \left(u_{\alpha\beta} a^{\dagger}_{\beta} + v_{\alpha\beta} a_{\beta} \right) \tag{2.2}$$

$$q_{\alpha} = \sum_{\beta} \left(u^{*}_{\alpha\beta} a_{\beta} + v^{*}_{\alpha\beta} a^{\dagger}_{\beta} \right) \tag{2.3}$$

The particle and quasiparticle operators satisfy the fermion anti-commutation relations

$$[a^{\dagger}_{\alpha}, a_{\beta}] = \delta_{\alpha\beta} \ ; \qquad [a^{\dagger}_{\alpha}, a^{\dagger}_{\beta}] = [a_{\alpha}, a_{\beta}] = 0 \tag{2.4}$$

$$[q^{\dagger}_{\alpha}, q_{\beta}] = \delta_{\alpha\beta} \ ; \qquad [q^{\dagger}_{\alpha}, q^{\dagger}_{\beta}] = [q_{\alpha}, q_{\beta}] = 0 \tag{2.5}$$

The transformation coefficients are real and satisfy appropriate orthonormality conditions. The 2n×2n linear transformation

$$\begin{bmatrix} q^{\dagger} \\ q \end{bmatrix} = \begin{bmatrix} u & v \\ v^{*} & u^{*} \end{bmatrix} \begin{bmatrix} a^{\dagger} \\ a \end{bmatrix} \tag{2.6}$$

is required to be unitary, and it follows from the unitarity condition that

$$uu^{\dagger} + vv^{\dagger} = u^{\dagger}u + \widetilde{v}v^{*} = I \tag{2.7}$$

$$u\widetilde{v} + v\widetilde{u} = u^{\dagger}v + \widetilde{v}u^{*} = 0 \tag{2.8}$$

The quasiparticle vacuum is defined through the relation

$$q_\alpha|\Phi_0\rangle = 0 \tag{2.9}$$

or

$$|\Phi_0\rangle = N\prod_\alpha q_\alpha|0\rangle \tag{2.10}$$

where $|0\rangle$ is the particle vacuum and N is the normalization constant, which is to be inserted appropriately.

The many-body Hamiltonian can be written with respect to the quasiparticle vacuum as

$$H' = H'_0 + H'_2 + H'_4 \tag{2.11}$$

where

$$\begin{aligned}
H'_0 &= Tr\left[\left(T - \lambda_\pi N_\pi - \lambda_\nu N_\nu + \frac{1}{2}\Gamma\right)\rho + \frac{1}{2}\Delta t^\dagger\right] && (2.12)\\
H'_2 &= \sum_{\alpha\beta}\left(h - \lambda_\pi N_\pi - \lambda_\nu N_\nu\right)_{\alpha\beta} : a^\dagger_\alpha a_\beta : \\
&\quad + \frac{1}{2}\sum_{\alpha\beta}\left[\Delta_{\alpha\beta} : a^\dagger_\alpha a^\dagger_\beta : + \Delta^\dagger_{\alpha\beta} : a_\alpha a_\beta :\right] && (2.13)\\
H'_4 &= \frac{1}{4}\sum_{\alpha\beta\gamma\delta}\langle\alpha\beta|\ V\ |\gamma\delta\rangle : a^\dagger_\alpha a^\dagger_\beta a_\delta a_\gamma : && (2.14)
\end{aligned}$$

The HF Hamiltonian h, the HF potential Γ and the pair potential Δ are given by

$$\begin{aligned}
h &= T + \Gamma && (2.15)\\
\Gamma_{\alpha\beta} &= \sum_{\gamma\delta}\langle\alpha\gamma|\ V\ |\beta\delta\rangle\rho_{\delta\gamma} && (2.16)\\
\Delta_{\alpha\beta} &= \frac{1}{2}\sum_{\gamma\delta}\langle\alpha\beta|\ V\ |\gamma\delta\rangle t_{\gamma\delta} && (2.17)
\end{aligned}$$

where the density matrix ρ and the pairing potential t are defined as

$$\begin{aligned} \rho_{\alpha\beta} &= \langle\Phi_0|a^\dagger_\beta a_\alpha|\Phi_0\rangle & (2.18)\\ &= \sum_\delta v_{\delta\beta}v^*_{\delta\alpha} = (v^\dagger v)_{\alpha\beta} & (2.19)\\ t_{\alpha\beta} &= \langle\Phi_0|a_\beta a_\alpha|\Phi_0\rangle = v^\dagger u & (2.20)\end{aligned}$$

Using Wick's theorem

$$\begin{aligned} \langle\Phi_0|H'|\Phi_0\rangle &= \langle\Phi_0|H'_0|\Phi_0\rangle \\ &= Tr\left[\left(T-\lambda_\pi N_\pi-\lambda_\nu N_\nu+\frac{1}{2}\Gamma\right)\rho+\frac{1}{2}\Delta t^\dagger\right] & (2.21)\end{aligned}$$

where by construction

$$\langle\Phi_0|H'_2+H'_4|\Phi_0\rangle = 0 \qquad (2.22)$$

The first term in Eq. (2.21) is the HF binding energy and the second term is the pairing energy. The quasiparticle excitation energies are obtained from H'_2 and the remaining H'_4 contains the quasiparticle interaction energies, which are neglected in the HFB theory. In time dependent HFB (TDHFB) or the quasiparticle random phase approximation (QRPA), some effects of quasiparticle interaction can be included.

The HFB theory is a generalized HF procedure in which the HF field and the pairing interaction are treated simultaneously and on equal footing. However, the quasiparticle transformations do not conserve the number of particles. Hence, one imposes constraints via the use of Lagrange multipliers while minimizing the complete Hamiltonian H such that the average number of nucleons in the state $|\Phi_0\rangle$ be equal to the given number of nucleons of the nucleus under consideration. That is, one minimizes

$$H' = H-\lambda_\pi N_\pi-\lambda_\nu N_\nu \qquad (2.23)$$

where

$$N_\pi = \sum_{\alpha_\pi} a^\dagger_{\alpha_\pi} a_{\alpha_\pi} \quad and \quad N_\nu = \sum_{\alpha_\nu} a^\dagger_{\alpha_\nu} a_{\alpha_\nu} \tag{2.24}$$

possess the expectation values

$$\langle \Phi_0 | N_\pi | \Phi_0 \rangle = Z \ , \ \langle \Phi_0 | N_\nu | \Phi_0 \rangle = A - Z \tag{2.25}$$

Further, the Lagrange's multipliers λ_π and λ_ν turn out to have the physical interpretation of proton and neutron fermi energies.

There are several equivalent methods for deriving the HFB equations such as (i) variational procedure, (ii) the equation of motion and (iii) elimination of dangerous diagrams. Here, we follow the equation of motion method. Further, we use time reversal symmetry as our concern is with even Z-even N nuclei only. The quasiparticle transformation are rewritten as

$$q^\dagger_k = \sum_\alpha \left(u_{k\alpha} a^\dagger_\alpha + v_{k\alpha} a_{\overline{\alpha}} \right) \tag{2.26}$$

$$q^\dagger_{\overline{k}} = \sum_\alpha \left(u_{k\alpha} a^\dagger_{\overline{\alpha}} - v_{k\alpha} a_\alpha \right) \tag{2.27}$$

and the HFB equations are given by

$$\begin{aligned} E_k u_{k\alpha} &= \sum_\gamma h'_{\alpha\gamma} u_{\alpha\gamma} + \Delta_{\alpha\overline{\gamma}} v_{\alpha\gamma} \\ E_k v_{k\alpha} &= \sum_\gamma \Delta_{\alpha\overline{\gamma}} u_{\alpha\gamma} - h'_{\alpha\gamma} v_{\alpha\gamma} \end{aligned} \tag{2.28}$$

where E_k is the quasiparticle energy. Further

$$h'_{\alpha\gamma} = T_{\alpha\gamma} - \lambda \delta_{\alpha\gamma} + \Gamma_{\alpha\gamma} \tag{2.29}$$

where

$$\Gamma_{\alpha\gamma} = \sum_{\beta\delta} \left[\langle\alpha\beta|\ V\ |\gamma\delta\rangle + \langle\alpha\overline{\beta}|\ V\ |\gamma\overline{\delta}\rangle\right] \sum_{k=1}^{n} v_{k\beta} v_{k\delta} \tag{2.30}$$

$$= \sum_{\beta\delta} \left[\langle\alpha\beta|\ V\ |\gamma\delta\rangle + \langle\alpha\overline{\beta}|\ V\ |\gamma\overline{\delta}\rangle\right] \rho_{\beta\delta} \tag{2.31}$$

and

$$\rho_{\beta\delta} = \sum_{k} v_{k\beta} v_{k\delta} \tag{2.32}$$

with

$$\Delta_{\alpha\overline{\gamma}} = \sum_{\beta\delta} \langle\alpha\overline{\gamma}|\ V\ |\beta\overline{\delta}\rangle \sum_{k=1}^{n} v_{k\beta} u_{k\delta} \tag{2.33}$$

Using the Bloch-Messiah theorem [Bloch and Messiah (1962)], the coupled HFB equations can be written in a simplified form. We define transformations

$$b_k^{\dagger} = \sum_{\alpha} C_{k,\alpha} a_{\alpha}^{\dagger} \qquad and \qquad b_{\overline{k}}^{\dagger} = \sum_{\alpha} C_{k,\alpha}^{*} a_{\overline{\alpha}}^{\dagger} \tag{2.34}$$

where the expansion coefficients appearing in Eq. (2.34) can be obtained by diagonalizing the HF like potential h' in spherical basis

$$h_{\alpha\beta}^{'} = \langle\alpha|T - \lambda_{\pi} N_{\pi} - \lambda_{\nu} N_{\nu}|\beta\rangle + \sum_{k} \langle\alpha k|\ V\ |\beta k\rangle v_k^2 \tag{2.35}$$

which includes the appropriate density $\rho_k = v_k^2$. The occupation probabilities v_k^2 are obtained by solving the BCS equation

$$\Delta_k = \Delta_{k\overline{k}} = \sum_{k'} \langle k\overline{k}|\ V\ |k'\overline{k'}\rangle u_{k'} v_{k'} \tag{2.36}$$

The calculation involves iteration between Eqs. (2.35) and (2.36) until a reasonable convergence is achieved in terms of both the expansion coefficients $C_{k,\alpha}$ and v_k^2. Denoting

by θ_k the eigenvalue of $h'_{\alpha\beta}$ given by Eq. (2.35), the probability amplitudes u_k and v_k in Eqs. (2.26 and 2.27) are given by

$$u_k^2 = \frac{1}{2}\left[1 + \frac{\theta_k}{E_k}\right] \tag{2.37}$$

and

$$v_k^2 = \frac{1}{2}\left[1 - \frac{\theta_k}{E_k}\right] \tag{2.38}$$

where

$$E_k = \sqrt{\theta_k^2 + \Delta_k^2} \tag{2.39}$$

with

$$\Delta_{k\overline{k}} = \frac{1}{2}\sum_{k'}\langle k\overline{k}|\ V\ |k'\overline{k'}\rangle \left(\frac{\Delta_{k\overline{k'}}}{\sqrt{\theta_{k'}^2 + \Delta_{k'\overline{k'}}^2}}\right) \tag{2.40}$$

The chemical potential λ is obtained by solving the equation

$$\sum_{k=1}^{n}\left[1 - \frac{\theta_k}{\sqrt{\theta_k^2 + \Delta_k^2}}\right] = N \tag{2.41}$$

The ground state energy E_{HFB} is given by

$$E_{HFB} = \sum_{k=1}^{n}(T_{kk} + \lambda - E_k)v_k^2 \tag{2.42}$$

where

$$\begin{aligned} T_{kk} &= \sum_{\alpha\gamma}\langle k\alpha\,|T|\,k\gamma\rangle \\ &= \sum_{\alpha\gamma} T_{\alpha\gamma}C_{k\alpha}\ C_{k\gamma} \end{aligned} \tag{2.43}$$

The quadrupole moment of the axially symmetric HFB intrinsic state is given by

$$Q_{HFB} = 2\sum_{k=1}^{n} Q_{20}\ v_k^2 \tag{2.44}$$

where

$$Q_{20} = \left(\frac{16\pi}{5}\right)^{1/2} \; r^2 \; Y_{20} \tag{2.45}$$

is the quadrupole moment operator.

The axially symmetric HFB intrinsic state $|\Phi_0\rangle$ can be written as

$$|\Phi_0\rangle = \prod_{im}(u_{im} + v_{im} b^\dagger_{im} b^\dagger_{i\bar{m}})|0\rangle \tag{2.46}$$

$$= N \; exp\left(\frac{1}{2}\sum_{\alpha\beta} f_{\alpha\beta} a^\dagger_{\alpha,m} a^\dagger_{\alpha,-m}|0\rangle\right) \tag{2.47}$$

where the creation operators $b^\dagger_{im}$ and $b^\dagger_{i\bar{m}}$ are defined as

$$b^\dagger_{im} = \sum_\alpha C_{i\alpha,m} a^\dagger_{\alpha,m} \quad \text{and} \quad b^\dagger_{i\bar{m}} = \sum_\alpha (-1)^{l+j-m} C_{i\alpha,m} a^\dagger_{\alpha,-m} \tag{2.48}$$

with

$$f_{\alpha\beta} = \sum_i C_{i,j_\alpha m_\alpha} C_{i,j_\beta m_\beta} \left(\frac{v_{im_\alpha}}{u_{im_\alpha}}\right) \delta_{m_\alpha - m_\beta} \tag{2.49}$$

where N is a normalization constant.

2.1.2 Projection of angular momentum

The intrinsic state $|\Phi_K\rangle$ can be expanded in terms of states of good angular momentum **J** as

$$|\Phi_K\rangle = \sum_J a_J |\Psi_{JK}\rangle \tag{2.50}$$

Applying the rotation operator $R(\Omega)$, one obtains

$$\hat{R}(\Omega) \; |\Phi_K\rangle = \sum_{JM} a_J \; D^J_{MK}(\Omega) \; |\Psi_{JM}\rangle \tag{2.51}$$

where

$$\hat{R}(\Omega) = e^{-i\alpha J_Z} e^{-i\beta J_Y} e^{-i\gamma J_Z} \tag{2.52}$$

and $D^J_{MK}(\Omega)$ is the rotation matrix. Multiplying by D^J_{MK} and integrating, one gets

$$\begin{aligned} |\Psi_{JM}\rangle &= \frac{2J+1}{8\pi^2 a_J}\int d\Omega D^J_{MK}(\Omega)\hat{R}(\Omega)\ |\Phi_K\rangle \\ &= P^J_{MK}|\Phi_K\rangle \end{aligned} \tag{2.53}$$

where

$$P^J_{MK} = \frac{2J+1}{8\pi^2 a_J}\int d\Omega D^J_{MK}(\Omega)\hat{R}(\Omega) \tag{2.54}$$

Restricting to the axially symmetric HFB intrinsic state $|\Phi_0\rangle$ with $K=0$, one obtains

$$\begin{aligned} |\Psi_{J0}\rangle &= P^J_{00}\,|\Phi_0\rangle \\ &= \frac{2J+1}{8\pi^2}\int D^J_{00}(\Omega)R(\Omega)\,|\Phi_0\rangle\,d\Omega \end{aligned} \tag{2.55}$$

2.2 Spectroscopic properties of yrast states

In the below, we present expressions to calculate various nuclear spectroscopic properties, namely Sub-shell occupation number, yrast energy spectra, reduced $B(E2{:}J_i \rightarrow J_f)$ transition probabilities [Dixit *et al.* (2002)] and magnetic dipole moments $\mu(J)$ [Rath *et al.* (1988)].

2.2.1 Sub-shell occupation number

The sub-shell occupation numbers η_J in a yrast state J is given by

$$\eta_J = \frac{\left\langle \Phi_0 \left| \left(\sum_m C^\dagger_{jm} C_{jm} \right) P^J_{00} \right| \Phi_0 \right\rangle}{\langle \Phi_0 \left| P^J_{00} \right| \Phi_0 \rangle} = \frac{\int_0^\pi P(\theta) d^J_{00}(\theta) \sin\theta d\theta}{\int_0^\pi n(\theta) d^J_{00}(\theta) \sin\theta d\theta} \tag{2.56}$$

where

$$P(\theta) = n(\theta) \left[\sum_m \left(\frac{M}{1+M} \right)_{jm,jm} \right] \tag{2.57}$$

An approximate estimate of the subshell occupation numbers can be easily obtained in terms of the expectation value of the operator η_J with respect to the intrinsic state $|\Phi_0\rangle$

$$\eta_J^{intrinsic} = \langle \Phi_0 \left| \widehat{\eta}_J \right| \Phi_0 \rangle = \sum_{i,m} |c_{Ji}^m|^2 \, (V_i^m)^2 \tag{2.58}$$

2.2.2 Yrast spectra

The energy E_J of a state with good angular momentum $\mathbf{J}$ is given by

$$E_J = \frac{\langle \Psi_{J0} | H | \Psi_{J0} \rangle}{\langle \Psi_{J0} | \Psi_{J0} \rangle} = \frac{\int_0^\pi h(\theta) d_{00}^J(\theta) \sin\theta \; d\theta}{\int_0^\pi n(\theta) d_{00}^J(\theta) \sin\theta \; d\theta} \tag{2.59}$$

The overlap integrals $h(\theta)$ and $n(\theta)$ are given by

$$\begin{aligned} h(\theta) &= \left\langle \Phi_0 | H e^{-i\theta J_y} | \Phi_0 \right\rangle \\ &= \sum_\alpha \varepsilon_\alpha \left(\frac{M}{1+M} \right)_{\alpha\alpha} + \frac{1}{4} \sum_{\alpha\beta\gamma\delta} \langle \alpha\beta | \; V \; | \gamma\delta \rangle \\ &\quad \times \left\{ 2 \left(\frac{M}{1+M} \right)_{\gamma\alpha} \left(\frac{M}{1+M} \right)_{\delta\beta} \right. \\ &\quad \left. + \sum_{\nu\rho} \left(\frac{1}{1+M} \right)_{\gamma\rho} F_{\rho\delta} \left(\frac{1}{1+M} \right)_{\nu\alpha} f_{\nu\beta} \right\} \end{aligned} \tag{2.60}$$

and

$$n(\theta) = \left\langle \Phi_0 | e^{-i\theta J_y} | \Phi_0 \right\rangle = \left\{ \det[1 + M(\theta)] \right\}^{1/2} \tag{2.61}$$

where

$$M(\theta) = F(\theta) f^\dagger \tag{2.62}$$

with

$$F_{\alpha\beta}(\theta) = \sum_{m'_\alpha, m'_\beta} d^{j_\alpha}_{m_\alpha, m'_\alpha}(\theta) d^{j_\beta}_{m_\beta, m'_\beta}(\theta) f_{j_\alpha m'_\alpha, j_\beta m'_\beta} \tag{2.63}$$

and

$$\rho_{\alpha\beta}(\theta) = \left[\frac{M(\theta)}{1+M(\theta)}\right]_{\alpha\beta} = \delta_{\alpha\beta} - \left[\frac{1}{1+M(\theta)}\right]_{\alpha\beta} \tag{2.64}$$

The projection calculation is carried out as follows. In the first step, f matrix is set up using the HFB wave functions. In the next step F, M and $(1/1+M)$ are evaluated for 20 values of Gaussian quadrature points between the range $(0, \pi)$.

2.2.3 Reduced $B(E2{:}J_i \to J_f)$ transition probabilities

The reduced $B(E2)$ transition probability is given by

$$B(E2{:}J_i \to J_f) = \left(\frac{5}{16\pi}\right) \left[e_\pi \left\langle Q_{20}\right\rangle_\pi + e_\nu \left\langle Q_{20}\right\rangle_\nu\right]^2 \tag{2.65}$$

where

$$\begin{aligned}
\left\langle Q_{20}\right\rangle_{\tau_3} &= \left\langle \Psi_{J_i K} \left| Q_{20} \right| \Psi_{J_f K} \right\rangle \\
&= \left[n_{J_i} n_{J_f}\right]^{-1/2} \int_0^\pi \sum_\mu \begin{pmatrix} J_i & 2 & J_f \\ -\mu & \mu & 0 \end{pmatrix} \\
&\quad \times d^{J_i}_{-\mu 0}(\theta) n(\theta) \left[b^2 \sum_{\tau_3 \alpha\beta} e_{\tau_3} \left\langle \alpha \left| Q_{2\mu} \right| \beta \right\rangle \rho^{\tau_3}_{\alpha\beta}(\theta)\right] \sin\theta \; d\theta
\end{aligned} \tag{2.66}$$

with

$$n_J = \int_0^\pi n(\theta) d^J_{00}(\theta) \sin\theta \; d\theta \tag{2.67}$$

$$\rho^{\tau_3}_{\alpha\beta}(\theta) = \left[\frac{M(\theta)}{1+M(\theta)}\right]^{\tau_3}_{\alpha\beta} \tag{2.68}$$

and

$$Q_{2\mu} = \sqrt{\frac{16\pi}{5}} \frac{r^2}{b^2} Y_{2\mu}(\theta, \phi) \tag{2.69}$$

The deformation parameter β_2 is given by

$$\beta_2 = \frac{4\pi}{3ZR_0^2} \left[\frac{B(E2)}{e^2} \right]^{1/2} \tag{2.70}$$

where $R_0 = 1.2\ A^{1/3}$ and $B(E2)$ is in units of $\mathrm{e}^2\mathrm{b}^2$.

2.2.4 Magnetic dipole moments $\mu(J)$

Usually, experimentalists prefer to report g-factors defined by $g(J) = \mu(J)/J$. The expression to calculate magnetic diploe moment $\mu(J)$ is given by

$$\begin{aligned} \mu(J) &= \langle \Psi_{J0} \left| \mu_z \right| \Psi_{J0} \rangle \\ &= n_J^{-1} \int_0^{\pi} n(\theta) \sum_m \begin{pmatrix} J & 1 & J \\ -m & m & 0 \end{pmatrix} \\ &\quad \times d^J_{-m0}(\theta) \sum_{\tau_3 \alpha\beta} \langle \alpha \left| \mu_m \right| \beta \rangle \, \rho^{\tau_3}_{\alpha\beta}(\theta) \sin\theta \ d\theta \end{aligned} \tag{2.71}$$

where in general [Bohr and Mottelson (1998)]

$$\boldsymbol{\mu} = g_l' \mathbf{l} + g_s' \mathbf{s} + g_p \left(Y^{(2)} \times S^{(2)} \right)^{(1)} \tag{2.72}$$

Here g_l' (g_s') are the effective orbital (spin) g-factors and g_p provides a measure of the spin-polarization effects. In the present calculation, we have neglected the contributions of spin-polarization effects.

2.3 Results and discussions

In case of ^{94,96}Zr, ^{94,96,100}Mo, ^{100,104}Ru, ^{104,110}Pd and ^{110}Cd nuclei, we treat the doubly even ^{76}Sr ($N = Z = 38$) nucleus as an inert core with the valence space spanned by $1p_{1/2}$, $2s_{1/2,}$ $1d_{3/2}$, $1d_{5/2}$, $0g_{7/2}$, $0g_{9/2}$ and $0h_{11/2}$ orbits for protons and neutrons. For ^{128,130}Te, ^{128,130}Xe, ^{150}Nd and ^{150}Sm nuclei, the doubly even ^{100}Sn ($N = Z = 50$) nucleus has been treated as an inert core with the valence space spanned by $2s_{1/2,}1d_{3/2}$, $1d_{5/2}$, $1f_{7/2}$, $0g_{7/2}$, $0h_{9/2}$ and $0h_{11/2}$ orbits for protons and neutrons. The change of model space is forced upon due to the following reason. The number of neutrons increase to about 50 for nuclei occurring in the mass region $A \sim 150$ in the model space with ^{76}Sr as the core. With the increase in neutron number, the yrast energy spectra gets compressed due to increase in the attractive part of effective two-body interaction. The single particle energies (SPEs) for ^{94,96}Zr, ^{94,96,100}Mo, ^{100,104}Ru, ^{104,110}Pd, ^{110}Cd, ^{128,130}Te, ^{128,130}Xe, ^{150}Nd and ^{150}Sm are derived from Woods-Saxon potential as proposed by Blomqvist and Wahlborn (1960) given as

$$V(r) = -V_0 \frac{1}{1+\exp((r-R_0)/a)} - \lambda \left(\frac{\hbar}{2Mc}\right)^2 \mathbf{l}.\boldsymbol{\sigma}\ \frac{1}{r}\frac{d}{dr}\left(\frac{V_0}{1+\exp((r-R_0)/a)}\right) + V_C(r) \tag{2.73}$$

where $\lambda = 32.0$ is a dimensionless parameter, $a = 0.67$ is diffusitivity and V_C is the coulomb potential given as

$$V_C(r) = \begin{cases} Ze^2(3 - r^2/R_0^2)/2R_0 & , \quad r \leqslant R_0 \\ Ze^2/r & , \quad r \geqslant R_0 \end{cases} \tag{2.74}$$

with $R_0 = r_0 A^{1/3}$ and $r_0 = 1.2$ fm. The potential V_0 for proton and neutron is taken as 57.0 MeV and 47.0 MeV, respectively. The calculated SPEs are given in Table 2.1.

We use a Hamiltonian with Pairing plus Quadrupole-Quadrupole plus Hexadecapole-Hexadecapole (*PQQHH)* type of effective two-body interaction. The Hamiltonian is explicitly written as

$$H = H_{sp} + V(P) + \zeta_{qq}\left[V(QQ) + V(HH)\right] \tag{2.75}$$

where ζ_{qq} is an arbitrary parameter and the final results are obtained by setting $\zeta_{qq} = 1$. The purpose of introducing ζ_{qq} is to study the role of deformation by varying the strength of $QQHH$ interaction. Further, H_{sp} denotes the single particle Hamiltonian. The pairing part of the effective two-body interaction $V(P)$ is given by

$$V(P) = -\left(\frac{G}{4}\right)\sum_{\alpha\beta}(-1)^{j_\alpha+j_\beta-m_\alpha-m_\beta}a^\dagger_\alpha a^\dagger_{\bar{\alpha}}a_{\bar{\beta}}a_\beta, \tag{2.76}$$

where α denotes the quantum numbers $(nljm)$. The state $\bar{\alpha}$ is same as α but with the sign of m reversed. For $A \leq 110$ nuclei, the strengths of the pairing interaction is fixed through the relation $G_p = 30/A$ MeV and $G_n = 25/A$ MeV. For ^{94}Zr and ^{94}Mo, we have used $G_n = 20/A$ MeV. The strengths of the pairing interaction fixed for $A \geq 128$ nuclei are $G_p = G_n = 35/A$ MeV.

The QQ part of the effective interaction $V(QQ)$ is expressed as

$$V(QQ) = -\left(\frac{\chi_2}{2}\right)\sum_{\alpha\beta\gamma\delta}\sum_{\mu}(-1)^\mu\langle\alpha|q_{2\mu}|\gamma\rangle\langle\beta|q_{2-\mu}|\delta\rangle\ a^\dagger_\alpha a^\dagger_\beta\ a_\delta\ a_\gamma \tag{2.77}$$

where

$$q_{2\mu} = \left(\frac{16\pi}{5}\right)^{1/2} r^2 Y_{2\mu}(\theta,\phi) \tag{2.78}$$

The HH part of the effective interaction $V(HH)$ is given as

$$V(HH) = -\left(\frac{\chi_4}{2}\right)\sum_{\alpha\beta\gamma\delta}\sum_{\nu}(-1)^\nu\langle\alpha|q_{4\nu}|\gamma\rangle\langle\beta|q_{4-\nu}|\delta\rangle\ a^\dagger_\alpha a^\dagger_\beta\ a_\delta\ a_\gamma \tag{2.79}$$

where

$$q_{4\nu} = r^4 Y_{4\nu}(\theta, \phi) \tag{2.80}$$

The relative magnitudes of the parameters of the hexadecapole-hexadecapole part of the two body interaction were calculated from a relation suggested by Bohr and Mottelson [Bohr and Mottelson (1975)]. According to them the approximate magnitude of these constants for isospin $T = 0$ is given by

$$\chi_\lambda = \frac{4\pi}{2\lambda + 1} \frac{m\omega_0^2}{A \langle r^{2\lambda-2} \rangle} \qquad \text{for } \lambda = 1, 2, 3, 4 \cdots \tag{2.81}$$

and the parameters for the $T = 1$ case are approximately half of their $T = 0$ counterparts. Using $b = 1.0032A^{1/6}$, one obtains

$$\begin{aligned} \chi_4 &= \left[\left(\frac{16}{25} \right) \left(\frac{2}{3} \right)^{2/3} \right] \chi_2 A^{-2/3} b^{-4} \\ &= 0.4884 \chi_2 A^{-2/3} b^{-4} \end{aligned} \tag{2.82}$$

The spectroscopic properties of ^{94,96}Zr, ^{94,96,100}Mo, ^{100,104}Ru, ^{104,110}Pd, ^{110}Cd, ^{128,130}Te, ^{128,130}Xe, ^{150}Nd and ^{150}Sm nuclei have been calculated in PHFB model using four parametrizations of the effective two-body interaction, namely $PQQ1$, $PQQ2$ (without hexadecapole-hexadecapole term), $PQQHH1$ and $PQQHH2$ (with hexadecapole-hexadecapole term). In $PQQ1$ and $PQQHH1$ parametrizations, the strengths of the like particle components of the QQ interaction are taken as $\chi_{2pp} = \chi_{2nn} = -0.0105$ MeV b^{-4}, where b is oscillator parameter and an optimum yrast spectra of nuclei under consideration was obtained by varying the strength of proton-neutron (pn) component of the QQ interaction χ_{2pn}. Thus, χ_{2pn} was fixed through the experimentally available energy spectra for a given model space, SPE's, G_p, G_n and χ_{2pp}. These values of the strength of the QQ interaction were comparable to those suggested by Arima on the basis of an empirical analysis of the effective

two-body interactions [Arima (1981)]. In the other two parametrizations, namely $PQQ2$ and $PQQHH2$ parametrizations, χ_{2pn} is taken as twice of χ_{2pp} i.e. $\chi_{2pn} = 2\chi_{2pp} = 2\chi_{2nn}$ and vary the three parameters together to obtain an optimum yrast spectra. The theoretical spectra was considered to be the optimum if the excitation energy of the 2^+ state E_{2^+} is reproduced as closely as possible in comparison to the experimental results. All these input parameters were kept fixed to calculate other nuclear spectroscopic properties.

The experimental sub-shell occupation numbers in case of ^{100}Mo, ^{100}Ru, ^{128,130}Te and ^{130}Xe are available. For these nuclei we adjusted the calculated SPEs to reproduce these occupation numbers which provides more reliability to the wave functions. In Tables 2.2 – 2.3, the calculated occupation numbers in $PQQ1$ parametrization are given along with the experimentally observed data [Freeman *et al.* (2017), Kay *et al.* (2013)]. The calculated occupation numbers in $PQQ1$ parametrization for rest of the nuclei are given in Tables 2.4 – 2.5. The occupation numbers calculated in other three parametrizations, namely $PQQHH1$, $PQQ2$ and $PQQHH2$ are found almost similar to those calculated in $PQQ1$ parametrization.

In Table 2.6, we have presented the theoretically calculated yrast energies for the E_{2^+} to E_{6^+} levels of the nuclei under consideration in all four parametrizations, namely $PQQ1$, $PQQHH1$, $PQQ2$ and $PQQHH2$ along with the experimental ones [Sakai (1984)]. From Table 2.6 it can be seen that the theoretical spectra is more expanded in comparison to the experimental spectra for all nuclei although the agreement between the theoretically calculated and experimentally observed E_{2^+} is quite good. This can be taken care by invoking the VAP prescription [Khosa *et al.* (1982), Tripathi *et al.* (1984), Sharma *et al.* (1988)]. However, our aim is to reproduce the properties of only low-lying 2^+ state and

hence, we have not attempted the VAP calculation. Employing either parametrization, the calculated excitation energies of 2^+ state E_{2^+} agree with the experimental values within about 2% accuracy.

The calculated as well as the experimentally observed reduced transition probabilities $B(E2{:}0^+ \rightarrow 2^+)$ and deformation parameters β_2 of the above mentioned nuclei are presented in Table 2.7. The $B(E2{:}0^+ \rightarrow 2^+)$ and β_2 are calculated for effective charges $e_{eff} =$ 0.40, 0.50 and 0.60. In case of ^{94}Zr, ^{96}Mo, ^{100}Ru and ^{150}Sm, the observed $B(E2{:}0^+ \rightarrow 2^+)$ and β_2 values are in overall agreement with calculated values, but for $PQQ2$ parametrization in case of ^{94}Zr, for $e_{eff} = 0.40$. The observed $B(E2{:}0^+ \rightarrow 2^+)$ as well as β_2 values are in good agreement with calculated values in all four parametrizations in case of ^{96}Zr, ^{104,110}Pd, ^{110}Cd, ^{128,130}Xe, ^{130}Te, ^{150}Nd isotopes for $e_{eff} = 0.50$. In case of ^{94,100}Mo, ^{104}Ru and ^{128}Te isotopes, the calculated values agree with experimental limits at $e_{eff} = 0.60$.

The gyromagnetic factors $g(2^+)$ are calculated with $g_l^\pi = 1.0$, $g_l^\nu = 0.0$, and $g_s^\pi = g_s^\nu =$ 0.50. The calculated and available experimental $g(2^+)$ values are given Table 2.8. No experimental result is available for ^{96}Zr and ^{94,96}Mo. The theoretical $g(2^+)$ value of ^{94}Zr is a pathological case. The calculated $g(2^+)$ values in present work are 0.177, 0.162, 0.522 and 0.106 nm in $PQQ1$, $PQQHH1$, $PQQ2$ and $PQQHH2$ parametrization, respectively while the most recent measured value is -0.329 ± 0.015 nm [Speidel *et al.* (2002)]. The calculated and experimentally observed $g(2^+)$ values are in good agreement for ^{100,104}Ru, ^{104}Pd and ^{128}Xe nuclei. The maximum discrepancy between calculated and experimentally observed $g(2^+)$ values is about 30% for ^{110}Pd, ^{130}Xe and ^{150}Sm nuclei. For rest of the nuclei there is a large discrepancy between theoretically calculated and experimentally observed $g(2^+)$ values.

2.4 Conclusions

To summarize, we have calculated the yrast spectra, reduced $B(E2{:}0^+ \rightarrow 2^+)$ transition probabilities, deformation parameters β_2 and g-factors $g(2^+)$ of ^{94,96}Zr, ^{94,96,100}Mo, ^{100,104}Ru, ^{104,110}Pd, ^{110}Cd, ^{128,130}Te, ^{128,130}Xe, ^{150}Nd and ^{150}Sm isotopes, participating in $\beta^-\beta^-$ decay, and compared them with the available experimental data as a test of the "goodness of the wave functions". The overall agreement between the calculated and observed spectroscopic properties of the nuclei suggests that the PHFB wave functions for all four parametrizations, namely $PQQ1$, $PQQHH1$, $PQQ2$ and $PQQHH2$ generated by fixing χ_{2pn}, χ_{2pp}, χ_{2nn} to reproduce the E_{2^+} are quite reliable. Hence, we proceed to calculate the NTMEs $M_{2\nu}$ and half-lives $T^{2\nu}_{1/2}$ of $2\nu\beta^-\beta^-$ decay for the $0^+ \rightarrow 0^+$ transition of the nuclei under consideration using same PHFB wave functions.

Table 2.1: Adjusted Woods-Saxon single particle energies for ^{94,96}Zr, ^{94,96,100}Mo, ^{100,104}Ru, ^{104}Pd, ^{110}Pd and ^{110}Cd, ^{128,130}Te, ^{128,130}Xe, ^{150}Nd and ^{150}Sm nuclei.

Nuclei		$2s_{1/2}$	$1p_{1/2}$	$1d_{3/2}$	$1d_{5/2}$	$0g_{7/2}$	$0g_{9/2}$	$0h_{11/2}$
^{94}Zr	Proton	7.881	-1.076	7.390	5.615	9.021	0.0	9.076
	Neutron	6.559	-1.276	7.949	4.700	7.811	0.0	9.099
^{94}Mo	Proton	7.815	-1.043	7.329	5.385	9.011	0.0	9.037
	Neutron	6.587	-1.270	5.978	4.715	7.827	0.0	9.108
^{96}Zr	Proton	8.002	-1.052	9.453	5.67	8.903	0.0	9.032
	Neutron	6.54	-2.269	7.878	4.681	7.64	0.0	9.013
^{96}Mo	Proton	7.994	-1.008	9.451	5.676	8.922	0.0	9.009
	Neutron	6.690	-2.235	5.530	4.767	7.727	0.0	9.062
^{100}Mo	Proton	8.144	-0.938	7.670	5.841	8.760	0.0	8.959
	Neutron	10.567	-1.560	7.950	5.980	6.997	0.0	8.250
^{100}Ru	Proton	9.999	-0.112	9.747	7.451	8.680	0.0	8.885
	Neutron	9.998	-1.174	8.210	7.656	7.677	0.0	8.878
^{104}Ru	Proton	9.408	-0.178	9.645	7.878	8.305	0.0	8.542
	Neutron	9.859	-1.153	8.806	7.840	8.442	0.0	8.924
^{104}Pd	Proton	9.806	-0.177	9.149	7.175	8.407	0.0	8.743
	Neutron	9.920	-1.426	8.983	8.379	8.968	0.0	9.999
^{110}Pd	Proton	8.480	-0.820	9.570	5.905	8.115	0.0	8.636
	Neutron	6.033	-2.286	7.063	4.350	6.417	0.0	8.354
^{110}Cd	Proton	8.673	-0.788	9.528	5.888	8.106	0.0	9.071
	Neutron	7.043	-2.079	8.058	4.929	6.964	0.0	8.688

Table 2.1 continued

Nuclei		$2s_{1/2}$	$1d_{3/2}$	$1d_{5/2}$	$1f_{7/2}$	$0g_{7/2}$	$0h_{9/2}$	$0h_{11/2}$
^{128}Te	Proton	2.763	3.465	0.0	12.444	3.195	12.208	6.131
	Neutron	4.080	4.765	0.0	12.997	1.152	11.467	4.342
^{128}Xe	Proton	2.742	3.445	0.0	10.373	3.198	12.154	6.112
	Neutron	2.118	2.801	0.0	10.073	3.147	11.725	6.320
^{130}Te	Proton	2.779	3.444	0.0	12.459	3.098	12.072	6.084
	Neutron	2.972	3.310	0.0	12.963	0.499	11.196	2.850
^{130}Xe	Proton	2.751	3.416	0.0	10.374	3.101	12.005	6.068
	Neutron	3.102	4.955	0.0	11.522	1.066	10.256	3.286
^{150}Nd	Proton	2.774	3.119	0.0	10.190	3.288	10.568	3.634
	Neutron	2.210	2.584	0.0	10.045	3.359	10.244	3.851
^{150}Sm	Proton	2.722	3.069	0.0	10.064	1.791	10.462	5.631
	Neutron	2.201	2.575	0.0	10.027	1.861	10.229	5.857

Table 2.2: Calculated and experimental [Freeman *et al.* (2017)] occupation numbers for protons and neutrons in ^{100}Mo and ^{100}Ru isotopes in $PQQ1$ parametrization.

	^{100}Mo		^{100}Ru	
Orbits	Theory	Exp.	Theory	Exp.
Protons				
$2s_{1/2}$	0.035	–	0.079	–
$1p_{1/2}$	0.013	–	0.044	–
$1d_{3/2}$+$1d_{5/2}$	0.544	–	0.858	–
$0g_{7/2}$	0.019	–	0.105	–
$0g_{9/2}$	3.380	4.06±0.30	4.969	5.56±0.22
$0h_{11/2}$	0.008	–	-0.056	–
Neutrons				
$2s_{1/2}$	0.309	0.33±0.02	0.535	0.23±0.01
$1p_{1/2}$	1.986	–	1.989	–
$1d_{3/2}$+$1d_{5/2}$	3.677	3.40±0.17	2.814	2.50±0.12
$0g_{7/2}$	2.558	2.48±0.19	2.336	2.19±0.15
$0g_{9/2}$	9.666	–	9.112	–
$0h_{11/2}$	1.804	1.89±0.13	1.214	1.13±0.08

Table 2.3: Calculated and experimental [Kay *et al.* (2013)] occupation numbers for protons and neutrons in ^{128,130}Te, ^{130}Xe isotopes in $PQQ1$ parametrization.

	^{128}Te		^{130}Te		^{130}Xe	
Orbits	Theory	Exp.	Theory	Exp.	Theory	Exp.
Protons						
$2s_{1/2}$	0.382	–	0.385	–	0.465	–
$1d_{3/2}$+$1d_{5/2}$	1.563	–	1.553	–	2.767	–
$1f_{7/2}$	0.000	–	0.000	–	0.010	–
$0g_{7/2}$	0.055	–	0.062	–	0.791	–
$0h_{9/2}$	0.000	–	0.000	–	0.004	–
$0h_{11/2}$	0.000	–	0.000	–	-0.037	–
Neutrons						
$2s_{1/2}$	1.329	1.28±0.2	1.517	1.50±0.2	1.251	1.44±0.2
$1d_{3/2}$+$1d_{5/2}$	7.973	7.94±0.2	8.626	8.55±0.2	7.353	7.29±0.2
$1f_{7/2}$	0.264	–	0.207	–	0.538	–
$0g_{7/2}$	7.635	8.00	7.707	8.00	7.490	8.00
$0h_{9/2}$	0.201	–	0.139	–	0.403	–
$0h_{11/2}$	8.597	8.66±0.3	9.803	9.79±0.3	8.964	9.01±0.3

Table 2.4: Calculated occupation numbers for protons and neutrons in ^{94,96}Zr, ^{94,96}Mo, ^{104}Ru, ^{104,110}Pd and ^{110}Cd isotopes in $PQQ1$ parametrization.

Orbits	^{94}Zr	^{94}Mo	^{96}Zr	^{96}Mo	^{104}Ru	^{104}Pd	^{110}Pd	^{110}Cd
Protons								
$2s_{1/2}$	0.012	0.019	0.005	0.033	0.054	0.027	0.139	0.015
$1p_{1/2}$	0.145	0.580	0.814	0.132	0.045	1.891	1.735	2.000
$1d_{3/2}$+$1d_{5/2}$	0.178	0.306	0.036	0.509	0.675	0.510	1.054	0.432
$0g_{7/2}$	0.011	0.024	0.015	0.020	0.076	0.048	0.150	0.034
$0g_{9/2}$	1.613	2.987	1.068	3.323	5.162	5.490	4.960	7.516
$0h_{11/2}$	0.041	0.083	0.063	-0.016	-0.013	0.033	-0.039	0.001
Neutrons								
$2s_{1/2}$	0.421	0.445	0.409	0.482	0.582	0.573	0.833	0.712
$1p_{1/2}$	1.998	2.000	1.986	1.990	1.994	1.994	1.993	1.990
$1d_{3/2}$+$1d_{5/2}$	3.380	1.684	4.683	3.401	3.29	3.367	5.219	5.355
$0g_{7/2}$	0.186	0.110	0.628	0.693	2.527	2.355	3.971	3.604
$0g_{9/2}$	9.903	9.761	9.844	9.363	9.736	9.809	9.698	9.828
$0h_{11/2}$	0.112	0.000	0.450	0.070	3.864	1.901	4.285	2.510

Table 2.5: Calculated occupation numbers for protons and neutrons in ^{128}Xe, ^{150}Nd and ^{150}Sm isotopes in $PQQ1$ parametrization.

Orbits	^{128}Xe	^{150}Nd	^{150}Sm
Protons			
$2s_{1/2}$	0.492	0.500	0.589
$1d_{3/2}$+$1d_{5/2}$	2.603	4.013	5.142
$1f_{7/2}$	0.015	0.723	0.453
$0g_{7/2}$	0.887	1.492	3.863
$0h_{9/2}$	0.003	0.019	0.054
$0h_{11/2}$	-0.001	3.253	1.898
Neutrons			
$2s_{1/2}$	1.610	1.992	1.982
$1d_{3/2}$+$1d_{5/2}$	8.572	9.969	9.935
$1f_{7/2}$	1.367	4.191	3.327
$0g_{7/2}$	6.178	7.943	7.946
$0h_{9/2}$	0.383	5.920	5.056
$0h_{11/2}$	5.889	9.985	9.753

Table 2.6: Theoretically calculated excitation energies E_{J^π} (MeV) of $J^\pi = 2^+$, 4^+ and 6^+ yrast states of ^{94,96}Zr, ^{94,96,100}Mo, ^{100,104}Ru, ^{104,110}Pd, ^{110}Cd, ^{128,130}Te, ^{128,130} Xe, ^{150}Nd and ^{150}Sm nuclei along with the experimental values [Sakai (1984)].

Nuclei		$PQQ1$	$PQQHH1$	$PQQ2$	$PQQHH2$	Exp.
^{94}Zr	χ_{2pp}	0.0105	0.0105	0.015798	0.0132	
	χ_{2pn}	0.032122	0.03095	0.031596	0.0264	
	E_{HFB}	11.5512	11.6760	10.3745	11.6550	
	Q_{HFB}	24.5837	23.0302	39.1223	20.6325	
	E_{2^+}	0.9192	0.9183	0.9184	0.9159	0.9183
	E_{4^+}	1.6883	1.6669	1.9877	1.9148	1.4688
	E_{6^+}	2.2558	2.1809	3.0807	2.6756	
^{94}Mo	χ_{2pp}	0.0105	0.0105	0.01195	0.011727	
	χ_{2pn}	0.02511	0.02445	0.0239	0.023454	
	E_{HFB}	0.1558	0.1019	0.0009	0.0017	
	Q_{HFB}	31.5209	31.8086	31.7552	31.8953	
	E_{2^+}	0.8714	0.8708	0.8790	0.8811	0.8711
	E_{4^+}	1.6786	1.6883	1.7156	1.7191	1.5737
	E_{6^+}	3.0112	3.0412	3.0723	3.0868	2.4234
^{96}Zr	χ_{2pp}	0.0105	0.0105	0.01022	0.01016	
	χ_{2pn}	0.026	0.02603	0.02044	0.02032	
	E_{HFB}	19.3916	19.3404	19.2733	19.2672	
	Q_{HFB}	2.5893	2.6300	0.4081	0.3933	
	E_{2^+}	1.7553	1.7567	1.7508	1.7876	1.7507
	E_{4^+}	2.7365	2.8147	2.9876	3.1821	3.1202
	E_{6^+}	5.9094	6.5165	5.5507	-	
^{96}Mo	χ_{2pp}	0.0105	0.0105	0.011779	0.01171	
	χ_{2pn}	0.02473	0.0245	0.023558	0.02342	
	E_{HFB}	5.2814	5.3053	5.1103	5.1520	
	Q_{HFB}	44.2408	43.2944	44.7574	43.8116	
	E_{2^+}	0.7758	0.7774	0.7781	0.7753	0.7782
	E_{4^+}	1.9447	1.9011	1.9560	1.9165	1.6281
	E_{6^+}	3.3426	3.2421	3.3665	3.2792	2.4406

Table 2.6 continued

Nuclei		$PQQ1$	$PQQHH1$	$PQQ2$	$PQQHH2$	Exp.
^{100}Mo	χ_{2pp}	0.0105	0.0105	0.010505	0.0104	
	χ_{2pn}	0.02102	0.020717	0.02101	0.0208	
	E_{HFB}	34.7380	34.8100	34.7247	34.8261	
	Q_{HFB}	51.2172	51.2645	51.1874	51.1959	
	E_{2^+}	0.5306	0.5321	0.5329	0.5347	0.5355
	E_{4^+}	1.5343	1.5334	1.5383	1.5378	1.1359
	E_{6^+}	2.8864	2.8842	2.8908	2.8891	
^{100}Ru	χ_{2pp}	0.0105	0.0105	0.01362	0.01349	
	χ_{2pn}	0.0313	0.0306	0.02724	0.02698	
	E_{HFB}	21.7229	22.1349	22.1605	22.2494	
	Q_{HFB}	60.2840	58.4752	60.0208	58.5762	
	E_{2^+}	0.5385	0.5399	0.5399	0.5320	0.5396
	E_{4^+}	1.7190	1.7246	1.7215	1.6990	1.2265
	E_{6^+}	3.4189	3.4358	3.4198	3.3835	2.0777
^{104}Ru	χ_{2pp}	0.0105	0.0105	0.01135	0.01142	
	χ_{2pn}	0.0238	0.0240	0.0227	0.02284	
	E_{HFB}	55.8788	55.4580	55.8676	55.4490	
	Q_{HFB}	64.6017	65.1667	64.4541	64.9618	
	E_{2^+}	0.3578	0.3573	0.3578	0.3574	0.35799
	E_{4^+}	1.1515	1.1524	1.1505	1.1524	0.8885
	E_{6^+}	2.3030	2.3111	2.2991	2.3104	1.5563
^{104}Pd	χ_{2pp}	0.0105	0.0105	0.01035	0.0104	
	χ_{2pn}	0.02054	0.0207	0.02070	0.0208	
	E_{HFB}	48.4522	48.4397	48.4667	48.4514	
	Q_{HFB}	55.8686	56.2952	55.8584	56.2814	
	E_{2^+}	0.5582	0.5555	0.5582	0.5556	0.5558
	E_{4^+}	1.7461	1.7481	1.7461	1.7485	1.32359
	E_{6^+}	3.4044	3.4310	3.4049	3.4318	2.2498

Table 2.6 continued

Nuclei		$PQQ1$	$PQQHH1$	$PQQ2$	$PQQHH2$	Exp.
^{110}Pd	χ_{2pp}	0.0105	0.0105	0.011273	0.01085	
	χ_{2pn}	0.023299	0.02230	0.022546	0.02170	
	E_{HFB}	54.3496	55.3412	54.3884	55.4540	
	Q_{HFB}	66.9156	62.6100	66.8010	62.3623	
	E_{2^+}	0.3733	0.3733	0.3748	0.3739	0.3738
	E_{4^+}	1.1929	1.2000	1.1985	1.2015	0.9208
	E_{6^+}	2.3692	2.4013	2.3818	2.4032	1.5739
^{110}Cd	χ_{2pp}	0.0105	0.0105	0.00957	0.00951	
	χ_{2pn}	0.01704	0.01849	0.01914	0.019020	
	E_{HFB}	55.5796	54.6336	54.9926	55.0943	
	Q_{HFB}	48.7175	53.2976	51.1335	50.1360	
	E_{2^+}	0.6574	0.6585	0.6576	0.6645	0.6577
	E_{4^+}	1.9580	1.9898	1.9602	2.0070	1.5424
	E_{6^+}	3.6863	3.7839	3.6822	3.8337	2.4799
^{128}Te	χ_{2pp}	0.0105	0.0105	0.01037	0.01045	
	χ_{2pn}	0.0206	0.02082	0.02074	0.02090	
	E_{HFB}	50.7831	50.6258	50.7241	50.6009	
	Q_{HFB}	37.4959	37.5739	37.4785	37.5923	
	E_{2^+}	0.7451	0.7432	0.7440	0.7424	0.7432
	E_{4^+}	1.5605	1.5534	1.5581	1.5528	1.4971
	E_{6^+}	2.6952	2.6810	2.6906	2.6802	1.8111
^{128}Xe	χ_{2pp}	0.0105	0.0105	0.0117	0.0112	
	χ_{2pn}	0.025458	0.02453	0.0234	0.0224	
	E_{HFB}	51.1383	52.3971	51.6475	52.7784	
	Q_{HFB}	61.8537	59.7865	61.6242	59.2707	
	E_{2^+}	0.4389	0.4510	0.4473	0.4484	0.4429
	E_{4^+}	1.3154	1.3382	1.3337	1.3183	1.0329
	E_{6^+}	2.4594	2.4909	2.4826	2.4352	1.7370

Table 2.6 continued

Nuclei		$PQQ1$	$PQQHH1$	$PQQ2$	$PQQHH2$	Exp.
^{130}Te	χ_{2pp}	0.0105	0.0105	0.01271	0.01057	
	χ_{2pn}	0.026	0.0204	0.02542	0.02114	
	E_{HFB}	35.8669	37.2704	35.5374	36.9659	
	Q_{HFB}	32.9693	27.1567	34.3438	28.3824	
	E_{2^+}	0.8397	0.8339	0.8366	0.8345	0.8395
	E_{4^+}	1.3582	1.2094	1.4198	1.2357	1.6325
	E_{6^+}	2.1162	1.9140	2.2462	1.9067	1.8145
^{130}Xe	χ_{2pp}	0.0105	0.0105	0.01200	0.010504	
	χ_{2pn}	0.0237	0.02200	0.02400	0.021008	
	E_{HFB}	34.2376	35.9352	32.8358	36.5554	
	Q_{HFB}	55.0921	52.3544	57.3170	51.0835	
	E_{2^+}	0.5370	0.5322	0.5344	0.5425	0.5361
	E_{4^+}	1.5356	1.5031	1.5761	1.4994	1.2046
	E_{6^+}	2.8467	2.7883	2.9788	2.7488	1.9444
^{150}Nd	χ_{2pp}	0.0105	0.0105	0.01042	0.01057	
	χ_{2pn}	0.02085	0.0212	0.02084	0.02114	
	E_{HFB}	153.6883	152.9843	153.6278	152.9235	
	Q_{HFB}	85.8091	85.9210	85.8360	85.9738	
	E_{2^+}	0.1303	0.1301	0.1302	0.1306	0.13012
	E_{4^+}	0.4316	0.4314	0.4313	0.4330	0.3815
	E_{6^+}	0.8982	0.8987	0.8974	0.9021	
^{150}Sm	χ_{2pp}	0.0105	0.0105	0.00819	0.00826	
	χ_{2pn}	0.0141	0.0143	0.01638	0.01652	
	E_{HFB}	156.5900	156.3113	156.9469	156.8386	
	Q_{HFB}	73.5688	75.0803	73.0783	74.6417	
	E_{2^+}	0.3348	0.3334	0.3339	0.3387	0.3339
	E_{4^+}	1.0281	1.0454	1.0243	1.0619	0.7733
	E_{6^+}	1.9694	2.0394	1.9607	2.0720	1.2788

Table 2.7: Comparison of calculated and experimentally observed [Raman *et al.* (2001)] reduced transition probabilities $B(E2{:}0^+ \rightarrow 2^+)$ and deformation parameter β_2 of ^{94,96}Zr, ^{94,96,100}Mo, ^{100,104}Ru, ^{104,110}Pd, ^{110}Cd, ^{128,130}Te, ^{128,130}Xe, ^{150}Nd and ^{150}Sm nuclei. Here $B(E2)$ is calculated for effective charge $e_p = 1 + e_{eff}$ and $e_n = e_{eff}$. Here (a), (b), (c) and (d) denote the $PQQ1$, $PQQHH1$, $PQQ2$ and $PQQHH2$ parametrizations, respectively. '*' denotes average $B(E2)$ values.

Nucleus		$B(E2{:}0^+ \rightarrow 2^+)$ $(e^2\mathrm{b}^2)$				β_2			
		Theory			Exp.	Theory			Exp.
		e_{eff}				e_{eff}			
		0.40	0.50	0.60		0.40	0.50	0.60	
^{94}Zr	(a)	0.065	0.086	0.111	0.066±0.014*	0.0899	0.1035	0.1171	0.090±0.010
	(b)	0.058	0.077	0.099	0.081±0.017	0.0849	0.0979	0.1109	
	(c)	0.173	0.225	0.284	0.056±0.014	0.1463	0.1669	0.1875	
	(d)	0.048	0.065	0.084		0.0773	0.0896	0.1019	
^{94}Mo	(a)	0.141	0.180	0.225	0.203±0.004*	0.1259	0.1423	0.1588	0.1509±0.0015
	(b)	0.145	0.185	0.230	0.230±0.040	0.1276	0.1442	0.1608	
	(c)	0.142	0.182	0.226	0.270±0.035	0.1263	0.1429	0.1595	
	(d)	0.144	0.184	0.230		0.1274	0.1440	0.1607	
^{96}Zr	(a)	0.045	0.060	0.078	0.055±0.022*	0.0738	0.0853	0.0968	0.080±0.017
	(b)	0.046	0.062	0.079		0.0745	0.0861	0.0977	
	(c)	0.042	0.056	0.072		0.0711	0.0820	0.0929	
	(d)	0.043	0.057	0.073		0.0716	0.0825	0.0935	
^{96}Mo	(a)	0.284	0.360	0.445	0.271±0.005*	0.1760	0.1982	0.2204	0.1720±0.0016
	(b)	0.274	0.348	0.430	0.310±0.047	0.1728	0.1948	0.2167	
	(c)	0.287	0.364	0.451	0.302±0.039	0.1769	0.1994	0.2218	
	(d)	0.277	0.353	0.437		0.1740	0.1962	0.2183	

Table 2.7 continued

Nucleus		$B(E2{:}0^+ \rightarrow 2^+)$ $(e^2\mathrm{b}^2)$				β_2			
		Theory			Exp.	Theory			Exp.
		e_{eff}				e_{eff}			
		0.40	0.50	0.60		0.40	0.50	0.60	
^{100}Mo	(a)	0.364	0.466	0.580	0.516±0.010*	0.1940	0.2194	0.2448	0.2309±0.0022
	(b)	0.367	0.469	0.584	0.511±0.009	0.1947	0.2202	0.2457	
	(c)	0.364	0.465	0.579	0.526±0.026	0.1939	0.2193	0.2447	
	(d)	0.366	0.468	0.583		0.1945	0.2200	0.2454	
^{100}Ru	(a)	0.534	0.677	0.837	0.490±0.005*	0.2242	0.2524	0.2807	0.2148±0.0011
	(b)	0.512	0.648	0.801	0.493±0.003	0.2195	0.2471	0.2747	
	(c)	0.518	0.659	0.816	0.494±0.006	0.2209	0.2490	0.2772	
	(d)	0.503	0.639	0.791		0.2177	0.2453	0.2730	
^{104}Ru	(a)	0.556	0.717	0.898	0.820±0.012*	0.2230	0.2532	0.2833	0.2707±0.0020
	(b)	0.566	0.729	0.913	0.93±0.06	0.2250	0.2553	0.2857	
	(c)	0.550	0.709	0.889	1.04±0.16	0.2217	0.2517	0.2818	
	(d)	0.558	0.720	0.902		0.2234	0.2536	0.2839	
^{104}Pd	(a)	0.449	0.575	0.716	0.535±0.035*	0.1917	0.2168	0.2420	0.209±0.007
	(b)	0.455	0.582	0.724	0.61±0.09	0.1928	0.2181	0.2433	
	(c)	0.450	0.575	0.717	0.535±0.035	0.1918	0.2169	0.2421	
	(d)	0.455	0.582	0.724		0.1929	0.2181	0.2433	
^{110}Pd	(a)	0.667	0.850	1.054	0.870±0.040*	0.2250	0.2539	0.2828	0.257±0.006
	(b)	0.583	0.746	0.928	0.780±0.120	0.2104	0.2379	0.2653	
	(c)	0.660	0.841	1.044	0.820±0.080	0.2237	0.2526	0.2814	
	(d)	0.578	0.739	0.919		0.2094	0.2368	0.2641	

Table 2.7 continued

Nucleus		$B(E2{:}0^+ \rightarrow 2^+)$ $(e^2\mathrm{b}^2)$				β_2			
		Theory			Exp.	Theory			Exp.
		e_{eff}				e_{eff}			
		0.40	0.50	0.60		0.40	0.50	0.60	
^{110}Cd	(a)	0.351	0.451	0.562	0.450±0.020*	0.1565	0.1772	0.1980	0.1770±0.0039
	(b)	0.416	0.534	0.666	0.504±0.040	0.1702	0.1929	0.2155	
	(c)	0.387	0.496	0.619	0.467±0.019	0.1642	0.1859	0.2076	
	(d)	0.375	0.481	0.600		0.1617	0.1831	0.2045	
^{128}Te	(a)	0.247	0.315	0.392	0.383±0.006*	0.1094	0.1237	0.1380	0.1363±0.0011
	(b)	0.253	0.323	0.403	0.380±0.009	0.1107	0.1252	0.1398	
	(c)	0.247	0.316	0.393	0.387±0.011	0.1095	0.1237	0.1380	
	(d)	0.253	0.324	0.403		0.1108	0.1253	0.1399	
^{128}Xe	(a)	0.601	0.771	0.961	0.750±0.040*	0.1644	0.1862	0.2079	0.1836±0.0049
	(b)	0.576	0.739	0.922	0.790±0.040	0.1610	0.1823	0.2037	
	(c)	0.593	0.761	0.950	0.890±0.230	0.1634	0.1850	0.2067	
	(d)	0.572	0.733	0.914		0.1604	0.1816	0.2028	
^{130}Te	(a)	0.221	0.277	0.339	0.295±0.07*	0.1024	0.1147	0.1270	0.1184±0.0014
	(b)	0.181	0.226	0.276	0.290±0.011	0.0928	0.1037	0.1146	
	(c)	0.230	0.289	0.356	0.260±0.050	0.1046	0.1173	0.1300	
	(d)	0.191	0.239	0.292		0.0952	0.1065	0.1178	
^{130}Xe	(a)	0.524	0.665	0.822	0.65±0.05*	0.1519	0.1711	0.1904	0.169±0.007
	(b)	0.488	0.620	0.769	0.631±0.048	0.1466	0.1654	0.1841	
	(c)	0.551	0.702	0.870	0.640±0.160	0.1559	0.1758	0.1958	
	(d)	0.469	0.596	0.738		0.1438	0.1620	0.1803	

Table 2.7 continued

Nucleus		$B(E2{:}0^+ \rightarrow 2^+)$ $(e^2\mathrm{b}^2)$				β_2			
		Theory			Exp.	Theory			Exp.
		e_{eff}				e_{eff}			
		0.40	0.50	0.60		0.40	0.50	0.60	
^{150}Nd	(a)	2.201	2.667	3.178	2.760±0.040*	0.2548	0.2805	0.3062	0.2853±0.0021
	(b)	2.220	2.692	3.210	2.640±0.080	0.2558	0.2818	0.3077	
	(c)	2.203	2.670	3.182	2.670±0.100	0.2549	0.2806	0.3063	
	(d)	2.223	2.696	3.215		0.2560	0.2820	0.3079	
^{150}Sm	(a)	1.460	1.785	2.143	1.350±0.030*	0.2008	0.2221	0.2433	0.1931±0.0021
	(b)	1.538	1.881	2.259	1.470±0.090	0.2061	0.2279	0.2498	
	(c)	1.421	1.739	2.090	1.440±0.150	0.1981	0.2192	0.2402	
	(d)	1.500	1.837	2.208		0.2035	0.2253	0.2470	

Table 2.8 : Comparison of calculated and experimentally observed g factors $g(2^+)$ [Raghavan (1989)] of ^{94,96}Zr, ^{94,96,100}Mo, ^{100,104}Ru, ^{104,110}Pd, ^{110}Cd, ^{128,130}Te, ^{128,130} Xe, ^{150}Nd and ^{150}Sm nuclei. The $g(2^+)$ has been calculated in units of nuclear magneton for$g_l^\pi = 1.0$, $g_l^\nu = 0.0$ and $g_s^\pi = g_s^\nu = 0.50$. '*' value taken from [Speidel *et al.* (2002)].

Nuclei	Theory				Exp.
	$PQQ1$	$PQQHH1$	$PQQ2$	$PQQHH2$	
^{94}Zr	0.177	0.162	0.522	0.106	-0.329±0.015*
^{94}Mo	0.282	0.293	0.277	0.286	-
^{96}Zr	0.385	0.396	0.414	0.420	-
^{96}Mo	0.610	0.596	0.598	0.586	-
^{100}Mo	0.645	0.654	0.644	0.655	0.34±0.18
^{100}Ru	0.514	0.520	0.506	0.508	0.51±0.07
^{104}Ru	0.384	0.379	0.378	0.374	0.41±0.05
^{104}Pd	0.489	0.499	0.490	0.500	0.46±0.04
^{110}Pd	0.431	0.478	0.429	0.480	0.37±0.03
^{110}Cd	0.510	0.449	0.477	0.506	0.31±0.07
^{128}Te	0.635	0.639	0.636	0.639	0.35±0.04
^{128}Xe	0.447	0.456	0.443	0.454	0.41±0.07
^{130}Te	0.709	0.837	0.681	0.809	0.33±0.08
^{130}Xe	0.483	0.495	0.469	0.502	0.38±0.07
^{150}Nd	0.602	0.603	0.601	0.602	0.422±0.039
^{150}Sm	0.490	0.498	0.474	0.483	0.411±0.032

Chapter 3

$2\nu\beta^-\beta^-$ decay of ^{94,96}Zr, ^{100}Mo, ^{104}Ru, ^{110}Pd, ^{128,130}Te and ^{150}Nd isotopes for the $0^+ \rightarrow 0^+$ transition

Over the past three decades, many a remarkable advances have been achieved in the experimental observations of $2\nu\beta^-\beta^-$ decay in the mass range $A = 90 - 150$ [Tretyak *et al.* (1995), (2002), Barabash (2010), (2019)]. The $2\nu\beta^-\beta^-$ decay modes have been observed experimentally for the $0^+ \rightarrow 0^+$ transitions in case of eleven nuclei, namely ^{48}Ca, ^{76}Ge, ^{82}Se, ^{96}Zr, ^{100}Mo, ^{116}Cd, ^{128,130}Te, ^{136}Xe, ^{150}Nd and ^{238}U isotopes. It is found that NTMEs $M_{2\nu}$ extracted from the observed half-life $T^{2\nu}_{1/2}(0^+ \rightarrow 0^+)$ of $2\nu\beta^-\beta^-$ decay are highly quenched. In spite of putting the best theoretical efforts over the last three decades, understanding of this observed quenching and reproduce them theoretically is a challenging task. We also do not have a complete solution of this problem. However, we try a systematic approach based on the basic principles of nuclear many-body theory.

The present chapter is organized as follows. In Section 3.1, we present the theoretical formalism to calculate the half-life of the $2\nu\beta^-\beta^-$ decay. In Section 3.2, the results of $2\nu\beta^-\beta^-$ decay of ^{94,96}Zr, ^{100}Mo, ^{104}Ru, ^{110}Pd, ^{128,130}Te and ^{150}Nd nuclei for the $0^+ \rightarrow 0^+$ transition are given and discussed. In the same section, the effect of deformation on $M_{2\nu}$ is also investigated. Finally, the conclusions are given in Section 3.3.

3.1 Theoretical formalism

The theoretical formalism to calculate the half-life of the $2\nu\beta^-\beta^-$ decay has been given in a number of reviews [Haxton and Stephenson (1984), Doi *et al.* (1985), (1992), Tomoda (1991) and Suhonen and Civitarese (1998)]. We briefly outline steps to derive the $2\nu\beta^-\beta^-$ decay rate formula following the notations of Doi *et al.* (1985).

3.1.1 Effective Hamiltonian for β^- decay

In LR symmetric models, the charged-current interaction Lagrangian L_{LR} due to the addition of extra gauge boson W_R is given by

$$L_{LR} = \frac{g}{2\sqrt{2}} \left[j_L^{\mu} W_{L\mu} + j_R^{\mu} W_{R\mu} \right] + h.c. \tag{3.1}$$

where the left and right handed weak leptonic $V \pm A$ currents are written as

$$j_L^{\mu} = \overline{e}\gamma^{\mu} \left(1 - \gamma_5\right) \nu_{eL} \qquad j_R^{\mu} = \overline{e}\gamma^{\mu} \left(1 + \gamma_5\right) \nu_{eR}^{'} \tag{3.2}$$

with

$$\nu_{eL} = \sum_i U_{ei} N_{ji} \qquad \nu_{eR}^{\prime} = \sum_i V_{ei} N_{iR} \tag{3.3}$$

The mixing matrices U and V satisfy the following orthonormality conditions.

$$\sum_i |U_{ei}|^2 = 1 \qquad \sum_i |V_{ei}|^2 = 1 \qquad \sum_i U_{ei}V_{ei} = 0 \tag{3.4}$$

The gauge bosons W_L and W_R are related to mass eigenstates W_1 and W_2 with masses M_1 and M_2 respectively by

$$\begin{pmatrix} W_L \\ W_R \end{pmatrix} = \begin{pmatrix} \cos\zeta & \sin\zeta \\ -\sin\zeta & \cos\zeta \end{pmatrix} \begin{pmatrix} W_1 \\ W_2 \end{pmatrix} \tag{3.5}$$

Including hadronic currents, the Lagrangian L_{LR} leads to the weak interaction effective Hamiltonian H_W given by

$$H_W = \left(\frac{G}{\sqrt{2}}\right)\left[j_{L\mu}J_L^{\mu\dagger} + \kappa j_{L\mu}J_R^{\mu\dagger} + \eta j_{R\mu}J_L^{\mu\dagger} + \lambda j_{R\mu}J_R^{\mu\dagger}\right] + h.c. \tag{3.6}$$

where

$$\frac{G}{\sqrt{2}} = \frac{g^2}{8M_1^2}\left[\cos^2\zeta + \left(\frac{M_1}{M_2}\right)^2 \sin^2\zeta\right] \tag{3.7}$$

$$\lambda = \frac{\left[\left(\frac{M_1}{M_2}\right)^2 + \tan^2\zeta\right]}{\left[1 + \left(\frac{M_1}{M_2}\right)^2 \tan^2\zeta\right]} \tag{3.8}$$

and

$$\eta = \kappa = \frac{\left[1 - \left(\frac{M_1}{M_2}\right)^2\right]\tan\zeta}{\left[1 + \left(\frac{M_1}{M_2}\right)^2 \tan^2\zeta\right]} \tag{3.9}$$

Here, the coupling constants κ, η and λ are small ($\ll 1$) parameters and $G = 1.16637\times10^{-5}$ GeV^{-2}. The left and right handed weak $V \pm A$ hadronic currents are given by

$$J_L^{\mu\dagger} = g_V\overline{u}\gamma^\mu(1-\gamma_5)\,d \qquad J_R^{\mu\dagger} = g'_V\overline{u}\gamma^\mu(1+\gamma_5)\,d \tag{3.10}$$

where

$$g_V = \cos\theta_c \qquad g'_V = e^{i\alpha}\cos\theta'_c \tag{3.11}$$

In Eq. (3.11), the θ_c and θ'_c are the Cabibbo-Kobayashi-Maskawa (CKM) mixing angles for the left- and right-handed d and s quarks. The CP violating phase α is due to both the mixing of right handed quarks and the mixing of left and right gauge bosons.

In the nonrelativistic impulse approximation, the left and right handed hadronic currents for nuclear $\beta^-\beta^-$ decay in $V \pm A$ forms are given by

$$J_L^{\mu\dagger}(x) = \sum_{n=1}^{A}\left[(g_V - g_A C_n)g^{\mu 0} + (g_A\sigma_n^k - g_V \mathbf{D}_n^k)g^{\mu k}\right]\delta(\mathbf{x} - \mathbf{r}_n)\,\tau_n^+ \tag{3.12}$$

$$J_R^{\mu\dagger}(x) = \sum_{n=1}^{A}\left[(g_V + g_A C_n)g^{\mu 0} + (-g_A\sigma_n^k - g_V \mathbf{D}_n^k)g^{\mu k}\right]\delta(\mathbf{x} - \mathbf{r}_n)\,\tau_n^+ \tag{3.13}$$

The nuclear recoil terms C_n and $\mathbf{D}_n$ are defined as follows

$$C_n = \frac{1}{2M}\left[(\mathbf{P}_n + \mathbf{P}'_n)\cdot\boldsymbol{\sigma}_n - \left(\frac{g_P}{g_A}\right)(E_n - E'_n)\,\boldsymbol{\sigma}_n\cdot\mathbf{Q}_n\right] \tag{3.14}$$

$$\mathbf{D}_n = \frac{1}{2M}\left[(\mathbf{P}_n + \mathbf{P}'_n) - i\left(1 - 2M\left(\frac{g_W}{g_V}\right)\right)\boldsymbol{\sigma}_n\times\mathbf{Q}_n\right] \tag{3.15}$$

where $\mathbf{Q}_n = \mathbf{P}_n - \mathbf{P}'_n$. The g_V, g_A, g_P and g_W are vector, axial vector, pseudoscalar and weak magnetism terms. At $q^2 = 0$,

$$g_V(0) = 1.0 \qquad g_A(0) = 1.25 \qquad \frac{g_p}{g_A} = \frac{2M_P}{m_\pi^2} \tag{3.16}$$

where M_P and m_π are the proton and pion masses. By the CVC hypothesis $g_W(0) = \kappa_\beta/2M$ and $\kappa_\beta = 3.70$, where M and κ_β are the mass and isovector anomalous magnetic moment of nucleons respectively.

3.1.2 Decay rate of $2\nu\beta^-\beta^-$ mode for the $0^+ \rightarrow 0^+$ transition

The $2\nu\beta^-\beta^-$ decay is allowed in the *SM* of electroweak unification and therefore, processes which involve left handed currents only, give dominant contribution. The following assumptions are made in deriving the $2\nu\beta^-\beta^-$ decay rate formula for the $0^+ \rightarrow 0^+$ transition.

(i) The light neutrino species are considered only. Hence, the normalization condition for the left handed neutrinos given by Eq. (3.4) can be recast in to the form

$$\sum_i{}' |U_{ei}|^2 \approx 1 \tag{3.17}$$

(ii) The masses of these light neutrinos are assumed to be much smaller than $Q_{\beta\beta} = E_I - E_F - 2m_e$.

(iii) The s-wave state of the electron and the neutrino wave functions are retained. The total angular momentum of four s-wave leptons can be 0, 1 or 2 and is equal to the total angular momentum transferred from the nucleus.

(iv) The initial and the final nucleus differ by two units of isospin for any $\beta^-\beta^-$ decay of practical interest. The contributions of the successive Fermi transitions can be safely neglected as they come from isospin mixing effects.

(v) The recoil terms are usually neglected.

Under these assumptions, the inverse half-life of the $2\nu\beta^-\beta^-$ decay for the $0^+ \rightarrow 0^+$ transition is written as

$$[T^{2\nu}_{1/2}(0^+ \rightarrow 0^+)]^{-1} = \frac{a_{2\nu}}{\ln 2} \int d\Omega_{2\nu}\, a(\varepsilon_1, \varepsilon_2) \left| \sum_N \left[M^{2\nu}_{GTN} - \left(\frac{g_V}{g_A}\right)^2 M^{2\nu}_{FN} \right] \frac{1}{2} (K_N + L_N) \right|^2 \tag{3.18}$$

where the constant term $a_{2\nu}$ is expressed as

$$a_{2\nu} = \left[\frac{(G g_A)^4 m_e^9}{64\pi^7} \right] \xi_p \tag{3.19}$$

and the phase space volume element $d\Omega_{2\nu}$ is given by

$$\begin{aligned} d\Omega_{2\nu} &= m_e^{-11} q_1 q_2 \omega_1 \omega_2 p_1 p_2 \varepsilon_1 \varepsilon_2 \delta(\varepsilon_1 + \varepsilon_2 + \omega_1 + \omega_2 + E_F - E_I) \\ &\quad \times d\omega_1 d\omega_2 d\varepsilon_1 d\varepsilon_2 d(\widehat{\mathbf{p}}_1 \cdot \widehat{\mathbf{p}}_2) \end{aligned} \tag{3.20}$$

Here, $\varepsilon_k = \sqrt{p_k^2 + m_e^2}$ and $\omega_k = \sqrt{q_k^2 + m_\nu^2}$ are the energies of the k^{th} electron and neutrino respectively. Further, E_I and E_F are the masses of the parent and daughter nuclei. The neutrino mixing effect represented by ξ_p is practically equal to 1. The Coulomb correction factor $a(\varepsilon_1,\varepsilon_2)$ is approximately given by

$$a\left(\varepsilon_1, \varepsilon_2\right) \approx F_0\left(Z, \varepsilon_1\right) F_0\left(Z, \varepsilon_2\right) \tag{3.21}$$

where, the Fermi function $F_0\left(Z, \varepsilon\right)$ is defined as the square of the ratio of relativistic s-wave scattering solution for a point charge Z to a plane wave evaluated at the nuclear surface, and is written as

$$F_{k-1}(Z, \varepsilon) = \left[\frac{\Gamma(2k+1)}{\Gamma(k)\Gamma(2\gamma_k+1)}\right]^2 (2pR)^{2(\gamma_k - k)} \left|\Gamma(\gamma_k + iy)\right|^2 e^{\pi y} \tag{3.22}$$

with

$$\gamma_k = \sqrt{k^2 - (\alpha Z)^2} \qquad \text{and} \qquad y = \frac{\alpha Z \varepsilon}{p} \tag{3.23}$$

The combination of energy denominators, which appear in the second order perturbation are

$$K_N = \frac{2m_e}{\mu_N + (\varepsilon_1 + \omega_1 - \varepsilon_2 - \omega_2)} + \frac{2m_e}{\mu_N - (\varepsilon_1 + \omega_1 - \varepsilon_2 - \omega_2)} \tag{3.24}$$

$$L_N = \frac{2m_e}{\mu_N + (\varepsilon_1 + \omega_2 - \varepsilon_2 - \omega_1)} + \frac{2m_e}{\mu_N - (\varepsilon_1 + \omega_2 - \varepsilon_2 - \omega_1)} \tag{3.25}$$

where

$$\mu_N m_e = E_N - \left(E_I + E_F\right) / 2 \tag{3.26}$$

where E_N is the energy of the intermediate nucleus N. The reduced nuclear matrix element due to the double Fermi and double Gamow-Teller transitions are given by

$$M^{2\nu}_{FN} \equiv \langle 0^+_F || \sum_n \tau^+_n || 0^+_N \rangle \langle 0^+_N || \sum_m \tau^+_m || 0^+_I \rangle \tag{3.27}$$

$$M^{2\nu}_{GTN} \equiv -\langle 0^+_F || \sum_n \boldsymbol{\sigma}_n \tau^+_n || 1^+_N \rangle \langle 1^+_N || \sum_m \boldsymbol{\sigma}_m \tau^+_m || 0^+_I \rangle \tag{3.28}$$

The minus sign in the definition $M^{(2\nu)}_{GTN}$ is introduced so that by the closure property, we have

$$M^{2\nu}_{GTc} \equiv \sum_N M^{2\nu}_{GTN} = \langle 0^+_F || \sum_{n,m} \boldsymbol{\sigma}_n \cdot \boldsymbol{\sigma}_m \tau^+_n \tau^+_m || 0^+_I \rangle \tag{3.29}$$

The energy denominators K_N and L_N depend on the energies of electrons and neutrinos. Hence, the integration to calculate phase space factor is to be made for each intermediate state and is a time consuming procedure. However, there is a procedure to bypass it. It is observed that the energy spectrum peaks at

$$(\varepsilon_1 - m_e) \sim (\varepsilon_2 - m_e) \sim \omega_1 \sim \omega_2 \sim \frac{Tm_e}{4} \tag{3.30}$$

where Tm_e is the maximum kinetic energy release,

$$Tm_e = Q_{\beta^-\beta^-} = E_I - E_F - 2m_e \tag{3.31}$$

Therefore, one can take

$$(\varepsilon_k + \omega_l - \varepsilon_{k'} - \omega_{l'}) \approx 0 \tag{3.32}$$

as a good approximation and thus,

$$K_N \simeq L_N \simeq \frac{2}{\mu_N} \tag{3.33}$$

The error of the above approximation is of the order of $[(\varepsilon_k + \omega_l - \varepsilon_{k'} - \omega_{l'})/\mu_N m_e]^2$. With

these assumptions, the inverse half-life of $2\nu\beta^-\beta^-$ decay is given by

$$[T^{2\nu}_{1/2}(0^+ \to 0^+)]^{-1} = G_{GT}(<\mu_N>) \left| \left(\sum_N \frac{M^{2\nu}_{GTN}}{\mu_N} \right) - \left(\frac{g_V}{g_A} \right)^2 \left(\sum_N \frac{M^{(2\nu)}_{FN}}{\mu_N} \right) \right|^2 \tag{3.34}$$

with

$$G_{GT}\,(<\mu_N>) = \frac{a_{2\nu}}{\ln 2} \int d\Omega_{2\nu}\, a(\varepsilon_1, \varepsilon_2) <\mu_N>^2 \left(\frac{<K_N> + <L_N>}{2} \right)^2 \tag{3.35}$$

Here $<\mu_N>$ is some average value of μ_N, and $<K_N>$ and $<L_N>$ are the quantities obtained from K_N and L_N by replacing μ_N with $<\mu_N>$. To derive the above formula, first we replace K_N and L_N by $2/\mu_N$ and the sum over N is taken. Next, the factor $<\mu_N>^2\ [(<K_N> + <L_N>)/2]^2$ is introduced for the phase space integration in order to take into account the energy dependence of leptons in K_N and L_N. If the $<\mu_N>$ dependence of the integrated kinematical factor $G_{GT}(<\mu_N>)$ is minor, the above approximation is valid. The half-life formula is further simplified if one uses the fact that

$$\left| \sum_N \frac{M^{2\nu}_{GTN}}{\mu_N} \right| \gg \left| \sum_N \frac{M^{(2\nu)}_{FN}}{\mu_N} \right| \tag{3.36}$$

Finally, the inverse half-life of the $2\nu\beta^-\beta^-$ decay for the $0^+ \to 0^+$ transition is given by

$$[T^{2\nu}_{1/2}(0^+ \to 0^+)]^{-1} = G_{2\nu}|M_{2\nu}|^2 \tag{3.37}$$

where the integrated kinematical factor $G_{2\nu}$ can be calculated with good accuracy [Doi *et al.* (1985), (1992) and Boehm and Vogel (1992)]. The phase space integral of $2\nu\beta^-\beta^-$ decay for the $0^+ \to 0^+$ transition can be rewritten as

$$G_{2\nu} = \frac{2(Gg_A)^4}{64\pi^7 m_e^2 \ln(2)} \int_{m_e}^{T+m_e} F_0\,(Z, \varepsilon_1)\, p_1 \varepsilon_1 I^{(0)}\,(T, \varepsilon_1)\, d\varepsilon_1 \tag{3.38}$$

$$= g_{2\nu} \int_{m_e}^{T+m_e} F_0\,(Z, \varepsilon_1)\, p_1 \varepsilon_1 I^{(0)}\,(T, \varepsilon_1)\, d\varepsilon_1 \tag{3.39}$$

where

$$g_{2\nu} = \frac{2(Gg_A)^4}{64\pi^7 m_e^2 \ln(2)} \tag{3.40}$$

$$I^{(0)}(T, \varepsilon_1) = \int_{m_e}^{T+2m_e-\varepsilon_1} F_0(Z, \varepsilon_2)\, p_2 \varepsilon_2 \left(T + 2 - \varepsilon_1 - \varepsilon_2\right)^5 d\varepsilon_2 \tag{3.41}$$

and the total kinetic energy release T is given by

$$T m_e = \varepsilon_1 + \varepsilon_2 \tag{3.42}$$

The NTME $M_{2\nu}$ is given by

$$\begin{aligned} M_{2\nu} &= \sum_N \frac{\langle 0_F^+ || \boldsymbol{\sigma}\tau^+ || 1_N^+ \rangle \langle 1_N^+ || \boldsymbol{\sigma}\tau^+ || 0_I^+ \rangle}{E_N - (E_I + E_F)/2} \\ &= \sum_N \frac{\langle 0_F^+ || \boldsymbol{\sigma}\tau^+ || 1_N^+ \rangle \langle 1_N^+ || \boldsymbol{\sigma}\tau^+ || 0_I^+ \rangle}{E_0 + E_N - E_I} \end{aligned} \tag{3.43}$$

with

$$E_0 = \frac{1}{2}(E_I - E_F) = \frac{1}{2} Q_{\beta\beta} + m_e \tag{3.44}$$

One has to perform a sum over all the intermediate states 1_N^+ in order to compute Eq. (3.43). However, it is not possible to study the structure of odd-odd nuclei in the present version of the PHFB model. Hence, we have carried out the summation over intermediate states by using the *summation method* given by Civitarese and Suhonen (1993) [Chandra *et al.* (2005)].

3.1.3 NTME in the PHFB model

The energy denominator in Eq. (3.43) and $x_N = (E_N - E_I)/E_0$ are always positive. Hence, the Eq. (3.43) can be written as

$$M_{2\nu} = \frac{1}{E_0} \sum_N \left\langle 0_F^+ \left| \boldsymbol{\Gamma} \right| N \right\rangle \left\langle N \left| \boldsymbol{\Gamma} \right| 0_I^+ \right\rangle \int_0^\infty e^{-t(1+x_N)} dt \tag{3.45}$$

where the Gamow-Teller (GT) operator $\mathbf{\Gamma} = \boldsymbol{\sigma}\tau^+$. The variable of integration is changed from t to $\omega = t/E_0$, which is allowed as $E_0 > 0$. By replacing $e^{-\omega E_N}\ |N\rangle$ by $e^{-\omega H}\ |N\rangle$ and $e^{-\omega E_I}\ \left|0_I^+\right\rangle$ by $e^{-\omega H}\ \left|0_I^+\right\rangle$, which is again possible as the intermediate states $|N\rangle$ and the initial states $\left|0_I^+\right\rangle$ are eigenstates of the nuclear Hamiltonian H, one obtains after summing over all the intermediate states

$$M_{2\nu} = \int_0^\infty \left\langle 0_F^+ \left| \mathbf{\Gamma} e^{-\omega H} \mathbf{\Gamma} e^{\omega H} \right| 0_I^+ \right\rangle e^{-\omega E_0} d\omega \tag{3.46}$$

Using the Baker-Hausdorff lemma, we make the multiple commutators expansion as

$$e^{-\omega H} \mathbf{\Gamma} e^{\omega H} = \sum_{k=0}^{\infty} \frac{(-1)^k \omega^k}{k!} \left[H, [H, ..., [H, \mathbf{\Gamma}] .....]\right]^{(k\ times)} \tag{3.47}$$

Integrating Eq. (3.46), one obtains

$$M_{2\nu} = \frac{1}{E_0} \left\langle 0_F^+ \left| \sum_\mu (-1)^\mu \Gamma_{-\mu} F_\mu \right| 0_I^+ \right\rangle \tag{3.48}$$

where Γ_μ is given by

$$\Gamma_\mu = \sigma_\mu \tau^+ \tag{3.49}$$

and

$$F_\mu = \sum_{\lambda=0}^{\infty} \frac{(-1)^\lambda}{E_0^\lambda} D_\lambda \Gamma_\mu \tag{3.50}$$

with

$$D_\lambda \Gamma_\mu = \left[H, [H, ..., [H, \Gamma_\mu] .....]\right]^{(\lambda\ \text{times})} \tag{3.51}$$

The Eq. (3.48) can be further simplified, when the GT operator commutes with the effective two-body interaction. For example, the GT operator commutes with the two-body interaction in the case of pseudo-SU(3) model [Castaños *et al.* (1994), Hirsch *et al.* (1995), Ceron *et al.* (1999)], and the energy denominator is a well-defined quantity

without any free parameter. It has been evaluated exactly for $2\nu\beta^-\beta^-$ [Castaños *et al.* (1994), Hirsch *et al.* (1995)] and $2\nu ECEC$ modes [Ceron *et al.* (1999)] in the pseudo-SU(3) scheme.

In the present work, we use a Hamiltonian with $PQQHH$ type of effective two-body interaction, which does not commute with the GT operator. Hence, the energy denominator is not a well-defined quantity. However, the violation of isospin symmetry for the $QQHH$ part of our model Hamiltonian is negligible as is evident from the parameters of the two-body interaction given in Section 2.3. Further, the violation of isospin symmetry for the pairing part of the two-body interaction is presumably small. With these assumptions, the NTME $M_{2\nu}$ of $2\nu\beta^-\beta^-$ decay for the $0^+ \rightarrow 0^+$ transition in the PHFB model in conjunction with the summation method can be derived as follows. Using

$$\begin{aligned} \left[H, a_\pi^\dagger a_\nu\right] &= \left[H_\pi + H_\nu, a_\pi^\dagger a_\nu\right] \\ &= \sum_{nljm} \left(\varepsilon_\pi - \varepsilon_\nu\right) a_\pi^\dagger a_\nu \end{aligned} \tag{3.52}$$

where H_α consists of one-body part of the Hamiltonian only,

$$H_\alpha = \sum_{nljm} \varepsilon_\alpha(n,l,j) a_\alpha^\dagger(nljm) a_\alpha(nljm) \tag{3.53}$$

one obtains

$$\begin{aligned} D_\lambda \Gamma_\mu &= [H_\pi + H_\nu, [H_\pi + H_\nu, ..., [H_\pi + H_\nu, \Gamma_\mu] .....]]^{(\lambda \text{ times})} \\ &= \sum_{nljm} \left[\varepsilon(n_\pi, l_\pi, j_\pi) - \varepsilon(n_\nu, l_\nu, j_\nu)\right]^\lambda \sigma_\mu \tau^+ \end{aligned} \tag{3.54}$$

and F_μ is written as

$$\begin{aligned} F_\mu &= \sum_{\lambda=0}^{\infty} \frac{(-1)^\lambda}{E_0^\lambda} D_\lambda \Gamma_\mu \\ &= \sum_{\pi\nu} \sum_{\lambda=0}^{\infty} \left(\frac{-1}{E_0}\right)^\lambda \left[\varepsilon(n_\pi, l_\pi, j_\pi) - \varepsilon(n_\nu, l_\nu, j_\nu)\right]^\lambda \sigma_\mu \tau^+ \\ &= \sum_{\pi\nu} \frac{E_0}{E_0 + \varepsilon(n_\pi, l_\pi, j_\pi) - \varepsilon(n_\nu, l_\nu, j_\nu)} \sigma_\mu \tau^+ \end{aligned} \tag{3.55}$$

and the Eq. (3.46) can be further simplified to

$$M_{2\nu} = \sum_{\pi,\nu} \frac{\langle 0_F^+ || \boldsymbol{\sigma} \cdot \boldsymbol{\sigma} \tau^+ \tau^+ || 0_I^+ \rangle}{E_0 + \varepsilon(n_\pi, l_\pi, j_\pi) - \varepsilon(n_\nu, l_\nu, j_\nu)} \tag{3.56}$$

We have evaluated the energy denominator as follows. With the assumption that the difference in single particle energies of protons in the intermediate nucleus and neutrons in the parent nucleus is mainly due to the difference in Coulomb energies, one obtains

$$\varepsilon(n_\pi, l_\pi, j_\pi) - \varepsilon(n_\nu, l_\nu, j_\nu) = \begin{cases} \Delta_C & for \quad n_\nu = n_\pi, l_\nu = l_\pi, j_\nu = j_\pi \\ \Delta_C + \Delta E_{s.o.splitting} & for \quad n_\nu = n_\pi, l_\nu = l_\pi, j_\nu \neq j_\pi \end{cases}, \tag{3.57}$$

where the Coulomb energy difference Δ_C is given by Bohr and Mottelson (1998).

$$\Delta_C = \frac{0.70}{A^{1/3}} \left[(2Z+1) - 0.76 \left\{(Z+1)^{4/3} - Z^{4/3}\right\}\right] \; MeV \tag{3.58}$$

Finally, one obtains the following expression for the NTME $M_{2\nu}$ of $2\nu\beta^-\beta^-$ decay for the $0^+ \rightarrow 0^+$ transition [Chandra *et al.* (2005)].

$$\begin{aligned} M_{2\nu} &= \sum_{\pi,\nu} \frac{\langle \Psi_{00}^{J_f=0} || \boldsymbol{\sigma} \cdot \boldsymbol{\sigma} \tau^+ \tau^+ || \Psi_{00}^{J_i=0} \rangle}{E_0 + \varepsilon(n_\pi, l_\pi, j_\pi) - \varepsilon(n_\nu, l_\nu, j_\nu)} \\ &= \left[n_{(Z,N)}^{Ji=0} n_{(Z+2,N-2)}^{J_f=0}\right]^{-1/2} \int_0^\pi n_{(Z,N),(Z+2,N-2)}(\theta) \sum_{\alpha\beta\gamma\delta} \frac{\langle \alpha\beta \,|\boldsymbol{\sigma}_1.\boldsymbol{\sigma}_2 \tau^+\tau^+| \,\gamma\delta\rangle}{E_0 + \varepsilon_\alpha(n_\pi, l_\pi, j_\pi) - \varepsilon_\gamma(n_\nu, l_\nu, j_\nu)} \\ &\quad \times \sum_{\varepsilon\eta} \frac{\left(f_{Z+2,N-2}^{(\pi)*}\right)_{\varepsilon\beta} \left(F_{Z,N}^{(\nu)*}\right)_{\eta\delta}}{\left[\left(1 + F_{Z,N}^{(\pi)}(\theta) f_{Z+2,N-2}^{(\pi)*}\right)\right]_{\varepsilon\alpha} \left[\left(1 + F_{Z,N}^{(\nu)}(\theta) f_{Z+2,N-2}^{(\nu)*}\right)\right]_{\gamma\eta}} sin\theta d\theta \end{aligned} \tag{3.59}$$

where

$$n^J = \int_0^\pi \left[det\left(1 + F^{(\pi)} f^{(\pi)\dagger}\right)\right]^{1/2} \left[det\left(1 + F^{(\nu)} f^{(\nu)\dagger}\right)\right]^{1/2} d^J_{00}(\theta) sin(\theta) d\theta \tag{3.60}$$

and

$$n_{(Z,N),(Z+2,N-2)}(\theta) = \left[det\left(1 + F^{(\nu)}_{Z,N} f^{(\nu)\dagger}_{Z+2,N-2}\right)\right]^{1/2} \times \left[det\left(1 + F^{(\pi)}_{Z,N} f^{(\pi)\dagger}_{Z+2,N-2}\right)\right]^{1/2} \tag{3.61}$$

The $\pi(\nu)$ represents the proton (neutron) of nuclei involved in the $2\nu\beta^-\beta^-$ decay process. The matrices $f_{Z,N}$ and $F_{Z,N}(\theta)$ are given by

$$f_{Z,N} = \sum_i C_{ij_\alpha,m_\alpha} C_{ij_\beta,m_\beta} \left(v_{im_\alpha}/u_{im_\alpha}\right) \delta_{m_\alpha,-m_\beta} \tag{3.62}$$

$$F_{Z,N}(\theta) = \sum_{m'_\alpha m'_\beta} d^{j_\alpha}_{m_\alpha,m'_\alpha}(\theta) d^{j_\beta}_{m_\beta,m'_\beta}(\theta) f_{j_\alpha m'_\alpha, j_\beta m'_\beta} \tag{3.63}$$

The results of PHFB calculations are summarized by amplitudes (u_{im}, v_{im}) and expansion coefficients $C_{ij,m}$. The required NTME $M_{2\nu}$ is calculated as follows. In the first step, matrices $f_{Z,N}$ and $F_{Z,N}(\theta)$ given by Eqs. (3.62) and (3.63) are setup for the nuclei involved in the $2\nu\beta^-\beta^-$ decay making use of 20 Gaussian quadrature points in the range (0, π). Finally, the required NTME can be calculated in a straightforward manner using the Eq. (3.59).

3.2 Results and discussions

Our aim is to study the $2\nu\beta^-\beta^-$ decay of ^{94,96}Zr, ^{100}Mo, ^{104}Ru, ^{110}Pd, ^{128,130}Te and ^{150}Nd isotopes for the $0^+ \rightarrow 0^+$ transition. The experimental results of all the nuclei have been presented in Table 3.1. The NTMEs $M_{2\nu}$ calculated with PHFB wave functions generated with four different parametrizations of effective two-body interactions, namely $PQQ1$,

$PQQHH1$, $PQQ2$ and $PQQHH2$ along with the estimated average $\overline{M}_{2\nu}$, uncertainties $\Delta\overline{M}_{2\nu}$ and experimental $M_{2\nu}$ [Barabash (2010)] are presented in Table 3.2. To calculate the uncertainty, we have done a statistical analysis in the following manner. The mean and standard deviation are defined for a finite series of calculations as

$$\overline{M}_i = \frac{\sum_{k=1}^{N} M_i^k}{N} \tag{3.64}$$

and

$$\Delta\overline{M}_i = \frac{1}{\sqrt{N-1}} \left[\sum_{k=1}^{N} \left(\overline{M}_i - M_i^k \right)^2 \right]^{1/2} \tag{3.65}$$

The Eqs. (3.64) and (3.65) define the best estimate of the mean and standard deviation for a Gaussian distribution. In the average NTMEs $\overline{M}_{2\nu}$, the maximum uncertainty $\Delta\overline{M}_{2\nu}$ turns out to be about 45%, which shows that the NTMEs $M_{2\nu}$ are highly sensitive to the deformation content of the intrinsic wave functions. We also present the experimental $M_{2\nu}$ [Barabash (2010)] in the last column of Table 3.2. The experimental $M_{2\nu}$ are not available for ^{94}Zr, ^{104}Ru and ^{110}Pd isotopes. The calculated $\overline{M}_{2\nu}$ in the present work agrees very well with the experimental $M_{2\nu}$ for ^{96}Zr, ^{100}Mo and ^{128}Te isotopes within error bars. In case of ^{130}Te and ^{150}Nd, the calculated $\overline{M}_{2\nu}$ are about 2.5 times larger and 3.4 times smaller, respectively than the experimental $M_{2\nu}$.

In Table 3.3, we compile all the available theoretical results along with our calculated $\overline{M}_{2\nu}$ and corresponding half-lives $T^{2\nu}_{1/2}$ of above mentioned nuclei for the $0^+ \rightarrow 0^+$ transition. We present only the theoretical $T^{2\nu}_{1/2}$ for those models for which no direct or indirect information about $M_{2\nu}$ is available to us. We use the phase space factors $G_{2\nu}$ calculated by Stoica and Mirea (2013) and rescale them at $g_A = 1.2701$ [Beringer *et al.* (2012)]. However, the $G_{2\nu}$ of ^{94}Zr and ^{104}Ru isotopes are not available. We take them from Boehm and

Vogel (1992) and rescale them at $g_A = 1.2701$. The phase space factors $G_{2\nu}$ (in the unit of yr^{-1}) used in the present work are 2.456×10^{-21}, 1.55×10^{-17}, 7.573×10^{-18}, 9.778×10^{-21}, 3.123×10^{-19}, 6.58×10^{-22}, 3.799×10^{-18} and 8.9×10^{-17} for ^{94,96}Zr, ^{100}Mo, ^{104}Ru, ^{110}Pd, ^{128,130}Te and ^{150}Nd isotopes, respectively. However, it is more justified to use g_A around 1.0 for heavy nuclei. Hence, the theoretical $T^{2\nu}_{1/2}$ are calculated for $g_A = 1.2701$ and 1.0.

A large number of experimental and theoretical studies have been done for the $0^+ \rightarrow 0^+$ transition of $2\nu\beta^-\beta^-$ decay. All the available theoretical results are compiled in Table 3.3 for the nuclei under study. We present only the theoretical $T^{2\nu}_{1/2}$ for those models for which no direct or indirect information about $M_{2\nu}$ is available to us. In case of heavy nuclei, it is more justified to use g_A around 1.0. Hence, the theoretical $T^{2\nu}_{1/2}$ are calculated both for $g_A = 1.2701$ and 1.0.

From the Table 3.3 it can be observed that there is a remarkable spread in the calculated NTMEs $M_{2\nu}$ within different nuclear models. Specifically, the NTMEs $M_{2\nu}$ calculated with the QRPA model vary by a factor of about 1.4–2.5, corresponding to ^{130}Te and ^{100}Mo isotopes, respectively and within all the extensions of QRPA, the variation is about 3.9–12.3, corresponding to ^{100}Mo and ^{128}Te isotopes, respectively. The calculated NTMEs within all the models vary by a factor of about 1.2–20, corresponding to ^{150}Nd and ^{128}Te isotopes, respectively.

The average NTMEs $\overline{M}_{2\nu}$ evaluated using the PHFB approach are suppressed, except for ^{130}Te isotope, by a factor between 1.7–2.5 approximately with respect to those of QRPA [Simkovic *et al.* (2013)], corresponding to ^{96}Zr and ^{110}Pd isotopes, respectively. The $\overline{M}_{2\nu}$ calculated within PHFB model is larger by a factor of about 1.3 with respect to QRPA [Simkovic *et al.* (2013)] value.

It is clear from above discussion that the validity of nuclear models presently employed to calculate $M_{2\nu}$ can not be uniquely established due to large error bars in experimental results as well as uncertainty in g_A. Further work is necessary both in the experimental as well as theoretical front to judge the relative applicability, success and failure of various models used so far for the study of $\beta\beta$ decay processes.

3.2.1 Deformation effects

To quantify the deformation effect on $M_{2\nu}$, we define a quantity $D_{2\nu}$ as the ratio of $M_{2\nu}$ at zero deformation ($\zeta_{qq} = 0$) and full deformation ($\zeta_{qq} = 1$). The deformation effect ratio $D_{2\nu}$ is given by

$$D_{2\nu} = \frac{M_{2\nu}(\zeta_{qq} = 0)}{M_{2\nu}(\zeta_{qq} = 1)} \tag{3.66}$$

The values of $D_{2\nu}$ are 2.37, 3.80, 3.41, 25.85, 5.27, 3.50, 4.81 and 12.30 for ^{94,96}Zr, ^{100}Mo, ^{104}Ru, ^{110}Pd, ^{128,130}Te and ^{150}Nd nuclei, respectively, which suggest that the deformation play a crucial role in the evaluation of NTMEs $M_{2\nu}$.

3.3 Conclusions

Presently, a number of nuclear models have been employed to calculate $M_{2\nu}$ and the calculated $M_{2\nu}$ in these models vary substantially. The validity of these nuclear models can not be uniquely established due to large error bars in experimental results as well as uncertainty in g_A. Further work is necessary both in the experimental as well as theoretical front to judge the relative applicability, success and failure of various models used so far for the study of $\beta\beta$ decay processes. In the present work, we have shown that

the deformations of the intrinsic states play a crucial role in reproducing a realistic NTME. A reasonable agreement between the calculated and observed spectroscopic properties and $M_{2\nu}$ of $2\nu\beta^-\beta^-$ decay for $0^+ \rightarrow 0^+$ transition of considered nuclei makes us confident to employ the same PHFB wave functions to study the $0\nu\beta^-\beta^-$ decay of the mentioned nuclei, which is given in the Chapter 4.

Table 3.1: Experimental half lives $T^{2\nu}_{1/2}$ of $2\nu\beta^-\beta^-$ decay of A = 48, 76, 82, 94, 96, 100, 110, 116, 128, 130, 136, 150, 238 and 244 nuclei for the $0^+ \rightarrow 0^+$ transition. †denotes all modes.

Transition	$T^{2\nu}_{1/2}$ (yr)	Project	Reference
^{48}Ca→^{48}Ti	$(6.4^{+0.7}_{-0.6})\times10^{19}$	NEMO 3	[Arnold.*et al.*(2016)]
	$(4.4^{+0.5}_{-0.4}\pm0.4)\times10^{19}$	NEMO 3	[Barabash *et al.*(2011)]
	9.0×10^{19}	ITEP+CSNS+ JINR+FNSPE	[Bakalyarov *et al.* (2002)]
	$(4.2^{+3.3}_{-1.3})\times10^{19}$	TGV	[Brudanin *et al.* (2000)]
	$(4.3^{+2.4}_{-1.1}\pm1.4)\times10^{19}$	UC Irvine	[Balysh *et al.*(1996)]
	$>3.6\times10^{19}$		[Bardin *et al.* (1970)]
	$(5.3^{+1.2}_{-0.8})\times10^{19}$	Average	[Barabash (2019)]
^{76}Ge→^{76}Se	$(1.925\pm0.094)\times10^{21}$	GERDA	[Agostini *et al.* (2015)]
	$(1.84^{+0.14}_{-0.10})\times10^{21}$	GERDA	[Agostini *et al.* (2013)]
	$(1.74\pm0.01^{+0.18}_{-0.16})\times10^{21}$		[Dorr *et al.*(2003)]
	$(1.55\pm0.01^{+0.19}_{-0.15})\times10^{21}$	HM	[Klapdor *et al.* (2001)]
	$(1.45\pm0.15)\times10^{21}$	IGEX	[Morales (1999)]
	$(1.77^{+0.01\ +0.13}_{-0.01\ -0.11})\times10^{21}$	HM	[Gunther *et al.* (1997)]
	$(1.1\pm0.2)\times10^{21}$	IGEX	[Aalseth *et al.* (1996)]
	$(1.2^{+0.2}_{-0.1})\times10^{21}$		[Avignone (1994)]
	$(8.4^{+1.0}_{-0.8})\times10^{20}$	IGEX	[Brodzinski *et al.* (1993)]
	$(9.2^{+0.7}_{-0.4})\times10^{20}$	USC+PNL+ ITEP+YPI	[Avignone *et al.* (1991)]
	$(1.1^{+0.6}_{-0.3})\times10^{21}$	PNL+USC	[Miley *et al.* (1991)]
	$(0.9\pm0.1)\times10^{21}$	ITEP+Yerevan	[Vasenko *et al.* (1990)]
	$>5.0\times10^{20}$		[Vuilleumier *et al.* (1988)]
	$>3.0\times10^{20}$	USC+PNL	[Avignone *et al.* (1986)]
	$(1.88\pm0.08)\times10^{21}$	Average	[Barabash (2019)]

Table 3.1 continued

Transition	$T^{2\nu}_{1/2}$ (yr)	Project	Reference
^{82}Se→^{82}Kr	$(0.939\pm0.017)\times10^{20}$	NEMO 3	[Arnold *et al.* (2018)]
	$(9.6\pm0.3\pm1.0)\times10^{19}$	NEMO 3	[Arnold *et al.* (2005)]
	$(10.3\pm0.2\pm1.0)\times10^{19}$	NEMO 3	[Lalanne (2005)]
	$(0.83\pm0.09\pm0.06)\times10^{20}$	NEMO 2	[Piquemal *et al.* (1999)]
	$(8.3\pm1.0\pm0.7)\times10^{19}$	NEMO 2	[Arnold *et al.* (1998)]
	$(1.08^{+0.26}_{-0.06})\times10^{20}$	UC Irvine	[Elliott *et al.* (1992)]
	1.0×10^{20}	Geochemical	[Manuel *et al.* (1991)]
	$(1.2\pm0.1)\times10^{20}$	Geochemical	[Lin *et al.* (1988)]
	$(1.1^{+0.8}_{-0.3})\times10^{20}$	UC Irvine	[Elliott *et al.* (1987)]
	$(1.3\pm0.05)\times10^{20}$	Geochemical	[Kirsten *et al.* (1986)]
	$(0.93\pm0.05)\times10^{20}$	Average	[Barabash (2019)]
^{94}Zr→^{94}Mo	$>1.1\times10^{17}$	NEMO 2	[Arnold *et al.* (1999)]
^{96}Zr→^{96}Mo	$(2.35\pm0.14\pm0.16)\times10^{19}$	NEMO 3	[Argyriades *et al.* (2010)]
	$(2.0\pm0.3\pm0.2)\times10^{19}$	NEMO 3	[Lalanne (2005)]
	$(9.4\pm3.2)\times10^{18}$	Geochemical	[Wieser *et al.* (2001)]
	$(2.1^{+0.8}_{-0.4}\pm0.2)\times10^{19}$	NEMO 2	[Arnold *et al.* (1999)]
	$(2.0^{+0.9}_{-0.5}\pm0.5)\times10^{19}$	NEMO 2	[Barabash (1998)]
	$(3.9\pm0.9)\times10^{19}$	Geochemical	[Kawashima *et al.* (1993)]
	$(2.3\pm0.2)\times10^{19}$	Average	[Barabash (2019)]
^{100}Mo→^{100}Ru	$(6.81\pm0.01)\times10^{18}$	NEMO 3	[Arnold *et al.* (2019)]
	$(7.12^{+0.18}_{-0.14}\pm0.10)\times10^{18}$	CUPID	[Armengaud *et al.* (2019)]
	$(6.90\pm0.15\pm0.37)\times10^{18}$	CUPID	[Armengaud *et al.* (2017)]
	$(7.15\pm0.37\pm0.66)\times10^{18}$	INFN	[Cardani *et al.* (2014)]
	$(7.11\pm0.02\pm0.54)\times10^{18}$	NEMO 3	[Arnold *et al.* (2005)]

Table 3.1 continued

Transition	$T^{2\nu}_{1/2}$ (yr)	Project	Reference
	$(7.72\pm0.02\pm0.54)\times10^{18}$	NEMO 3	[Lalanne (2005)]
	$(2.1\pm0.3)\times10^{18}$	Geochemical	[Hidaka *et al.* (2004)]
	$(7.2\pm0.9\pm1.8)\times10^{18}$	ITEP+INFN	[Ashitkov *et al.* (2001)]
	8.5×10^{18}	ITEP+INFN	[Ashitkov *et al.* (1999)]
	$(6.82^{+0.38}_{-0.53}\pm0.68)\times10^{18}$	UC Irvine	[De Silva *et al.* (1997]
	$(7.6^{+2.2}_{-1.4})\times10^{18}$	LBL+MHC+ UNM+INEL	[Alston-Garnjost *et al.* (1997)]
	$(9.5\pm0.4\pm0.9)\times10^{18}$	NEMO 2	[Dassie *et al.* (1995)]
	$(11.6^{+3.4}_{-0.8})\times10^{18}$	UC Irvine	[Elliot *et al.,* (1991)]
	$(11.5^{+3.0}_{-2.0})\times10^{18}$	ELEGANT V	[Ejiri *et al.*(1991)]
	$(3.3^{+2.0}_{-1.0})\times10^{18}$	INS Baksan	[Vasilev *et al.* (1990)]
	$(6.88\pm0.25)\times10^{18}$	Average	[Barabash (2019)]
^{110}Pd$\rightarrow^{110}$Cd	$>6.0\times10^{16}$		[Winter (1952)]
^{116}Cd$\rightarrow^{116}$Sn	$(2.63^{+0.11}_{-0.12})\times10^{19}$	Aurora	[Barabash *et al.* (2018)]
	$(2.74\pm0.04\pm0.18)\times10^{19}$	NEMO 3	[Arnold *et al.* (2017)]
	$(2.80\pm0.05\pm0.4)\times10^{19}$	INR	[Poda *et al.* (2014)]
	$(2.88\pm0.04\pm0.16)\times10^{19}$	-	[Barabash (2011)]
	$(2.8\pm0.1\pm0.3)\times10^{19}$	NEMO 3	[Lalanne (2005)]
	$(2.9\pm0.1^{+0.4}_{-0.3})\times10^{19}$	INR	[Danevich *et al.* (2003)]
	$(2.6\pm0.1^{+0.7}_{-0.4})\times10^{19}$	INR+INFN	[Danevich *et al.* (2000)]
	$(3.75\pm0.35\pm0.21)\times10^{19}$	NEMO 2	[Arnold *et al.* (1996)]
	$(2.7^{+0.5}_{-0.4}\pm0.9)\times10^{19}$	INR	[Danevich *et al.* (1995)]
	$(2.6^{+0.9}_{-0.5})\times10^{19}$	Osaka	[Ejiri *et al.* (1995)]
	$(2.6^{+0.9}_{-0.5}\pm0.35)\times10^{19}$		[Kume *et al.,* (1994)]
	$(2.69\pm0.09)\times10^{19}$	Average	[Barabash (2019)]

Table 3.1 continued

Transition	$T^{2\nu}_{1/2}$ (yr)	Methods	Reference
^{128}Te$\rightarrow^{128}$Xe	$(2.41\pm0.39)\times10^{24}$	Geochemical	[Meshik *et al.*(2008)]
	$(2.3\pm0.3)\times10^{24}$	Geochemical	[Thomas *et al.*(2008)]
	$(2.2\pm0.3)\times10^{24}$	Geochemical	[Takaoka *et al.* (1996)]
	$(7.7\pm0.4)\times10^{24}$	Geochemical	[Bernatovicz *et al.* (1993)]
	2.2×10^{24}	Geochemical	[Manuel (1991)]
	$(1.8\pm0.7)\times10^{24}$	Geochemical	[Lin *et al.* (1988)]
	$>5\times10^{24}$	Geochemical	[Kirsten *et al.* (1986)]
	$(2.25\pm0.09)\times10^{24}$	Recommended	[Barabash (2019)]
^{130}Te$\rightarrow^{130}$Xe	$(7.9\pm0.1\pm0.2)\times10^{20}$	CUORE	[Caminata *et al.* (2019)]
	$(8.2\pm0.2\pm0.6)\times10^{20}$	CUORE 0	[Alduino *et al.* (2017)]
	$(7.0\pm0.9\pm1.1)\times10^{20}$	NEMO 3	[Arnold *et al.* (2011)]
	$6.1\pm1.4^{+2.9}_{-3.5}$	INFN+LNGS	[Arnaboldi *et al.* (2003)]
	$>3.0\times10^{20}$	INFN+LNGS	[Alessandrello *et al.* (2000)]
	$(7.9\pm1.0)\times10^{20}$	Geochemical	[Takaoka *et al.* (1996)]
	$(2.7\pm0.1)\times10^{21}$	Geochemical	[Bernatovicz *et al.* (1993)]
	0.8×10^{21}	Geochemical	[Manuel (1991)]
	$>8.0\times10^{20}$		[Bellotti *et al.* (1987)]
	$(2.7\pm0.1)\times10^{21}$	Recommended	[Elliott *et al.* (2002)]
	$(7.19\pm0.21)\times10^{20}$	Average	[Barabash (2019)]
^{136}Xe$\rightarrow^{136}$Ba	$(2.21\pm0.02\pm0.07)\times10^{21}$	KamLAND Zen	[Gando *et al.* (2016)]
	$(2.165\pm0.016\pm0.0059)\times10^{21}$	EXO-200	[Albert *et al.*(2014)]
	$(2.30\pm0.02\pm0.12)\times10^{21}$	KamLAND-Zen	[Gando *et al.*(2012)]
	$>1.0\times10^{22}$	INFN	[Bernabei *et al.* (2002)]
	$>8.1\times10^{20}$	INR	[Gavriljuk *et al.* (2000)]
	$>5.5\times10^{20}$	Gotthard tunnel	[Busto *et al.*,(1996)]

Table 3.1 continued

Transition	$T^{2\nu}_{1/2}$ (yr)	Project	Reference
	$(2.18\pm0.05)\times10^{21}$	Average	[Barabash (2019)]
^{150}Nd→^{150}Sm	$(9.34\pm0.22\pm0.63)\times10^{18}$	NEMO 3	[Arnold *et al.*(2016)]
	$(9.11^{+0.25}_{-0.22}\pm0.63)\times10^{18}$	NEMO 3	[Argyriades *et al.* (2009)]
	$(9.7\pm0.7\pm1.0)\times10^{18}$	NEMO 3	[Lalanne (2005)]
	$(6.75^{+0.37}_{-0.42}\pm0.68)\times10^{18}$	UC Irvine	[De Silva *et al.* (1997)]
	$(18.8^{+6.9}_{-3.9}\pm1.9)\times10^{18}$	ITEP +INR	[Artemiev *et al.* (1995)]
	$(17^{+10}_{-5.0}\pm3.5)\times10^{18}$	ITEP +INR	[Artemiev *et al.* (1993)]
	9.0×10^{18}	UC Irvine	[Elliott *et al.* (1993)]
	$>11.0\times10^{18}$	INS Baksan	[Vasilev *et al.* (1993)]
	$>18\times10^{18}$	INR	[Klimenko *et al.* (1986)]
	$(8.4\pm1.1)\times10^{18}$	Average	[Barabash (2019)]
^{238}U→^{238}Pu	$\geq8.1\times10^{10}$	INR	[Tretyak *et al.* (2005)]
	$(2.0\pm0.6)\times10^{21}$	Radiochemical	[Turkevich *et al.* (1991)]
^{244}Pu→^{244}Cm	$\geq1.1\times10^{18\dagger}$	Radiochemical	[Moody *et al.* (1992)]

Table 3.2: Theoretically calculated NTMEs $M_{2\nu}$ within the PHFB model with four different parametrizations and their average value $\overline{M}_{2\nu}$ along with experimental values [Barabash (2010)].

Nuclei	$M_{2\nu}$				$\overline{M}_{2\nu}$	$M_{2\nu}$(Exp.)
	$PQQ1$	$PQQHH1$	$PQQ2$	$PQQHH2$		
^{94}Zr	0.064	0.060	0.133	0.058	0.079±0.036	–
^{96}Zr	0.055	0.056	0.053	0.054	0.054±0.001	$0.048^{+0.002}_{-0.002}$
^{100}Mo	0.127	0.128	0.127	0.127	0.127±0.001	$0.123^{+0.004}_{-0.003}$
^{104}Ru	0.020	0.021	0.023	0.022	0.021±0.001	–
^{110}Pd	0.085	0.124	0.105	0.115	0.107±0.017	–
^{128}Te	0.026	0.022	0.027	0.021	0.024±0.003	$0.024^{+0.003}_{-0.002}$
^{130}Te	0.047	0.044	0.041	0.050	0.045±0.004	$0.017^{+0.002}_{-0.001}$
^{150}Nd	0.010	0.008	0.010	0.008	0.009±0.001	$0.031^{+0.002}_{-0.002}$

Table 3.3: Theoretically calculated NTME $M_{2\nu}$ and half-life $T^{2\nu}_{1/2}$ of $2\nu\beta^-\beta^-$ in different nuclear models for the $0^+ \rightarrow 0^+$ transition of ^{94,96}Zr, ^{100}Mo, ^{104}Ru, ^{110}Pd, ^{128,130}Te and ^{150}Nd nuclei. The numbers corresponding to (a) and (b) are calculated for $g_A = 1.2701$ and 1.0 respectively. "*" denotes present calculation.

Nuclei	Model	Reference	$\lvert M_{2\nu}\rvert$		$T^{2\nu}_{1/2}$
^{94}Zr	PHFB	*	0.079	(a)	6.52
(10^{22} yr)				(b)	16.98
	SRQRPA	[Bobyk *et al.* (2000)]			3.08–659
	OEM	[Hirsch *et al.* (1994)]			168
	QRPA	[Staudt *et al.* (1990)]			6.93
^{96}Zr	PHFB	*	0.054	(a)	2.21
(10^{19} yr)				(b)	5.76
	FSQP	[Eijri (2017)]	0.045	(a)	3.19
				(b)	8.29
	QRPA	[Simkovic *et al.* (2013)]	0.090	(a)	0.80
				(b)	2.07
	SRQRPA	[Bobyk *et al.* (2000)]			0.452–61
	$SU(4)_{\sigma\tau}$	[Rumyantsev *et al.* (1998)]	0.0678	(a)	1.40
				(b)	3.65
	RQRPA†	[Toivanen *et al.* (1997)]			4.4
	RQRPA‡	[Toivanen *et al.* (1997)]			4.2
	QRPA	[Barabash *et al.* (1996)]	0.12–0.31	(a)	0.45–0.067
				(b)	0.12–0.17
	SRPA	[Stoica *et al.* (1995)]	0.022	(a)	13.33
				(b)	34.69
	OEM	[Hirsch *et al.* (1994)]			20.2
	QRPA	[Staudt *et al.* (1990)]			1.08

Table 3.3 continued

Nuclei	Model	Reference	$\lvert M_{2\nu}\rvert$		$T^{2\nu}_{1/2}$
	QRPA	[Engel *et al.* (1988)]	0.124	(a)	0.42
				(b)	1.09
^{100}Mo	PHFB	*	0.127	(a)	8.19
(10^{18} yr)				(b)	21.30
	FSQP	[Eijri (2017)]	0.096	(a)	14.33
				(b)	37.29
	QRPA	[Simkovic *et al.* (2013)]	0.232	(a)	2.45
				(b)	6.38
	SSDH	[Simkovic *et al.* (2000)]		(a)	7.15–8.97
	SRQRPA	[Bobyk *et al.* (2000)]			5.04–16800
	$SU(4)_{\sigma\tau}$	[Rumyantsev *et al.* (1998)]	0.1606	(a)	5.12
				(b)	13.32
	SSDH	[Civitarese *et al.* (1998)]	0.18	(a)	4.08
				(b)	10.61
	SRPA	[Stoica *et al.* (1995)]	0.059	(a)	37.93
				(b)	98.71
	$pSU(3)^{+}$	[Hirsch *et al.* (1995*a*)]	0.152	(a)	5.71
				(b)	14.87
	$pSU(3)^{++}$	[Hirsch *et al.* (1995*a*)]	0.108	(a)	11.32
				(b)	29.46
	OEM	[Hirsch *et al.* (1994)]			35.8
	QRPA	[Suhonen *et al.* (1994)]	0.101	(a)	12.94
				(b)	33.69
	QRPA	[Griffith *et al.* (1992)]	0.256	(a)	2.01
				(b)	5.24
	QRPA	[Staudt *et al.* (1990)]			1.13
	QRPA	[Engel *et al.* (1988)]	0.211	(a)	2.97
				(b)	7.72

Table 3.3 continued

Nuclei	Model	Reference	$\lvert M_{2\nu}\rvert$		$T^{2\nu}_{1/2}$
^{104}Ru	PHFB	*	0.021	(a)	23.19
(10^{22} yr)				(b)	60.35
	OEM	[Hirsch *et al.* (1994)]			3.09
	QRPA	[Staudt *et al.* (1990)]			0.629
^{110}Pd	PHFB	*	0.107	(a)	2.80
(10^{20} yr)				(b)	7.28
	FSQP	[Eijri (2017)]	0.145	(a)	1.52
				(b)	3.96
	QRPA	[Simkovic *et al.* (2013)]	0.263	(a)	0.46
				(b)	1.20
	SSDH	[Semenov *et al.* (2000)]			1.6
	SSDH	[Civitarese *et al.* (1998)]	0.19	(a)	0.89
				(b)	2.31
	SRPA	[Stoica (1994)]	0.046	(a)	15.13
				(b)	39.38
	OEM	[Hirsch *et al.* (1994)]			12.4
	QRPA	[Staudt *et al.* (1990)]			0.116
^{128}Te	PHFB	*	0.024	(a)	2.64
(10^{24} yr)				(b)	6.87
	FSQP	[Eijri (2017)]	0.019	(a)	4.21
				(b)	10.96
	QRPA	[Simkovic *et al.* (2013)]	0.048	(a)	0.66
				(b)	1.71
	SSDH	[Semenov *et al.* (2000)]	0.048	(a)	0.66
				(b)	1.72
	SM	[Caurier *et al.* (1999)]			0.5

Table 3.3 continued

Nuclei	Model	Reference	$\lvert M_{2\nu}\rvert$		$T^{2\nu}_{1/2}$
	$SU(4)_{\sigma\tau}$	[Rumyantsev *et al.* (1998)]	0.053	(a)	0.54
				(b)	1.41
	SSDH	[Civitarese *et al.* (1998)]	0.013	(a)	8.99
				(b)	23.40
	MCM	[Aunola *et al.* (1996)]	0.046	(a)	0.72
				(b)	1.87
	SRPA	[Stoica (1994)]	0.006	(a)	42.22
				(b)	109.9
	OEM	[Hirsch *et al.* (1994)]			0.21
	QRPA	[Staudt *et al.* (1990)]			2.63
	QRPA	[Engel *et al.* (1988)]	0.074	(a)	0.28
				(b)	0.72
	IBM	[Scholten *et al.* (1985)]			0.09
	WCSM	[Haxton and Stephenson (1984)]	0.120	(a)	0.10
				(b)	0.27
^{130}Te	PHFB	*	0.045	(a)	1.30
(10^{20} yr)				(b)	3.38
	FSQP	[Eijri (2017)]	0.017	(a)	9.11
				(b)	23.70
	QRPA	[Simkovic *et al.* (2013)]	0.034	(a)	2.29
				(b)	5.96
	SM	[Caurier *et al.* (1999)]	0.030	(a)	2.92
				(b)	7.61
	$SU(4)_{\sigma\tau}$	[Rumyantsev *et al.* (1998)]	0.0468	(a)	1.20
				(b)	3.13
	RQRPA†	[Toivanen *et al.* (1997)]	0.009	(a)	32.50
				(b)	84.57

Table 3.3 continued

Nuclei	Model	Reference	$\lvert M_{2\nu}\rvert$		$T^{2\nu}_{1/2}$
	RQRPA[‡]	[Toivanen *et al.* (1997)]	0.009	(a)	32.50
				(b)	84.57
	MCM	[Aunola *et al.* (1996)]	0.028	(a)	3.36
				(b)	8.74
	$SU(4)_{\sigma\tau}$	[Rumyantsev *et al.* (1995)]			7.0
	SRPA	[Stoica (1994)]	0.016	(a)	10.28
				(b)	26.76
	OEM	[Hirsch *et al.* (1994)			0.79
	QRPA	[Staudt *et al.* (1990)]			18.4
	QRPA	[Engel *et al.* (1988)]	0.049	(a)	1.10
				(b)	2.85
	IBM	[Scholten *et al.* (1985)]			0.17
	WCSM	[Haxton and Stephenson (1984)]	0.114	(a)	0.20
				(b)	0.53
^{150}Nd	PHFB	*	0.009	(a)	138.7
(10^{18} yr)				(b)	361.0
	$SU(4)_{\sigma\tau}$	[Rumyantsev *et al.* (1998)]	0.0642	(a)	2.73
				(b)	7.09
	pSU(3)	[Castanos *et al.* (1994)]	0.055	(a)	3.71
				(b)	9.67
	OEM	[Hirsch *et al.* (1994)]			16.6
	QRPA	[Staudt *et al.* (1990)]			7.37

[†]AWS basis; [‡]WS basis; [+]Spherical occupation wave functions; [++]Deformed occupation wave functions

Chapter 4

$0\nu\beta^-\beta^-$ decay of ^{94,96}Zr, ^{100}Mo, ^{104}Ru, ^{110}Pd, ^{128,130}Te and ^{150}Nd nuclei in the left-right symmetric grand unified theory

The flavor oscillation of neutrinos has been confirmed at atmospheric [Fukuda *et al.* (1998),(1999)], solar [Ahmed *et al.* (2001),(2002),(2004)], reactor [Eguchi *et al.* (2003)] and accelerator [Aguilar *et al.* (2001)] sources, which imply that the neutrinos have mass. On the other hand, the possibility of finite neutrino mass has been already suggested by left-right symmetric models (*LRSM*) based on quark-lepton symmetry [Pati and Salam (1974), Mohapatra and Pati (1975), Senjanovic and Mohapatra (1975)]. The possible existence of right handed $V + A$ currents and right handed heavy Majorana neutrinos is suggested by *LRSM*. The non-vanishing mass of neutrinos suggest that the latter may

be Dirac or Majorana particles. The possible occurrence of $0\nu\beta^-\beta^-$ decay requires two necessary conditions, namely finite neutrino mass and helicity matching so that the neutrino is a Majorana particle and $\nu_{eL} = \overline{\nu}_{eL}$. The latter condition is also satisfied if the neutrino has a finite mass because the emitted neutrino ν_e can be in a minor helicity state $h = 1/2$ in proportion to (m_ν/ω), where m_ν and ω are the mass and the energy of the neutrino respectively. The transition amplitude will be proportional to (m_ν/m_e) and this is the well known mass mechanism. Alternatively, the helicity matching is also satisfied in the presence of right handed $V + A$ currents. In this case, a neutrino mass is also induced as a perturbative correction by the $0\nu\beta^-\beta^-$ decay. Thus, the two possibilities regarding the nature of neutrinos can be resolved only through the experimental study of $0\nu\beta^-\beta^-$ decay. Further, the study of $0\nu\beta^-\beta^-$ decay also provides information regarding the parameters of right handed currents and mass of heavy neutrinos.

The left-right symmetric models (*LRSM*) [Pati *et al.* (1974), Mohapatra *et al.* (1975) and Senjanovic *et al.* (1975)] aim at explaining two puzzling aspects of the SM, namely (i) violation of parity in the weak interactions and (ii) masslessness of neutrinos both of which are intimately related to $0\nu\beta^-\beta^-$ decay [Doi *et al.* (1985)]. There exists a common solution to both the above mentioned questions. The process of spontaneous symmetry breaking of the $SU(2)_R$ symmetry group suppresses the right handed $V + A$ currents at low energies and gives non-zero mass. The *LRSM* provides a very attractive explanation for non zero mass values of neutrinos, when compared to those of charged leptons via the well known seesaw mechanism [Gell Mann *et al.* (1979) and Mohapatra *et al.* (1981)].

The present chapter is organized as follows. The $0\nu\beta^-\beta^-$ decay has been already studied extensively in the light neutrino approximation [Haxton *et al.* (1984), Doi *et al.*

(1985), Vergados [(1986), (2002)], Tomoda (1991), Suhonen *et al.* (1998), Faessler *et al.* (1998)]. In *LRSM*, the $0\nu\beta^-\beta^-$ decay has been studied by Mohapatra [(1986)], Doi *et al.* (1993) and Hirsch *et al.* (1996). Therefore, the theoretical formalism for $0\nu\beta^-\beta^-$ decay in *LRSM* is given briefly in Section 4.1. In Section 4.2 , results of our calculation are presented and discussed. The role of deformation on the NTMEs due to light Majorana neutrino exchange $M^{(0\nu)}$ as well as heavy Majorana neutrino exchange $M^{(0N)}$ is studied in the same Section. Finally, we present concluding remarks in Section 4.3.

4.1 Theoretical formalism

The weak interaction effective Hamiltonian H_W including hadronic currents is written as

$$H_W = \left(\frac{G}{\sqrt{2}}\right)\left[j_{L\mu}J_L^{\mu\dagger} + \kappa j_{L\mu}J_R^{\mu\dagger} + \eta j_{R\mu}J_L^{\mu\dagger} + \lambda j_{R\mu}J_R^{\mu\dagger}\right] + h.c. \tag{4.1}$$

where

$$j_L^\mu = \overline{e}\gamma^\mu\left(1-\gamma_5\right)\nu_{eL} \qquad j_R^\mu = \overline{e}\gamma^\mu\left(1+\gamma_5\right)\nu_{eR}^{'} \tag{4.2}$$

and

$$\nu_{eL} = \sum_j U_{ej}N_{jL} \qquad \nu_{eR}^{\prime} = \sum_j V_{ej}N_{jR} \tag{4.3}$$

The left and right handed weak hadronic $V \pm A$ currents are given by

$$J_L^{\mu\dagger} = g_v\overline{u}\gamma^\mu\left(1-\gamma_5\right)d \qquad J_R^{\mu\dagger} = g_v^{\prime}\overline{u}\gamma^\mu\left(1+\gamma_5\right)d \tag{4.4}$$

The following approximations are taken in deriving the decay rate of $0\nu\beta^-\beta^-$ decay.

(i) The light neutrino species ($m_i < 10\ MeV$) and heavy neutrinos ($m_i > 1\ GeV$) are considered.

(ii) The total angular momentum transferred from the nucleus can be 0,1 or 2. The s and p waves are considered to describe the final leptonic states.

(iii) The nonrelativistic impulse approximation is considered for the hadronic currents. However, the recoil terms are retained.

(iv) In the case of $0\nu\beta^-\beta^-$ decay, the exchanged neutrinos are virtual particles. The energy of neutrinos are much larger than the typical excitation energy of the intermediate nuclear states. Hence, the closure approximation is valid and it is usually used.

(iv) No finite de Broglie wave length correction is considered. This assumption is helpful in the calculation of phase space factors.

(vi) The CP invariance is assumed so that the effective neutrino masses $\langle m_\nu \rangle$ and $\langle M_N \rangle$ for the light and heavy neutrinos are also real since U_{ei} and V_{ei} are both real or pure imaginary depending on the CP parity of the mass eigenstate neutrino N.

In the mass mechanism, the inverse half-life $T^{0\nu}_{1/2}$ of $0\nu\beta^-\beta^-$ decay for the $0^+ \rightarrow 0^+$ transition is given by

$$\left[T^{0\nu}_{1/2}(0^+ \rightarrow 0^+)\right]^{-1} = \left(\frac{\langle m_\nu \rangle}{m_e}\right)^2 C^{LL}_{mm} + \left(\frac{m_p}{\langle M_N \rangle}\right)^2 C^{NN}_{mm} + \left(\frac{\langle m_\nu \rangle}{m_e}\right)\left(\frac{m_p}{\langle M_N \rangle}\right) C^{NL}_{mm} \quad (4.5)$$

where

$$\langle m_\nu \rangle = \Sigma_i^{'} U^2_{ei} m_i \quad (4.6)$$

$$\langle M_N \rangle^{-1} = \Sigma_i^{''} U^2_{ei} m_i^{-1} \quad (4.7)$$

and the nuclear factors-of-merit C_{mm} are defined by the following relations.

$$C_{mm}^{LL} = G_{01}\left|M^{(0\nu)}\right|^2 = G_{01}\left(-M_F^{(0\nu)} + M_{GT}^{(0\nu)} + M_T^{(0\nu)}\right)^2 \quad (4.8)$$

$$C_{mm}^{NN} = G_{01}\left|M^{(0N)}\right|^2 = G_{01}\left(-M_{Fh}^{(0N)} + M_{GTh}^{(0N)} + M_{Th}^{(0N)}\right)^2 \quad (4.9)$$

$$C_{mm}^{NL} = 2G_{01}\left(-M_F^{(0\nu)} + M_{GT}^{(0\nu)} + M_T^{(0\nu)}\right)\left(-M_{Fh}^{(0N)} + M_{GTh}^{(0N)} + M_{Th}^{(0N)}\right) \quad (4.10)$$

where the NTMEs $M_K^{(I)}$ ($K = F,\ GT,\ T,\ Fh,\ GTh,\ Th$ and $I = 0\nu,\ 0N$) are [Simkovic *et al.* (2001), (2008), (2009)]

$$M_K^{(I)} = \sum_{n,m}\left\langle 0_F^+ \left\| O_{K,nm}\tau_n^+\tau_m^+ \right\| 0_I^+ \right\rangle \quad (4.11)$$

with

$$O_F = H_F\left(r_{nm}\right) \quad (4.12)$$

$$O_{GT} = \boldsymbol{\sigma}_n \cdot \boldsymbol{\sigma}_m H_{GT}\left(r_{nm}\right) \quad (4.13)$$

$$O_T = \left[3\left(\boldsymbol{\sigma}_n \cdot \widehat{\mathbf{r}}_{nm}\right)\left(\boldsymbol{\sigma}_m \cdot \widehat{\mathbf{r}}_{nm}\right) - \boldsymbol{\sigma}_n \cdot \boldsymbol{\sigma}_m\right] H_T\left(r_{nm}\right) \quad (4.14)$$

$$O_{Fh} = H_{Fh}\left(r_{nm}\right) \quad (4.15)$$

$$O_{GTh} = \boldsymbol{\sigma}_n \cdot \boldsymbol{\sigma}_m H_{GTh}\left(r_{nm}\right) \quad (4.16)$$

$$O_{Th} = \left[3\left(\boldsymbol{\sigma}_n \cdot \widehat{\mathbf{r}}_{nm}\right)\left(\boldsymbol{\sigma}_m \cdot \widehat{\mathbf{r}}_{nm}\right) - \boldsymbol{\sigma}_n \cdot \boldsymbol{\sigma}_m\right] H_{Th}\left(r_{nm}\right) \quad (4.17)$$

The neutrino potentials due to light Majorana neutrino exchange $H_\alpha(r_{nm})$ and heavy Majorana neutrino exchange $H_{\alpha h}(r_{nm})$ associated with Fermi, Gamow-Teller (GT) and tensor operators are given by

$$H_\alpha(r_{nm}) = \frac{2R}{\pi}\int \frac{f_\alpha\left(qr_{nm}\right)}{\left(q + \overline{A}\right)}\, h_\alpha(q) q dq \quad (4.18)$$

$$H_{\alpha h}(r_{nm}) = \frac{2R}{(m_p m_e)\pi}\int f_\alpha\left(qr_{nm}\right) h_\alpha(q) q^2 dq \quad (4.19)$$

where $f_\alpha\left(qr_{nm}\right) = j_0\left(qr_{nm}\right)$ for $\alpha = F,\ GT$ and $f_T\left(qr_{nm}\right) = j_2\left(qr_{nm}\right)$. The effects due to the FNS are incorporated through the dipole form factors and the form factor related functions $h_F(q)$, $h_{GT}(q)$ and $h_T(q)$ are written as

$$h_F(q) = g_V^2\left(q^2\right) \tag{4.20}$$

$$\begin{aligned} h_{GT}(q) &= \frac{g_A^2(q^2)}{g_A^2}\left[1 - \frac{2}{3}\frac{g_P(q^2)q^2}{g_A(q^2)2M_p} + \frac{1}{3}\frac{g_P^2(q^2)q^4}{g_A^2(q^2)4M_P^2}\right] + \frac{2}{3}\frac{g_M^2(q^2)q^2}{g_A^2 4M_p^2} \\ &\approx \left(\frac{\Lambda_A^2}{q^2+\Lambda_A^2}\right)^4\left[1 - \frac{2}{3}\frac{q^2}{(q^2+m_\pi^2)} + \frac{1}{3}\frac{q^4}{(q^2+m_\pi^2)^2}\right] \\ &\quad + \left(\frac{g_V}{g_A}\right)^2\frac{\kappa^2 q^2}{6M_p^2}\left(\frac{\Lambda_V^2}{q^2+\Lambda_V^2}\right)^4 \end{aligned} \tag{4.21}$$

$$\begin{aligned} h_T(q) &= \frac{g_A^2(q^2)}{g_A^2}\left[\frac{2}{3}\frac{g_P(q^2)q^2}{g_A(q^2)2M_p} - \frac{1}{3}\frac{g_P^2(q^2)q^4}{g_A^2(q^2)4M_P^2}\right] + \frac{1}{3}\frac{g_M^2(q^2)q^2}{g_A^2 4M_p^2} \\ &\approx \left(\frac{\Lambda_A^2}{q^2+\Lambda_A^2}\right)^4\left[\frac{2}{3}\frac{q^2}{(q^2+m_\pi^2)} - \frac{1}{3}\frac{q^4}{(q^2+m_\pi^2)^2}\right] \\ &\quad + \left(\frac{g_V}{g_A}\right)^2\frac{\kappa^2 q^2}{12M_p^2}\left(\frac{\Lambda_V^2}{q^2+\Lambda_V^2}\right)^4 \end{aligned} \tag{4.22}$$

where

$$\begin{aligned} g_V(q^2) &= \frac{g_V}{g_A}\left(\frac{\Lambda_V^2}{q^2+\Lambda_V^2}\right)^2 \\ g_A(q^2) &= g_A\left(\frac{\Lambda_A^2}{q^2+\Lambda_A^2}\right)^2 \\ g_M(q^2) &= \kappa g_V\left(\frac{\Lambda_V^2}{q^2+\Lambda_V^2}\right)^2 \end{aligned} \tag{4.23}$$

$$g_P(q^2) = \frac{2m_p g_A(q^2)}{(q^2+m_\pi^2)}\left(\frac{\Lambda_A^2 - m_\pi^2}{\Lambda_A^2}\right) \tag{4.24}$$

with $g_V = 1.0$, $g_A = 1.2701$, $\kappa = \mu_p - \mu_n = 3.70$, $\Lambda_V = 0.850$ GeV, $\Lambda_A = 1.086$ GeV and m_π is the pion mass. The presence of pseudoscalar and weak magnetism terms of the higher order currents (HOC) [Simkovic *et al.* (1999)] results in no change of the Fermi matrix element $M_F^{(I)}$ $(I = 0\nu, 0N)$, the addition of three new terms $M_{GT-PP}^{(I)}$, $M_{GT-AP}^{(I)}$, $M_{GT-MM}^{(I)}$ to the conventional GT $M_{GT}^{(I)} = M_{GT-AA}^{(I)}$ matrix element and the addition of

three new terms $M^{(I)}_{T-PP}$, $M^{(I)}_{T-AP}$, $M^{(I)}_{T-MM}$ as the tensor matrix element $M^{(I)}_{T}$.

The short range correlations (SRC) arise mainly from the repulsive nucleon-nucleon potential due to the exchange of ρ and ω mesons and have been incorporated by using effective transition operator [Wu *et al.* (1985)], the exchange of ω-meson [Hirsch *et al.* (1995)] , UCOM [Simkovic *et al.* (2008), Kortelainen *et al.* (2007)] and the self-consistent CCM [Simkovic *et al.* (2009)]. The SRC can also be incorporated phenomenologically by Jastrow type of correlations with Miller-Spenser parametrization [Miller *et al.* (1976)]. Further, it has been shown in the self-consistent CMM [Simkovic *et al.* (2009)] that the SRC effects of Argonne and CD-Bonn two nucleon potentials are weak and it is possible to parametrize them by Jastrow type of correlations within a few percent of accuracy. Explicitly,

$$f(r) = 1 - ce^{-ar^2}(1 - br^2) \tag{4.25}$$

where a = 1.1, 1.59 and 1.52 fm^{-2}, b = 0.68, 1.45 and 1.88 fm^{-2} and c = 1.0, 0.92 and 0.46 for Miller-Spencer parametrization, CD-Bonn and Argonne V18 NN potentials, respectively. In present work the NTMEs $M^{(I)}_{K}$ ($K = F,\ GT,\ T,\ Fh,\ GTh,\ Th$ and $I = 0\nu$, $0N$) are calculated in the PHFB model for the above mentioned three sets of parameters for the SRC, denoted as SRC1, SRC2 and SRC3, respectively.

Employing closure approximation in conjunction with the HFB wave functions, the NTMEs $M^{(I)}_{K}$ are calculated by using the expression [Rath *et al.* (2010), (2012)] as follows:

$$
\begin{aligned}
M_K^{(I)} &= \left\langle 0_f^+ \left\| O_K \right\| 0_i^+ \right\rangle \\
&= \left[n^{J_f=0} n^{Ji=0} \right]^{-1/2} \int_0^\pi n_{(Z,N),(Z+2,N-2)}(\theta) \times \sum_{\alpha\beta\gamma\delta} \left\langle \alpha\beta \left| O_K \right| \gamma\delta \right\rangle \\
&\quad \times \sum_{\varepsilon\eta} \frac{\left(f^{(\pi)*}_{Z+2,N-2} \right)_{\varepsilon\beta}}{\left[\left(1 + F^{(\pi)}_{Z,N}(\theta) f^{(\pi)*}_{Z+2,N-2} \right) \right]_{\varepsilon\alpha}} \\
&\quad \times \frac{\left(F^{(\nu)*}_{Z,N} \right)_{\eta\delta}}{\left[\left(1 + F^{(\nu)}_{Z,N}(\theta) f^{(\nu)*}_{Z+2,N-2} \right) \right]_{\gamma\eta}} \sin\theta d\theta
\end{aligned} \tag{4.26}
$$

where

$$
n^J = \int_0^\pi \left[det\left(1 + F^{(\pi)} f^{(\pi)^\dagger} \right) \right]^{1/2} \left[det\left(1 + F^{(\nu)} f^{(\nu)^\dagger} \right) \right]^{1/2} d^J_{00}(\theta) sin(\theta) d\theta \tag{4.27}
$$

and

$$
\begin{aligned}
n_{(Z,N),(Z+2,N-2)}(\theta) &= \left[det\left(1 + F^{(\nu)}_{Z,N} f^{(\nu)^\dagger}_{Z+2,N-2} \right) \right]^{1/2} \\
&\quad \times \left[det\left(1 + F^{(\pi)}_{Z,N} f^{(\pi)^\dagger}_{Z+2,N-2} \right) \right]^{1/2}
\end{aligned} \tag{4.28}
$$

The $\pi(\nu)$ represents the proton (neutron) of nuclei involved in the $0\nu\beta^-\beta^-$ decay process. The matrices $f_{Z,N}$ and $F_{Z,N}(\theta)$ are given by

$$
f_{Z,N} = \sum_i C_{ij_\alpha,m_\alpha} C_{ij_\beta,m_\beta} \left(v_{im_\alpha} / u_{im_\alpha} \right) \delta_{m_\alpha,-m_\beta} \tag{4.29}
$$

$$
F_{Z,N}(\theta) = \sum_{m'_\alpha m'_\beta} d^{j_\alpha}_{m_\alpha,m'_\alpha}(\theta) d^{j_\beta}_{m_\beta,m'_\beta}(\theta) f_{j_\alpha m'_\alpha, j_\beta m'_\beta} \tag{4.30}
$$

The phase space factor G_{01} of the $0\nu\beta^-\beta^-$ decay can be evaluated by using the following integral [Doi *et al.* (1985)]

$$
G_{01} = \frac{(G g_A)^4 m_e^9}{64\pi^5 \left(m_e R \right)^2 \ln(2)} \int b_{01} d\Omega_{0\nu} \tag{4.31}
$$

where

$$d\Omega_{0\nu} = 2m_e^{-5} p_1 p_2 \varepsilon_1 \varepsilon_2 \delta\left(\varepsilon_1 + \varepsilon_2 + M_F - M_I\right) d\varepsilon_1 d\varepsilon_2 \tag{4.32}$$

Using

$$\int d\Omega_{0\nu} = \frac{2}{m_e^5} \int p_1 p_2 \varepsilon_1 \varepsilon_2 d\varepsilon_1 \tag{4.33}$$

one obtains

$$\begin{aligned} G_{01} &= \frac{2(Gg_A)^4 m_e^4}{64\pi^5 \left(m_e R\right)^2 \ln(2)} \int b_{01} p_1 p_2 \varepsilon_1 \varepsilon_2 d\varepsilon_1 \\ &= \frac{g^{(0\nu)}}{\left(m_e R\right)^2} \int b_{01} p_1 p_2 \varepsilon_1 \varepsilon_2 d\varepsilon_1 \end{aligned} \tag{4.34}$$

where

$$g^{(0\nu)} = \frac{(Gg_A)^4 m_e^4}{32\pi^5 \ln(2)} \tag{4.35}$$

and the nuclear radius

$$R = 1.2A^{1/3}\ fm \tag{4.36}$$

The kinematical factors b_{01} is given by

$$b_{01} = \alpha_+ + \beta_+ \tag{4.37}$$

Using the approximate relation

$$\begin{pmatrix} \alpha_+ \\ \\ \beta_+ \end{pmatrix} = \frac{1}{2}\left(\varepsilon_1 \varepsilon_2 \pm m_e^2\right) C_{00} \tag{4.38}$$

and

$$C_{00} = F_0\left(Z, \varepsilon_1\right) F_0\left(Z, \varepsilon_2\right) / \varepsilon_1 \varepsilon_2 \tag{4.39}$$

the phase space integral is finally given by

$$G_{01} = \frac{g^{(0\nu)}}{\left(m_e R\right)^2} \int_{m_e}^{T+m_e} F_0\left(Z, \varepsilon_1\right) F_0\left(Z, \varepsilon_2\right) p_1 p_2 \varepsilon_1 \varepsilon_2 d\varepsilon_1 \tag{4.40}$$

4.2 Results and discussions

Employing the same PHFB wave functions generated with four parametrizaions of pairing plus multipolar type of effective two-body interaction as used in Chapter 2 and Chapter 3 to calculate spectroscopic properties and NTMEs $M_{2\nu}$, the required NTMEs due to light Majorana neutrino exchange $M^{(0\nu)}$ as well as heavy Majorana neutrino exchange $M^{(0N)}$ for ^{94,96}Zr, ^{100}Mo, ^{104}Ru, ^{110}Pd, ^{128,130}Te and ^{150}Nd isotopes are calculated with the consideration of three different parametrizations of the Jastrow type of SRC.

The decomposition of NTMEs $M_K^{(0\nu)}$ into Fermi, Gamow-Teller and tensor components due to light Majorana neutrino exchange for ^{100}Mo are presented in Table 4.1 for point case P (3rd column), including finite size effect FNS (4th column) and with the consideration of FNS and SRC simultaneously (F+SRC -5th to 7th columns) for all four parametrizations, namely $PQQ1$, $PQQHH1$, $PQQ2$ and $PQQHH2$ used in the present work. To test the validity of closure approximation, the NTMEs $M_K^{(0\nu)}$ are also calculated for $\overline{A}/2$ in the energy denominator in the case of F+SRC given in 8th to 10th columns of Table 4.1. The Fermi, Gamow-Teller and tensor components of NTMEs $M_K^{(0N)}$ due to heavy Majorana neutrino exchange for ^{100}Mo are given in Table 4.2 for P, FNS and F+SRC case. It is observed from Table 4.1 and 4.2 that the contribution of conventional Fermi matrix elements is about 20% to the total matrix element. The Gamow-Teller matrix element is noticeably modified by the inclusion of the pseudoscalar and weak magnetism terms in the hadronic currents. The tensor matrix elements have a very small contribution, smaller than 4%, to the total transition matrix elements. The inclusion of short range correlations changes the nuclear matrix elements significantly, whose effects are large for

the Gamow-Teller and Fermi matrix elements but small in the case of tensor ones.

In Table 4.3, we present NTMEs $M^{(0\nu)}$ due to light Majorana neutrino exchange for ^{94,96}Zr, ^{100}Mo, ^{104}Ru, ^{110}Pd, ^{128,130}Te and ^{150}Nd isotopes calculated in the same approximations as mentioned above. It is noticed in general but for ^{110}Pd isotope that the NTMEs evaluated for both $PQQ1$ and $PQQ2$ parameterizations are quite close. The inclusion of the hexadecapolar term tends to reduce them by magnitudes, specifically depending on the structure of nuclei. The maximum variation in $M^{(0\nu)}$ due to the $PQQHH1$, $PQQ2$ and $PQQHH2$ parameterizations with respect to $PQQ1$ for all nuclei except ^{110}Pd is about 15%. However, the maximum variation in case of ^{110}Pd is about 37%. The relative change in NTMEs $M^{(0\nu)}$, by changing the energy denominator to $\overline{A}/2$ instead of $\overline{A}$ is in between 7.5%–12.4%, which confirms that the dependence of NTMEs on average excitation energy $\overline{A}$ is small and thus, the validity of the closure approximation for $0\nu\beta^-\beta^-$ decay is supported. In Table 4.4, the NTMEs $M^{(0N)}$ due to heavy Majorana neutrino exchange are presented for all the nuclei under consideration and the effect of different parametrizations is found same as in case of NTMEs $M^{(0\nu)}$ due to light neutrino exchange.

In Table 4.5 and 4.6, we compare our results of NTMEs $M^{(0\nu)}$ and $M^{(0N)}$, respectively, with those of calculated in other nuclear models. In comparison to the recent SM and QRPA (including its extensions) values, presently calculated NTMEs $M^{(0\nu)}$ differ by a factor of about 0.5–0.9 and 0.5–2.5, respectively. However, the difference between the calculated values of $M^{(0N)}$ turns out to be a factor of about 1.3–1.6 and 1.5–7.5 in comparison to SM and QRPA (including its extensions) results.

4.2.1 Effect of FNS and SRC

In Table 4.7, the relative changes in NTMEs $M^{(I)}$(in %) ($I = 0\nu, 0N$) due to the different approximations are presented. It is noticed that the consideration of FNS induces changes about 9.0%–12.0% in the NTMEs $M^{(0\nu)}$ with respect to point nucleon case. The NTMEs $M^{(0\nu)}$ are further reduced by approximately 13.0%–17.0%, 1.0%–2.0% and 2%–3.0% with the addition of SRC1, SRC2 and SRC3, respectively, relative to the FNS case.

In case of heavy Majorana neutrino exchange, the change in $M^{(0N)}$ is about 29%–33% due to the FNS with respect to the point nucleon case. With the inclusion of effects due to both FNS and SRC, the NTMEs change by about 65%–68%, 39%–42% and 18%–20% for F+SRC1, F+SRC2 and F+SRC3, respectively.

4.2.2 Extraction of effective neutrino mass

The limits on the effective mass of light Majorana neutrino $\langle m_\nu \rangle$ as well as heavy Majorana neutrino $\langle M_N \rangle$ are extracted from the most recent observed limits on half-lives $T^{0\nu}_{1/2}$ of $0\nu\beta^-\beta^-$ decay using the average NTMEs $\overline{M}^{(I)}$ ($I = 0\nu, 0N$). We use the phase space factors G_{01} calculated by Stoica and Mirea (2013) and rescale them at $g_A = 1.2701$ [Beringer *et al.* (2012)]. However, the G_{01} of ^{94}Zr isotope is not available. We take G_{01} for ^{94}Zr isotope from Boehm and Vogel (1992) and rescale them at $g_A = 1.2701$. The experimental half-life limits $T^{0\nu}_{1/2}$ and phase space factors G_{01} used in the present work are given in Table 4.8. The average NTMEs $\overline{M}^{(I)}$ along with calculated parameters are presented in Table 4.9. It is observed that the extracted upper limits on $\langle m_\nu \rangle$ for ^{100}Mo and ^{130}Te nuclei are 0.45 eV and 0.17 eV, respectively. The predicted half-lives of $0\nu\beta^-\beta^-$

decay of ^{94,96}Zr, ^{100}Mo, ^{110}Pd, ^{128,130}Te and ^{150}Nd isotopes are also given for $\langle m_\nu \rangle = 50$ meV. We also extract lower limits on the effective mass of heavy Majorana neutrino $\langle M_N \rangle$ from the recent observed limits on half-lives $T^{0\nu}_{1/2}$ of $0\nu\beta^-\beta^-$ decay. The extracted lower limits on $\langle M_N \rangle$ are 3.27×10^7 GeV and 8.99×10^7 GeV, for ^{100}Mo and ^{130}Te nuclei, respectively.

In the same Table 4.9, we present the nuclear sensitivities $\xi^{(I)}$ $(I = 0\nu, 0N)$, which are related to mass sensitivities, defined by Simkovic *et al.* (1999)

$$\xi^{(I)} = 10^8 \sqrt{G_{01}} \left| M^{(I)} \right| \tag{4.41}$$

with an arbitrary normalization factor 10^8 so that the nuclear sensitivities turn out to be order of unity. It is observed that the nuclear sensitivities $\xi^{(0\nu)}$ for light neutrino exchange of ^{100}Mo, ^{130}Te, ^{150}Nd, ^{96}Zr, ^{110}Pd, ^{94}Zr and ^{128}Te isotopes are in the decreasing order of their magnitudes. The nuclear sensitivities $\xi^{(0N)}$ for heavy neutrino exchange of ^{100}Mo, ^{130}Te, ^{96}Zr, ^{150}Nd, ^{110}Pd, ^{94}Zr and ^{128}Te isotopes are in the decreasing order of their magnitudes.

4.2.3 Uncertainties in NTMEs

The uncertainties associated with the NTMEs $M^{(0\nu)}$ and $M^{(0N)}$ for $0\nu\beta^-\beta^-$ decay are estimated by preforming a statistical analysis by employing set of twelve NTMEs listed in the columns 4–6 of Table 4.3 and Table 4.4, respectively. The mean $\overline{M}^{(I)}$ and their variances $\Delta\overline{M}^{(I)}$ are calculated by using Eqs. (3.64) and (3.65) of Chapter 3. It turns out that the uncertainties $\Delta\overline{M}^{(0\nu)}$ are of the order of 10%, but for ^{110}Pd for which $\Delta\overline{M}^{(0\nu)}$ is approximately 14%. For the case of NTMEs associated with heavy Majorana neutrino

exchange, the maximum uncertainty $\Delta\overline{M}^{(0N)}$ is about 37%.

4.2.4 Deformation effect

The effect of deformation on $M^{(I)}$ is quantified by the quantity $D^{(I)}$ defined as the ratio of $M^{(I)}$ at zero deformation ($\zeta_{qq} = 0$) and full deformation ($\zeta_{qq} = 1$) [Chaturvedi *et al.* (2008)].

$$D^{(I)} = \frac{M^{(I)}(\zeta_{qq} = 0)}{M^{(I)}(\zeta_{qq} = 1)}, \tag{4.42}$$

In Table 4.10, we tabulate the values of $D^{(I)}$ for ^{94,96}Zr, ^{100}Mo, ^{104}Ru, ^{110}Pd, ^{128,130}Te and ^{150}Nd nuclei. It is observed that owing to deformation effects, the NTMEs $M^{(I)}$ are suppressed by factor of about 2–11 in the mass range $A = 90-150$. Thus, the deformation plays a crucial role in the nuclear structure aspects of $0\nu\beta^-\beta^-$ decay.

4.3 Conclusions

The required NTMEs to study the $0\nu\beta^-\beta^-$ decay of ^{94,96}Zr, ^{100}Mo, ^{104}Ru, ^{110}Pd, ^{128,130}Te and ^{150}Nd isotopes within mass mechanism are calculated within PHFB model using four different parametrization of pairing plus multipolar type of effective two body interaction with three different parametrizations of SRC. It is observed that the closure approximation is quite valid as expected. The effect due to FNS is about 12% and 33% for light and heavy neutrino exchange, respectively. With the consideration of the SRCs, the NTMEs $M^{(0\nu)}$ $\left(M^{(0N)}\right)$ are in addition reduced by approximately 17%(68%), 2.0%(42%) and 3%(20%) for SRC1, SRC2 and SRC3, respectively. The effects due to deformation are in between a factor of 2–11. We have also extracted limits on the effective neutrino mass

$\langle m_\nu \rangle$ and $\langle M_N \rangle$ from the available limits on experimental half-lives $T^{0\nu}_{1/2}$ using average NTMEs $\overline{M}^{(I)}(I = 0\nu, 0N)$ calculated in the PHFB model. The extracted limits on $\langle m_\nu \rangle$ and $\langle M_N \rangle$ for ^{130}Te nuclei is very stringent and equal to 0.17 eV and 8.99×10^7 GeV, respectively, from the observed limit on the half-live $T^{0\nu}_{1/2} > 1.5 \times 10^{25}$ yr of $0\nu\beta^-\beta^-$ decay [Alduino *et al.* (2018)].

Table 4.1: Decomposition of NTMEs $M^{(0\nu)}$ calculated in (a) $PQQ1$, (b) $PQQHH1$, (c) $PQQ2$ and (d) $PQQHH2$ parametrizations for the $0\nu\beta^-\beta^-$decay of ^{100}Mo nuclei due to the exchange of light Majorana neutrinos.

	NTME	P	FNS	F+SRC			F+SRC($\overline{A}/2$)		
				SRC1	SRC2	SRC3	SRC1	SRC2	SRC3
(a)	$M_F^{(0\nu)}$	1.2464	1.0823	0.9501	1.0830	1.1201	1.0401	1.1803	1.2191
	$M_{GT-AA}^{(0\nu)}$	-6.0238	-5.4951	-4.7297	-5.4237	-5.6420	-5.2338	-5.9633	-6.1901
	$M_{GT-PP}^{(0\nu)}$	-0.4786	-0.3625	-0.2354	-0.3251	-0.3627	-0.2431	-0.3348	-0.3730
	$M_{GT-AP}^{(0\nu)}$	1.5317	1.2486	0.9179	1.1747	1.2710	0.9584	1.2221	1.3204
	$M_{GT-MM}^{(0\nu)}$	-0.3044	-0.1892	-0.0945	-0.1458	-0.1755	-0.0982	-0.1505	-0.1806
	$M_{GT}^{(0\nu)}$	-5.2750	-4.7981	-4.1417	-4.7199	-4.9092	-4.6167	-5.2266	-5.4233
	$M_{T-PP}^{(0\nu)}$	-0.0498	-0.0366	-0.0371	-0.0379	-0.0378	-0.0380	-0.0388	-0.0387
	$M_{T-AP}^{(0\nu)}$	0.1356	0.1044	0.1059	0.1075	0.1073	0.1084	0.1101	0.1098
	$M_{T-MM}^{(0\nu)}$	0.0165	0.0095	0.0096	0.0100	0.0100	0.0098	0.0102	0.0102
	$M_T^{(0\nu)}$	0.1024	0.0774	0.0783	0.0797	0.0795	0.0802	0.0815	0.0813
	$\left\vert M^{(0\nu)}\right\vert$	6.4190	5.8031	5.0134	5.7232	5.9498	5.5767	6.3254	6.5610
(b)	$M_F^{(0\nu)}$	1.0816	0.9237	0.7956	0.9231	0.9590	0.8619	0.9964	1.0339
	$M_{GT-AA}^{(0\nu)}$	-5.7962	-5.2855	-4.5463	-5.2166	-5.4275	-5.0266	-5.7312	-5.9502
	$M_{GT-PP}^{(0\nu)}$	-0.4624	-0.3503	-0.2275	-0.3141	-0.3505	-0.2349	-0.3235	-0.3605
	$M_{GT-AP}^{(0\nu)}$	1.4804	1.2069	0.8875	1.1355	1.2286	0.9266	1.1813	1.2762
	$M_{GT-MM}^{(0\nu)}$	-0.2941	-0.1827	-0.0913	-0.1408	-0.1695	-0.0949	-0.1454	-0.1745
	$M_{GT}^{(0\nu)}$	-5.0723	-4.6116	-3.9776	-4.5361	-4.7189	-4.4298	-5.0189	-5.2089
	$M_{T-PP}^{(0\nu)}$	-0.0390	-0.0284	-0.0289	-0.0295	-0.0294	-0.0295	-0.0302	-0.0301
	$M_{T-AP}^{(0\nu)}$	0.1014	0.0767	0.0778	0.0791	0.0790	0.0793	0.0807	0.0805
	$M_{T-MM}^{(0\nu)}$	0.0131	0.0074	0.0074	0.0078	0.0078	0.0076	0.0079	0.0079
	$M_T^{(0\nu)}$	0.0755	0.0556	0.0563	0.0574	0.0573	0.0573	0.0584	0.0583
	$\left\vert M^{(0\nu)}\right\vert$	6.0783	5.4797	4.7169	5.4017	5.6206	5.2343	5.9568	6.1844

Table 4.1 continued

	NTME	P	FNS	F+SRC			F+SRC($\overline{A}$/2)		
				SRC1	SRC2	SRC3	SRC1	SRC2	SRC3
(c)	$M_F^{(0\nu)}$	1.2474	1.0834	0.9513	1.0842	1.1213	1.0414	1.1816	1.2203
	$M_{GT-AA}^{(0\nu)}$	-6.0033	-5.4753	-4.7108	-5.4041	-5.6221	-5.2127	-5.9415	-6.1679
	$M_{GT-PP}^{(0\nu)}$	-0.4780	-0.3621	-0.2351	-0.3247	-0.3623	-0.2428	-0.3344	-0.3726
	$M_{GT-AP}^{(0\nu)}$	1.5288	1.2460	0.9156	1.1722	1.2684	0.9560	1.2193	1.3175
	$M_{GT-MM}^{(0\nu)}$	-0.3040	-0.1889	-0.0944	-0.1456	-0.1753	-0.0981	-0.1504	-0.1804
	$M_{GT}^{(0\nu)}$	-5.2566	-4.7804	-4.1247	-4.7023	-4.8913	-4.5976	-5.2069	-5.4034
	$M_{T-PP}^{(0\nu)}$	-0.0519	-0.0382	-0.0387	-0.0395	-0.0394	-0.0397	-0.0405	-0.0404
	$M_{T-AP}^{(0\nu)}$	0.1415	0.1090	0.1106	0.1122	0.1120	0.1132	0.1149	0.1146
	$M_{T-MM}^{(0\nu)}$	0.0172	0.0099	0.0100	0.0104	0.0104	0.0102	0.0106	0.0106
	$M_T^{(0\nu)}$	0.1068	0.0808	0.0818	0.0831	0.0830	0.0837	0.0851	0.0849
	$\left\|M^{(0\nu)}\right\|$	6.3972	5.7830	4.9943	5.7034	5.9297	5.5553	6.3034	6.5388
(d)	$M_F^{(0\nu)}$	1.0654	0.9086	0.7814	0.9080	0.9437	0.8456	0.9792	1.0164
	$M_{GT-AA}^{(0\nu)}$	-5.7221	-5.2152	-4.4812	-5.1466	-5.3559	-4.9530	-5.6525	-5.8699
	$M_{GT-PP}^{(0\nu)}$	-0.4590	-0.3476	-0.2257	-0.3117	-0.3478	-0.2331	-0.3210	-0.3577
	$M_{GT-AP}^{(0\nu)}$	1.4674	1.1959	0.8787	1.1249	1.2173	0.9173	1.1701	1.2644
	$M_{GT-MM}^{(0\nu)}$	-0.2919	-0.1814	-0.0906	-0.1398	-0.1682	-0.0941	-0.1443	-0.1732
	$M_{GT}^{(0\nu)}$	-5.0057	-4.5483	-3.9188	-4.4732	-4.6547	-4.3629	-4.9477	-5.1363
	$M_{T-PP}^{(0\nu)}$	-0.0408	-0.0299	-0.0303	-0.0309	-0.0309	-0.0310	-0.0316	-0.0316
	$M_{T-AP}^{(0\nu)}$	0.1062	0.0804	0.0816	0.0830	0.0828	0.0832	0.0846	0.0844
	$M_{T-MM}^{(0\nu)}$	0.0136	0.0077	0.0078	0.0081	0.0081	0.0079	0.0083	0.0083
	$M_T^{(0\nu)}$	0.0790	0.0583	0.0591	0.0602	0.0600	0.0601	0.0612	0.0611
	$\left\|M^{(0\nu)}\right\|$	5.9921	5.3986	4.6411	5.3211	5.5384	5.1484	5.8657	6.0917

Table 4.2: Decomposition of NTMEs $M^{(0N)}$ calculated in (a) $PQQ1$, (b) $PQQHH1$, (c) $PQQ2$ and (d) $PQQHH2$ parametrizations for the $0\nu\beta^-\beta^-$decay of ^{100}Mo nuclei due to the exchange of heavy Majorana neutrinos.

	NTME	P	FNS	F+SRC		
				SRC1	SRC2	SRC3
(a)	$M^{(0N)}_{Fh}$	85.5809	55.4045	28.9452	43.6462	51.9028
	$M^{(0N)}_{GT-AA}$	-414.1650	-304.4840	-118.1970	-198.5860	-259.5880
	$M^{(0N)}_{GT-PP}$	-83.8104	-55.3411	-7.6215	-24.2524	-40.3074
	$M^{(0N)}_{GT-AP}$	208.8210	144.4150	36.4057	78.0266	113.9140
	$M^{(0N)}_{GT-MM}$	-68.8591	-34.1591	12.5725	5.5036	-11.3419
	$M^{(0N)}_{GTh}$	-358.0135	-249.5692	-76.8403	-139.3082	-197.3233
	$M^{(0N)}_{T-AP}$	23.9353	15.9262	15.6489	16.9109	16.9494
	$M^{(0N)}_{T-PP}$	-9.8403	-6.2621	-6.1031	-6.6918	-6.7148
	$M^{(0N)}_{T-MM}$	4.3340	2.0213	1.8079	2.1621	2.2050
	$M^{(0N)}_{Th}$	18.4290	11.6855	11.3537	12.3812	12.4396
	$\left\|M^{(0N)}\right\|$	425.1653	293.2883	94.4319	170.5732	236.7865
(b)	$M^{(0N)}_{Fh}$	82.6694	53.0080	27.5202	41.6264	49.5854
	$M^{(0N)}_{GT-AA}$	-400.0750	-294.1170	-114.1750	-191.8250	-250.7490
	$M^{(0N)}_{GT-PP}$	-80.9412	-53.4358	-7.3409	-23.4053	-38.9136
	$M^{(0N)}_{GT-AP}$	201.6890	139.4670	35.1355	75.3386	110.0040
	$M^{(0N)}_{GT-MM}$	-66.5406	-32.9884	12.1525	5.3243	-10.9477
	$M^{(0N)}_{GTh}$	-345.8678	-241.0742	-74.2278	-134.5674	-190.6063
	$M^{(0N)}_{T-AP}$	19.2273	12.6177	12.3731	13.4124	13.4468
	$M^{(0N)}_{T-PP}$	-7.9505	-4.9869	-4.8493	-5.3338	-5.3540
	$M^{(0N)}_{T-MM}$	3.6053	1.6338	1.4560	1.7471	1.7830
	$M^{(0N)}_{Th}$	14.8821	9.2646	8.9798	9.8257	9.8758
	$\left\|M^{(0N)}\right\|$	413.6552	284.8176	92.7683	166.3681	230.3159

Table 4.2 continued

	NTME	P	FNS	F+SRC		
				SRC1	SRC2	SRC3
(c)	$M_{Fh}^{(0N)}$	85.4586	55.4104	28.9733	43.6719	51.9204
	$M_{GT-AA}^{(0N)}$	-413.5740	-304.1090	-118.0630	-198.3560	-259.2780
	$M_{GT-PP}^{(0N)}$	-83.7057	-55.3005	-7.6434	-24.2537	-40.2876
	$M_{GT-AP}^{(0N)}$	208.5640	144.2940	36.4249	77.9955	113.8360
	$M_{GT-MM}^{(0N)}$	-68.6855	-34.1155	12.5533	5.4944	-11.3286
	$M_{GTh}^{(0N)}$	-357.4012	-249.2310	-76.7282	-139.1198	-197.0583
	$M_{T-AP}^{(0N)}$	24.8640	16.5860	16.3028	17.6076	17.6468
	$M_{T-PP}^{(0N)}$	-10.2133	-6.5176	-6.3546	-6.9634	-6.9869
	$M_{T-MM}^{(0N)}$	4.4743	2.0967	1.8764	2.2428	2.2870
	$M_{Th}^{(0N)}$	19.1250	12.1651	11.8246	12.8870	12.9469
	$\left\|M^{(0N)}\right\|$	423.7348	292.4763	93.8770	169.9046	236.0318
(d)	$M_{Fh}^{(0N)}$	82.0667	52.6416	27.3340	41.3432	49.2455
	$M_{GT-AA}^{(0N)}$	-397.1580	-291.9360	-113.3100	-190.3870	-248.8810
	$M_{GT-PP}^{(0N)}$	-80.4078	-53.0961	-7.3393	-23.2854	-38.6803
	$M_{GT-AP}^{(0N)}$	200.3270	138.5400	34.9725	74.8793	109.2920
	$M_{GT-MM}^{(0N)}$	-66.0566	-32.7720	12.0384	5.2596	-10.8935
	$M_{GTh}^{(0N)}$	-343.2954	-239.2641	-73.6384	-133.5335	-189.1628
	$M_{T-AP}^{(0N)}$	19.9498	13.1646	12.9189	13.9865	14.0209
	$M_{T-PP}^{(0N)}$	-8.2334	-5.1955	-5.0564	-5.5542	-5.5745
	$M_{T-MM}^{(0N)}$	3.6932	1.6894	1.5073	1.8066	1.8433
	$M_{Th}^{(0N)}$	15.4096	9.6585	9.3699	10.2389	10.2897
	$\left\|M^{(0N)}\right\|$	409.9525	282.2472	91.6026	164.6378	228.1186

Table 4.3: Calculated NTMEs $M^{(0\nu)}$ with (a) $PQQ1$, (b) $PQQHH1$, (c) $PQQ2$ and (d) $PQQHH2$ parametrizations for the $0\nu\beta^-\beta^-$ decay of ^{94,96}Zr, ^{100}Mo, ^{104}Ru, ^{110}Pd, ^{128,130}Te, ^{150}Nd isotopes due to the exchange of light Majorana neutrinos.

Nuclei		FNS	F+SRC			F+SRC($\overline{A}/2$)		
			SRC1	SRC2	SRC3	SRC1	SRC2	SRC3
^{94}Zr	(a)	3.7246	3.1870	3.6620	3.8170	3.5047	4.0050	4.1662
	(b)	3.4234	2.9215	3.3642	3.5089	3.2101	3.6765	3.8269
	(c)	4.0451	3.5364	3.9950	4.1419	3.9152	4.3983	4.5509
	(d)	3.3124	2.8224	3.2542	3.3954	3.1017	3.5565	3.7033
^{96}Zr	(a)	2.5806	2.1919	2.5336	2.6450	2.4317	2.7919	2.9077
	(b)	2.5258	2.1277	2.4764	2.5904	2.3528	2.7203	2.8389
	(c)	2.5140	2.1339	2.4679	2.5768	2.3671	2.7192	2.8324
	(d)	2.4626	2.0741	2.4143	2.5256	2.2937	2.6524	2.7681
^{100}Mo	(a)	5.8031	5.0134	5.7232	5.9498	5.5767	6.3254	6.5610
	(b)	5.4797	4.7169	5.4017	5.6206	5.2343	5.9568	6.1844
	(c)	5.7830	4.9943	5.7034	5.9297	5.5553	6.3034	6.5388
	(d)	5.3986	4.6411	5.3211	5.5384	5.1484	5.8657	6.0917
^{104}Ru	(a)	3.1853	2.6665	3.1506	3.3002	2.8886	3.3995	3.5551
	(b)	2.9767	2.4805	2.9421	3.0850	2.6794	3.1665	3.3152
	(c)	3.2979	2.7646	3.2617	3.4154	2.9982	3.5229	3.6828
	(d)	3.0190	2.5173	2.9838	3.1283	2.7205	3.2129	3.3633
^{110}Pd	(a)	3.8919	3.3612	3.8442	3.9962	3.7599	4.2703	4.4286
	(b)	5.3346	4.6238	5.2693	5.4730	5.1702	5.8524	6.0646
	(c)	5.0913	4.4049	5.0304	5.2272	4.9224	5.5834	5.7883
	(d)	4.7101	4.0666	4.6508	4.8350	4.5450	5.1623	5.3542
^{128}Te	(a)	2.8955	2.4823	2.8541	2.9729	2.7698	3.1639	3.2879
	(b)	2.6329	2.2211	2.5900	2.7082	2.4623	2.8533	2.9767
	(c)	2.9615	2.5421	2.9197	3.0404	2.8375	3.2377	3.3636
	(d)	2.6043	2.1902	2.5612	2.6800	2.4244	2.8175	2.9416
^{130}Te	(a)	4.3429	3.7772	4.2822	4.4452	4.2441	4.7795	4.9497
	(b)	3.9744	3.4207	3.9106	4.0699	3.8329	4.3523	4.5186
	(c)	3.9575	3.4266	3.8994	4.0522	3.8459	4.3472	4.5067
	(d)	4.3409	3.7584	4.2763	4.4440	4.2160	4.7650	4.9401
^{150}Nd	(a)	1.5651	1.3601	1.5489	1.6080	1.5187	1.7194	1.7812
	(b)	1.3442	1.1551	1.3286	1.3831	1.2803	1.4648	1.5217
	(c)	1.5389	1.3374	1.5230	1.5811	1.4934	1.6907	1.7515
	(d)	1.3313	1.1458	1.3162	1.3696	1.2712	1.4523	1.5082

Table 4.4 : Calculated NTMEs $M^{(0N)}$ with (a) $PQQ1$, (b) $PQQHH1$, (c) $PQQ2$ and (d) $PQQHH2$ parametrizations for the $0\nu\beta^-\beta^-$ decay of ^{94,96}Zr, ^{100}Mo, ^{104}Ru, ^{110}Pd, ^{128,130}Te, ^{150}Nd isotopes due to the exchange of heavy Majorana neutrinos.

Nuclei		FNS	F+SRC		
			SRC1	SRC2	SRC3
^{94}Zr	(a)	203.2751	67.8689	119.6413	164.7657
	(b)	189.5836	63.2916	111.5600	153.6496
	(c)	200.7418	71.5457	121.6008	164.6023
	(d)	184.4190	61.2271	108.2680	149.3274
^{96}Zr	(a)	141.9017	44.9432	81.8051	114.1234
	(b)	145.3457	46.1813	83.8631	116.9214
	(c)	138.5449	43.7558	79.7812	111.3773
	(d)	141.6329	44.8727	81.6315	113.8885
^{100}Mo	(a)	293.2883	94.4319	170.5732	236.7865
	(b)	284.8176	92.7683	166.3681	230.3159
	(c)	292.4763	93.8770	169.9046	236.0318
	(d)	282.2472	91.6026	164.6378	228.1186
^{104}Ru	(a)	203.8109	70.5058	122.7010	166.9829
	(b)	195.1071	67.8059	117.6135	159.9077
	(c)	209.0557	72.0996	125.6824	171.1804
	(d)	197.0849	68.3978	118.7301	161.4859
^{110}Pd	(a)	198.2846	63.9080	115.6405	160.3442
	(b)	270.9020	90.7743	160.3396	220.2645
	(c)	257.9370	83.8262	150.9320	208.8491
	(d)	244.1266	81.3110	144.1521	198.3176
^{128}Te	(a)	160.8075	55.2432	96.1106	131.2360
	(b)	159.6205	54.7378	95.3085	130.2117
	(c)	163.3688	56.1680	97.6757	133.3445
	(d)	160.5424	55.0992	95.8922	130.9814
^{130}Te	(a)	222.3150	77.7118	133.5565	181.6968
	(b)	216.9775	76.0308	130.3507	177.2936
	(c)	207.3902	71.9214	124.1740	169.2793
	(d)	229.7443	81.0846	138.4904	187.9900
^{150}Nd	(a)	80.4797	27.2294	47.9481	65.6449
	(b)	73.9475	24.9391	43.9845	60.2743
	(c)	79.1299	26.7764	47.1469	64.5455
	(d)	72.6078	24.5094	43.2064	59.1931

Table 4.5: Comparison of NTMEs due to light neutrino exchange $M^{(0\nu)}$ in different nuclear models.

Nuclei	Model	References	g_A	$M^{(0\nu)}$			
				Jastrow	AV18	CD Bonn	UCOM
^{96}Zr	$PQQ1$	Present work	1.2701	2.192	2.534	2.645	
	$PQQHH1$	Present work	1.2701	2.128	2.476	2.590	
	$PQQ2$	Present work	1.2701	2.134	2.468	2.577	
	$PQQHH2$	Present work	1.2701	2.074	2.414	2.526	
	QRPA	[Faessler *et al.* (2012)]	1.254	1.22	2.07	2.28	1.77
	pnQRPA	[Civitarese *et al.* (2009)]	1.25	2.065			3.117
	pnQRPA	[Hyvarinen *et al.* (2015)]	1.26			3.14	
	QRPA(I)	[Simkovic *et al.* (2013)]	1.27		2.717	2.957	
	RQRPA	[Faessler *et al.* (2012)]	1.254	1.31	2.01	2.19	1.77
	EDF	[Vaquero *et al.* (2013)]	1.25				6.498
	IBM-2	[Barea *et al.* (2013)]	1.254	2.53	2.89	3.00	
	IBM-2(I)	[Barea *et al.* (2015)]	1.269		2.83		
	CDFT	[Song *et al.* (2017)], [Yao *et al.* (2015)]	1.254	4.84	5.58	5.82	6.47
^{100}Mo	$PQQ1$	Present work	1.2701	5.013	5.723	5.950	
	$PQQHH1$	Present work	1.2701	4.717	5.402	5.621	
	$PQQ2$	Present work	1.2701	4.994	5.703	5.930	
	$PQQHH2$	Present work	1.2701	4.641	5.321	5.538	
	QRPA	[Faessler *et al.* (2012)]	1.254	3.64	5.18	5.73	4.71
	pnQRPA	[Civitarese *et al.* (2009)]	1.25	2.737			3.931
	pnQRPA	[Hyvarinen *et al.* (2015)]	1.26			3.90	
	QRPA(I)	[Simkovic *et al.* (2013)]	1.27		5.402	5.850	
	RQRPA	[Faessler *et al.* (2012)]	1.254	3.03	4.20	4.67	3.88
	EDF	[Vaquero *et al.* (2013)]	1.25				6.588
	IBM-2	[Barea *et al.* (2013)]	1.254	3.73	4.31	4.50	
	IBM-2(I)	[Barea *et al.* (2015)]	1.269		4.22		
	CDFT	[Song *et al.* (2017)], [Yao *et al.* (2015)]	1.254	9.38	10.80	11.27	6.58

Table 4.5 continued

Nuclei	Model	References	g_A	$M^{(0\nu)}$			
				Jastrow	AV18	CD Bonn	UCOM
^{110}Pd	$PQQ1$	Present work	1.2701	3.361	3.844	3.996	
	$PQQHH1$	Present work	1.2701	4.624	5.269	5.473	
	$PQQ2$	Present work	1.2701	4.405	5.030	5.227	
	$PQQHH2$	Present work	1.2701	4.067	4.651	4.835	
	pnQRPA	[Hyvarinen *et al.* (2015)]	1.26			6.52	
	QRPA(I)	[Simkovic *et al.* (2013)]	1.27		5.762	6.255	
	IBM-2	[Barea *et al.* (2013)]	1.254	3.62	4.15	4.31	
	IBM-2(I)	[Barea *et al.* (2015)]	1.269		4.05		
^{128}Te	$PQQ1$	Present work	1.2701	2.482	2.854	2.973	
	$PQQHH1$	Present work	1.2701	2.221	2.590	2.708	
	$PQQ2$	Present work	1.2701	2.542	2.920	3.040	
	$PQQHH2$	Present work	1.2701	2.190	2.561	2.680	
	ISM	[Menendez *et al.* (2009)], [Caurier *et al.* (2008)]	1.25	2.26			2.88
	QRPA	[Faessler *et al.* (2012)]	1.254	3.97	5.38	5.99	5.04
	pnQRPA	[Civitarese *et al.* (2009)]	1.25	3.383			4.790
	pnQRPA	[Hyvarinen *et al.* (2015)]	1.26			4.92	
	QRPA(I)	[Simkovic *et al.* (2013)]	1.27		4.563	5.084	
	RQRPA	[Faessler *et al.* (2012)]	1.254	3.52	4.71	5.26	4.45
	EDF	[Vaquero *et al.* (2013)]	1.25				5.687
	IBM-2	[Barea *et al.* (2013)]	1.254	4.48	4.97	5.13	
	IBM-2(I)	[Barea *et al.* (2015)]	1.269		4.10		
^{130}Te	$PQQ1$	Present work	1.2701	3.777	4.282	4.445	
	$PQQHH1$	Present work	1.2701	3.421	3.911	4.070	
	$PQQ2$	Present work	1.2701	3.427	3.900	4.052	
	$PQQHH2$	Present work	1.2701	3.758	4.276	4.444	
	SM	[Menendez *et al.* (2018)]	1.27		2.76	2.96	
	ISM	[Menendez *et al.* (2009)], [Caurier *et al.* (2008)]	1.25	2.04			2.65

Table 4.5 continued

Nuclei	Model	References	g_A	$M^{(0\nu)}$			
				Jastrow	AV18	CD Bonn	UCOM
	QRPA	[Faessler *et al.* (2012)]	1.254	3.56	4.77	5.37	4.53
	pnQRPA	[Civitarese *et al.* (2009)]	1.25	2.993			4.221
	pnQRPA	[Hyvarinen *et al.* (2015)]	1.26			4.00	
	QRPA(I)	[Simkovic *et al.* (2013)]	1.27		3.888	4.373	
	RQRPA	[Faessler *et al.* (2012)]	1.254	3.22	4.27	4.80	4.07
	DQRPA(I)	[Fang *et al.* (2018)]	1.27		2.90	3.22	
	EDF	[Vaquero *et al.* (2013)]	1.25				6.405
	IBM-2	[Barea *et al.* (2013)]	1.254	4.03	4.47	4.61	
	IBM-2(I)	[Barea *et al.* (2015)]	1.269		3.70		
	CDFT	[Song *et al.* (2017)], [Yao *et al.* (2015)]	1.254	8.03	9.38	9.82	4.98
^{150}Nd	$PQQ1$	Present work	1.2701	1.360	1.549	1.608	
	$PQQHH1$	Present work	1.2701	1.155	1.329	1.383	
	$PQQ2$	Present work	1.2701	1.337	1.523	1.581	
	$PQQHH2$	Present work	1.2701	1.146	1.316	1.370	
	DQRPA	[Fang *et al.* (2011)]	1.25			3.34	
	DQRPA(I)	[Fang *et al.* (2018)]	1.27		3.01	3.43	
	EDF	[Vaquero *et al.* (2013)]	1.25				2.190
	IBM-2	[Barea *et al.* (2013)]	1.254	2.32	2.74	2.88	
	IBM-2(I)	[Barea *et al.* (2015)]	1.269		2.67		
	CDFT	[Song *et al.* (2017)], [Yao *et al.* (2015)]	1.254	11.11	13.00	13.62	5.60

Table 4.6: Comparison of NTMEs $M^{(0N)}$ due to heavy neutrino exchange in different nuclear models.

Nuclei	Model	References	g_A	$M^{(0N)}$		
				Jastrow	AV18	CD Bonn
^{96}Zr	$PQQ1$	Present work	1.2701	44.943	81.805	114.123
	$PQQHH1$	Present work	1.2701	46.181	83.863	116.921
	$PQQ2$	Present work	1.2701	43.756	79.781	111.377
	$PQQHH2$	Present work	1.2701	44.872	81.631	113.888
	pnQRPA	[Hyvarinen *et al.* (2015)]	1.26			307.9
	IBM-2	[Barea *et al.* (2013)]	1.254	59.0	99.0	135
	IBM-2(I)	[Barea *et al.* (2015)]	1.269		98.7	
	CDFT	[Song *et al.* (2017)], [Yao *et al.* (2015)]	1.254	89.0	177.7	250.5
^{100}Mo	$PQQ1$	Present work	1.2701	94.432	170.573	236.786
	$PQQHH1$	Present work	1.2701	92.768	166.368	230.316
	$PQQ2$	Present work	1.2701	93.877	169.905	236.032
	$PQQHH2$	Present work	1.2701	91.603	164.638	238.119
	pnQRPA	[Hyvarinen *et al.* (2015)]	1.26			350.8
	RQRPA	[Simkovic *et al.* (2010)]	1.25			392
	IBM-2	[Barea *et al.* (2013)]	1.254	99.3	165	224
	IBM-2(I)	[Barea *et al.* (2015)]	1.269		164	
	CDFT	[Song *et al.* (2017)], [Yao *et al.* (2015)]	1.254	174.1	346.7	487.4
^{110}Pd	PQQ1	Present work	1.2701	63.908	115.640	160.344
	PQQHH1	Present work	1.2701	90.774	160.340	220.264
	PQQ2	Present work	1.2701	83.826	150.932	208.849
	PQQHH2	Present work	1.2701	81.311	144.152	198.318
	pnQRPA	[Hyvarinen *et al.* (2015)]	1.26			475.7
	IBM-2	[Barea *et al.* (2013)]	1.254	95.7	155	208
	IBM-2(I)	[Barea *et al.* (2015)]	1.269		154	
^{128}Te	$PQQ1$	Present work	1.2701	55.243	96.111	131.236
	$PQQHH1$	Present work	1.2701	54.738	95.308	130.212
	$PQQ2$	Present work	1.2701	56.168	97.676	133.344

Table 4.6 continued

Nuclei	Model	References	g_A	$M^{(0N)}$		
				Jastrow	AV18	CD Bonn
	$PQQHH2$	Present work	1.2701	55.010	95.892	130.981
	pnQRPA	[Hyvarinen *et al.* (2015)]	1.26			396.1
	IBM-2	[Barea *et al.* (2013)]	1.254	48.4	101	152
	IBM-2(I)	[Barea *et al.* (2015)]	1.269		101	
^{130}Te	$PQQ1$	Present work	1.2701	77.712	133.556	181.697
	$PQQHH1$	Present work	1.2701	76.031	130.351	177.294
	$PQQ2$	Present work	1.2701	71.921	124.174	169.279
	$PQQHH2$	Present work	1.2701	81.085	138.490	187.990
	SM	[Menendez *et al.* (2018)]	1.27		146	210
	pnQRPA	[Hyvarinen *et al.* (2015)]	1.26			338.3
	RQRPA	[Simkovic *et al.* (2010)]	1.25			362
	DQRPA(I)	[Fang *et al.* (2018)]	1.27		191.4	303.5
	IBM-2	[Barea *et al.* (2013)]	1.254	44.0	92.0	138
	IBM-2(I)	[Barea *et al.* (2015)]	1.269		91.8	
	CDFT	[Song *et al.* (2017)], [Yao *et al.* (2015)]	1.254	168.5	339.2	472.8
^{150}Nd	$PQQ1$	Present work	1.2701	27.229	47.948	65.645
	$PQQHH1$	Present work	1.2701	24.939	43.984	60.274
	$PQQ2$	Present work	1.2701	26.776	47.147	64.545
	$PQQHH2$	Present work	1.2701	24.509	43.206	59.193
	DQRPA(I)	[Fang *et al.* (2018)]	1.27		206.1	337.0
	IBM-2	[Barea *et al.* (2013)]	1.254	68.4	116	160
	IBM-2(I)	[Barea *et al.* (2015)]	1.269		116	
	CDFT	[Song *et al.* (2017)], [Yao *et al.* (2015)]	1.254	237.7	481.7	667.9

Table 4.7: Changes (in %) of the NTMEs $M^{(I)}$ ($I = 0\nu, 0N$) due to exchange of light and heavy Majorana neutrinos, for the $0\nu\beta^-\beta^-$ decay with the inclusion of FNS and F+SRC ((i) F+SRC1, (ii) F+SRC2, (iii) F+SRC3) for the four different parametrizations of the effective two-body interaction.

Parametrization	$M^{(0\nu)}$		$M^{(0N)}$	
	FNS	F+SRC	FNS	F+SRC
$PQQ1$	9.51–11.66	(i) 13.03–16.29	29.25–33.37	(i) 65.04–68.33
		(ii) 1.04–1.82		(ii) 39.80–42.35
		(iii) 2.35–3.61		(iii) 18.07–19.58
$PQQHH1$	9.55–11.93	(i) 13.32–16.67	29.43–33.46	(i) 64.96–68.23
		(ii) 1.16–1.96		(ii) 39.72–42.30
		(iii) 2.40–3.64		(iii) 18.04–19.56
$PQQ2$	9.44–11.57	(i) 12.57–16.17	29.29–32.91	(i) 64.36–68.42
		(ii) 1.03–1.83		(ii) 39.42–42.41
		(iii) 2.39–3.56		(iii) 18.00–19.61
$PQQHH2$	9.73–11.89	(i) 13.42–16.62	29.44–33.48	(i) 64.71–68.32
		(ii) 1.14–1.96		(ii) 39.72–42.36
		(iii) 2.38–3.62		(iii) 18.06–19.59

Table 4.8 : Experimental Half-life $T^{(0\nu)}_{1/2}$ and Phase space factor G_{01} [Stoica *et al.* (2013)] for the $0\nu\beta^-\beta^-$ decay of ^{94,96}Zr, ^{100}Mo, ^{110}Pd, ^{128,130}Te and ^{150}Nd isotopes.

Nuclei	$T^{(0\nu)}_{1/2}$ (Exp.)	Reference	G_{01} (yr^{-1})
^{94}Zr	1.9×10^{19}	[Arnold *et al.* (1999)]	1.750×10^{-15}*
^{96}Zr	9.2×10^{21}	[Barabash *et al.* (2011)]	5.283×10^{-14}
^{100}Mo	1.1×10^{24}	[Arnold *et al.* (2015)]	4.086×10^{-14}
^{110}Pd	6.0×10^{17}	[Winter (1952)]	1.246×10^{-14}
^{128}Te	1.1×10^{23}	[Arnaboldi *et al.* (2003)]	1.444×10^{-15}
^{130}Te	1.5×10^{25}	[Alduino *et al.* (2018)]	3.669×10^{-14}
^{150}Nd	2.0×10^{22}	[Arnold *et al.* (2016)]	1.613×10^{-13}

'*' Value taken from Boehm and Vogel (1992).

Table 4.9: Average NTMEs $\overline{M}^{(I)}$ $(I = 0\nu, 0N)$ and uncertainties $\Delta\overline{M}^{(I)}$ along with effective neutrino mass $\langle m_\nu \rangle$ (in eV), $\langle M_N \rangle$ (in GeV), predicted half-lives $T_{1/2}^{(0\nu)}$ (for light neutrino exchange at $\langle m_\nu \rangle$ = 50 meV) and nuclear sensitivities $\xi^{(I)}$ for the $0\nu\beta^-\beta^-$ decay of ^{94,96}Zr, ^{100}Mo, ^{110}Pd, ^{128,130}Te and ^{150}Nd isotopes.

Nuclei	Light neutrino exchange					Heavy neutrino exchange			
	$\overline{M}^{(0\nu)}$	$\Delta\overline{M}^{(0\nu)}$	$\langle m_\nu \rangle$	$T_{1/2}^{(0\nu)}$	$\xi^{(0\nu)}$	$\overline{M}^{(0N)}$	$\Delta\overline{M}^{(0N)}$	$\langle M_N \rangle$	$\xi^{(0N)}$
^{94}Zr	3.467	0.399	8.08×10^{2}	4.96×10^{27}	14.50	113.11	39.73	1.93×10^{4}	4.73×10^{2}
^{96}Zr	2.396	0.206	9.67	3.44×10^{26}	55.07	80.26	29.54	1.66×10^{6}	1.84×10^{3}
^{100}Mo	5.379	0.448	0.45	8.84×10^{25}	108.7	164.62	59.66	3.27×10^{7}	3.33×10^{3}
^{110}Pd	4.565	0.648	1.29×10^{3}	4.02×10^{26}	50.97	139.89	53.05	1.13×10^{4}	1.56×10^{3}
^{128}Te	2.647	0.273	15.32	1.03×10^{28}	10.06	94.33	32.51	1.12×10^{6}	3.58×10^{2}
^{130}Te	3.980	0.350	0.17	1.80×10^{26}	76.24	129.13	44.04	8.99×10^{7}	2.47×10^{3}
^{150}Nd	1.388	0.152	6.48	3.36×10^{26}	55.75	44.62	15.75	2.38×10^{6}	1.79×10^{3}

Table 4.10 : Deformation ratios $D^{(I)}$ $(I = 0\nu, 0N)$ of $0\nu\beta^-\beta^-$ decay of ^{94,96}Zr, ^{100}Mo, ^{104}Ru, ^{110}Pd, ^{128,130}Te and ^{150}Nd isotopes for the PQQ1 parametrization.

Nuclei	$D^{(0\nu)}$				$D^{(0N)}$			
	FNS	F+SRC			FNS	F+SRC		
		SRC1	SRC2	SRC3		SRC1	SRC2	SRC3
^{94}Zr	2.36	2.40	2.37	2.36	2.18	2.20	2.19	2.18
^{96}Zr	4.43	4.55	4.46	4.44	4.03	4.35	4.16	4.08
^{100}Mo	3.46	3.51	3.47	3.46	3.33	3.58	3.43	3.37
^{104}Ru	8.01	8.36	8.01	7.93	6.15	6.07	6.09	6.12
^{110}Pd	5.49	5.61	5.51	5.48	5.04	5.53	5.23	5.12
^{128}Te	3.08	3.14	3.09	3.08	2.74	2.78	2.77	2.75
^{130}Te	3.78	3.92	3.81	3.77	2.98	3.11	3.04	3.01
^{150}Nd	10.97	10.94	10.96	10.97	10.98	10.68	10.86	10.93

Chapter 5

Conclusions

The implications of present studies on nuclear $\beta\beta$ decay are far reaching in nature. The validity of different models employed for nuclear structure calculations can be tested by studying the $2\nu\beta^-\beta^-$ decay. It is observed that in all cases of the $2\nu\beta^-\beta^-$ decay, the NTMEs $M_{2\nu}$ are sufficiently quenched. The main motive of all the theoretical calculations is to understand the physical mechanism responsible for the suppression of $M_{2\nu}$. The $0\nu\beta^-\beta^-$ decay is a convenient tool to test the physics beyond the SM, and it has not been observed so far. Hence the models predict half-lives assuming certain value for the neutrino mass or conversely extract various parameters from the observed limits on half-lives $T^{0\nu}_{1/2}$ of the $0\nu\beta^-\beta^-$ decay. The reliability of predictions can be judged a priori only from the success of the nuclear model in explaining various observed physical properties of nuclei. The common practice is to calculate the $M_{2\nu}$ to start with and compare with the experimentally observed value as the two decay modes involve the same set of initial and final nuclear wave functions.

The PHFB model is one of the convenient many-body techniques to study the medium

and heavy mass nuclei in which the pairing and deformation degrees of freedom are treated on equal footing. The pairing part of the two body interaction is responsible for the reduction of collectivity where as the quadrupole-quadrupole plus hexadecapole-hexadecapole (QQ) interaction enhances the collectivity in the nuclear intrinsic wave functions. Hence, the $PQQHH$ interaction seems to be the most appropriate choice to examine the explicit role of deformation degrees of freedom vis-à-vis the suppression of $M_{2\nu}$. In the present work, our aim was to study the $0\nu\beta^-\beta^-$ decay of ^{94,96}Zr, ^{100}Mo, ^{104}Ru, ^{110}Pd, ^{128,130}Te and ^{150}Nd for the $0^+ \rightarrow 0^+$ transition within the PHFB model using pairing plus multipolar type of effective two-body interaction. Specifically, we use pairing plus quadrupole-quadrupole plus hexadecapole-hexadecapole interaction and derive four different parametrizations, namely $PQQ1$, $PQQHH1$, $PQQ2$ and $PQQHH2$. The single particle energies used in the present work were derived from Woods-Saxon potential for the nuclei participating in $\beta^-\beta^-$ decay and adjusted to reproduce the experimentally observed sub-shell occupation numbers where ever available. We have tested the quality of wave functions by comparing the calculated values of a number of nuclear properties with the available experimental data. To be more specific, we have computed the yrast spectra, reduced $B(E2{:}0^+ \rightarrow 2^+)$ transition probabilities, deformation parameters β_2, g-factors $g(2^+)$ and NTMEs $M_{2\nu}$ of $2\nu\beta^-\beta^-$ decay for the $0^+ \rightarrow 0^+$ transition. It is observed from the trends of results that the validity of nuclear models presently employed to calculate the NTME $M_{2\nu}$ as well as half-life $T^{2\nu}_{1/2}$ can not be uniquely established due to large error bars in experimental results as well as uncertainty in g_A. Hence, further work is necessary both in the experimental as well as theoretical front to judge the relative applicability, success and failure of various models used so far for the study of $2\nu\beta^-\beta^-$

decay processes.

In case of $0\nu\beta^-\beta^-$ decay, we have studied the $0^+ \rightarrow 0^+$ transition of ^{94,96}Zr, ^{100}Mo, ^{104}Ru, ^{110}Pd, ^{128,130}Te and ^{150}Nd nuclei in the mass mechanism and extracted limits on effective mass of light neutrino $\langle m_\nu \rangle$ and heavy neutrinos $\langle M_N \rangle$ from the observed limits on half-lives $T^{0\nu}_{1/2}$ for the $0^+ \rightarrow 0^+$ transition. The best limit comes from the $0\nu\beta^-\beta^-$ decay of ^{130}Te nucleus studied experimentally under the 'CUORE' project [Alduino *et al.* (2018)]. The extracted limits on $\langle m_\nu \rangle$ and $\langle M_N \rangle$ for ^{130}Te nuclei is 0.17 eV and 8.99×10^7 GeV, respectively, from the observed limit on the half-live $T^{0\nu}_{1/2} > 1.5 \times 10^{25}$ yr of $0\nu\beta^-\beta^-$ decay [Alduino *et al.* (2018)]. The study of role of deformation on the NTMEs $M^{(I)}$ $(I = 0\nu, 0N)$ of $0\nu\beta^-\beta^-$ decay for the $0^+ \rightarrow 0^+$ transition suggests that the nuclear structure effects are also important in case of $0\nu\beta^-\beta^-$ decay. The uncertainties associated with the NTMEs $M^{(0\nu)}$ and $M^{(0N)}$ for $0\nu\beta^-\beta^-$ decay are estimated by preforming a statistical analysis by employing set of twelve NTMEs listed in the columns 4–6 of Table 4.3 and Table 4.4, respectively in Chapter 4. The mean $\overline{M}^{(I)}$ and their standard deviations $\Delta\overline{M}^{(I)}$ are calculated and it turns out that the uncertainties $\Delta\overline{M}^{(0\nu)}$ are of the order of 10%, but for ^{110}Pd for which $\Delta\overline{M}^{(0\nu)}$ is approximately 14%. For the case of heavy Majorana neutrino exchange, the maximum uncertainty $\Delta\overline{M}^{(0N)}$ is about 37%.

The phase space factors are calculated exactly and the main uncertainty in the calculation of decay rates comes from the NTMEs, which are model dependent. The PHFB method includes the pairing and deformation degrees of freedom on equal footing. However, the trend of results suggest that it is necessary to incorporate a number of improvements in our study of $\beta\beta$ decay in general and $2\nu\beta^-\beta^-$ decay in particular, which are discussed in the below.

(1) The proton-neutron pairing should be included so that the Hamiltonian will be isospin symmetric and the summation method will be exact.

(2) In the present version of the PHFB model, it is not possible to study the structure of odd-odd nuclei. Hence, the single beta decay rates and the distribution of Gamow-Teller strength can not be calculated. On the other hand, the study of these processes has implications in the understanding of the role of the isoscalar part of the proton-neutron interaction. This is a serious draw back in the present formalism of the PHFB model. However, this limitation can be over come by extending the HFB formalism using complex Bogoliubov transformation.

(3) The fluctuations in average particle numbers is around 5%. None the less, it is necessary that number projection should be carried out for consistency.

(4) The study of $2\nu\beta^-\beta^-$ decay suggests that a reasonably large model space is more effective in reproducing the observed quenching of NTMEs. One needs appropriate effective two-body interaction for a large model space. Therefore, it will be illustrative to study $\beta\beta$ decay in the PHFB model using a large model space in conjunction with appropriate effective two-body interaction.

(5) The deformed Hartree-Fock (DHF) model [Ripka (1968), Brink (1966), Guney and Warke (1967), Praharaj (1988)] is one of the another convenient choices, in which pairing and deformation degrees of freedom can be treated on equal footing. Further, it has been shown by Ahlpara *et al.* (1985) that it is possible to get the shell-model results in DHF by mixing a few intrinsic states. This suggests that a band mixing in an extended PHFB model using complex Bogoliubov transformation will be the best alternative.

The $0\nu\beta^-\beta^-$ decay is possible in a number of gauge theoretical models in addition

to the GUT. Hence, the investigation of $0\nu\beta^-\beta^-$ decay in (i) GUT, (ii) Majoron models, (iii) R_p-MSSM, (iv) Lepto-quark exchange mechanism (v) sterile neutrino and (v) compositeness scenario has the potential to assess the validity of different gauge models. The study of other decay processes like positron emission, electron capture and double electron capture ($e^+\beta\beta$) of $\beta\beta$ decay will be interesting both from experimental as well as theoretical point of view. A reliable and timely prediction of the half-life of $e^+\beta\beta$ modes will be helpful in designing of an experimental set up and analysis of data. Once, the $0\nu\beta^-\beta^-$ decay is observed, the $e^+\beta\beta$ processes would play a crucial role in discriminating the finer issues like dominance of Majorana neutrino mass or the right handed current. Last but not the least, a study of $0\nu\beta^-\beta^-$ decay can draw inferences regarding the dark matter, dark energy and violation of weak equivalence principle.

Bibliography

[1] C. E. Aalseth *et al.,* Nucl. Phys. B (Proc. Suppl.) 48, 223 (1996).

[2] C. E. Aalseth *et al.,* Phys. Rev. D 65, 092007 (2002).

[3] C. E. Aalseth *et al.,* Phys Rev Lett. 120, 132502 (2018).

[4] J. N. Abdurashitov *et al.* (SAGE Collaboration), Phys. Lett. B 328, 234 (1994).

[5] P. Adamson *et al.* (MINOS Collaboration), Phys. Rev. Lett. 101, 131802 (2008); arXiv:0806.2237.

[6] P. Adamson *et al.* (MINOS Collaboration), Phys. Rev. D 86, 052007 (2012); arXiv:1208.2915 [hep-ex].

[7] M. Agostini *et al.* (GERDA Collaboration), Phys. Rev. Lett. 472 111, 122503 (2013).

[8] M. Agostini *et al.,* J. Phys. G 42 115201 (2015).

[9] M. Agostini *et al.* (GERDA Collaboration), Nature 544, 7648, 5-132 (2017).

[10] M Agostini *et al.* (GERDA Collaboration), Phys. Rev Lett. 120 132503 (2018).

[11] M. Agostini *et al.,* Science 10.1126/science.aav8613 (2019).

[12] A. Aguilar *et al.,* Phys. Rev. D 64 112007 (2001).

[13] D. P. Ahalpara, K. H. Bhatt and R. Sahu, J. Phys. G Nucl. Phys. 11 735 (1985).

[14] Q. R. Ahmad *et al.,* Phys. Rev. Lett. 87 071301 (2001).

[15] Q. R. Ahmad *et al.,* Phys. Rev. Lett. 89 011301 (2002).

[16] S. N. Ahmed *et al.,* Phys. Rev. Lett. 92 181301 (2004).

[17] M. H. Ahn *et al.* (K2K Collaboration), Phys. Rev. D 74, 072003 (2006); hep-ex/0606032.

[18] J. B. Albert *et al.,* Phys. Rev. C 89, 015502 (2014).

[19] J. B. Albert *et al.,* Phys. Rev. Lett. 120, 072701(2018).

[20] C. Alduino *et al.,* Phys. Rev. C 93, 045503 (2016).

[21] C. Alduino *et al.,* Eur. Phys. J C 77, 13 (2017).

[22] C. Alduino *et al.,* Phys. Rev. Lett. 120, 132501 (2018).

[23] A. Alessandrello *et al.,* Nucl. Phys. A 478, 453 (1988).

[24] A. Alessandrello *et al.,* Nucl. Phys. B 35 (Proc. Suppl.), 366 (1994).

[25] A. Alessandrello *et al.,* Phys. Lett. B 433 156(1998).

[26] A. Alessandrello *et al.,* Phys. Lett. B 486 13(2000).

[27] K. Alfonso *et al.,* Phys. Rev. Lett. 115, 102502 (2015).

[28] M. Alston-Garnjost *et al.,* Phys. Rev. Lett. 60 1928 (1988).

[29] M. Alston-Garnjost *et al.,* Phys. Rev. Lett. 63 1671 (1989).

[30] M. Alston-Garnjost *et al.,* Phys. Rev. Lett. 71 831 (1993).

[31] M. Alston-Garnjost *et al.,* Phys. Rev. C 55 474 (1997).

[32] M. Altmann *et al.* (GNO Collaboration), Phys. Lett. B 616, 174 (2005); hep-ex/0504037.

[33] M. Apollonio *et al.,* Eur. Phys. J C 27, 331 (2003).

[34] P. Anselmann *et al.* [GALLEX Collaboration], Phys. Lett. B 327, 377 (1994).

[35] J. Argyriades *et al.,* Phys. Rev. C 80, 032501(R) (2009).

[36] J. Argyriades *et al.,* Nucl. Phys. A 847, 168 (2010).

[37] A. Arima, Nucl. Phys. A 354, 19 (1981).

[38] E. Armengaud *et al.,* Eur. Phys. J. C 77, 785 (2017).

[39] E. Armengaud *et al.,* arXiv:1912.07272v1, [nucl-ex] (2019).

[40] C. Arnaboldi *et al.,* Phys. Lett. B 557, 167 (2003).

[41] C. Arnaboldi *et al.,* Phys. Lett. B 584, 260 (2004).

[42] C. Arnaboldi *et al.,* Phys. Rev. Lett. 95, 142501 (2005).

[43] G. Arnison *et al.,* Phys. Lett. B 122, 103 (1983).

[44] R. Arnold *et al.,* Z. Phys. C 72, 239 (1996).

[45] R. Arnold *et al.,* Nucl. Phys. A 636, 209 (1998).

[46] R. Arnold *et al.,* Nucl. Phys. A 658, 299 (1999).

[47] R. Arnold *et al.,* Nucl. Phys. A 678, 341 (2000).

[48] R. Arnold *et al.,* Phys. Rev. Lett. 95, 182302 (2005).

[49] R. Arnold *et al.,* Nucl. Phys. A 765, 483 (2006).

[50] R. Arnold *et al.,* Phys. Rev. Lett. 107, 062504 (2011).

[51] R. Arnold *et al.,* Nucl. Phys. A 925, 25 (2014).

[52] R. Arnold *et al.,*, Phys. Rev. D 92, 072011 (2015).

[53] R. Arnold *et al.,*, Phys. Rev. D 94, 072003 (2016).

[54] R. Arnold *et al.,*, Eur. Phys. J. C 78, 821 (2018).

[55] R. Arnold *et al.,*, Eur. Phys. J. C 79, 440 (2019).

[56] V. Artemiev *et al.,*, JETP Lett. 58, 262 (1993).

[57] V. Artemiev *et al.,*, Phys. Lett. B 345, 564 (1995).

[58] D. R. Artusa *et al.* (CUORE collaboration), arXiv:1402.6072v1 [physics.ins-det] (2014a).

[59] D. R. Artusa *et al.* (CUORE collaboration), arXiv:1402.0922v2 [physics.ins-det] (2014b).

[60] V. D. Ashitkov *et al.,* Phys. At. Nucl. 62, 2044 (1999).

[61] V. D. Ashitkov *et al.,* JETP Lett. 74, 529 (2001).

[62] M. Auger et al. (EXO-200 Collaboration), J. Instrum. 7, P05010 (2012).

[63] M. Aunola, O. Civitarese, J. Kauhanen and J. Suhonen, Nucl. Phys. A 596, 187 (1996).

[64] M. Aunola and J. Suhonen, Nucl. Phys. A 602, 133 (1996); Nucl. Phys. A 643, 207 (1998).

[65] N. Auerbach, G.F. Bertsch, B.A. Brown, L. Zhao, Nucl. Phys. A 556, 2, 190-200 (1993).

[66] F. T. Avignone III, R. L. Brodzinski, J. C. Evans Jr., W. K. Hensley, H. S. Miley, J. H. Reaves Phys. Rev. C 34,666 (1986).

[67] F. T. Avignone III and R. L. Brodzinski, Prog. Part. Nucl. Phys. 21, 99 (1988).

[68] F. T. Avignone III *et. al.*, Phys. Rev. Lett. 54, 2309 (1985); Phys. Lett. B 256, 559 (1991).

[69] F. T. Avignone, Prog. Part. Nucl. Phys. 32, 223 (1994).

[70] O. Azzolini *et al.,* Phys. Rev. Lett. 120 232502(2018).

[71] P. Bagnaia *et al.,* Phys Lett. B 129, 130 (1983).

[72] A. Bakalyarov *et al.,* Pis'ma Zh. Eksp. Teor. Fiz. 76, 643 (2002) [JEPT Lett. 76, 545 (2002)].

[73] A. Balysh *et al.*,, Phys. Lett. B 283, 32 (1992); ibid 322,176 (1994); ibid 356, 450 (1995); Phys. Rev. Lett. 77, 5186 (1996).

[74] I. R. Barabanov *et al.*,, Pis'ma Zh. Eksp. Teor. Fiz 43, 166 (1986).

[75] A. S. Barabash, Phys. Lett. B 216, 257 (1989).

[76] A. S. Barabash, R. Gurriaran, F. Hubert, Ph. Hubert, J. L. Reyss, J. Suhonen, V. I. Umatov, J. Phys. G 22, 487 (1996).

[77] A. S. Barabash, Nucl. Phys. A629, 517c (1998).

[78] A. S. Barabash, Eur. Phys. J. A 8, 137 (2000).

[79] A. S. Barabash, F. Hubert, Ph. Hubert, V.I. Umatov, Eur. Phys. J. A 11, 143 (2001).

[80] A. S. Barabash, Czech. J. Phys. 52, 567 (2002).

[81] A. S. Barabash, Phys. Atm. Nucl. 67, 438 (2004).

[82] A. S. Barabash *et al.,* Phys. Rev. C 79, 045501 (2009).

[83] A. S. Barabash, Phys. Rev. C 81, 035501 (2010).

[84] A. S. Barabash, V.B. Brudanin, Phys. At. Nucl. 74, 312 (2011).

[85] A. S. Barabash, Nuclear Physics, A 935, 52 (2015).

[86] A. S. Barabash *et al.,* Nucl Instrum Methods A 868:(2017).

[87] A. S. Barabash *et al.,* Phys. Rev. D 98, 092007 (2018).

[88] A. S. Barabash *et al.,* Int J Mod Phys A 33, 1843001 (2018).

[89] A. S. Barabash, AIP Conference Proceedings 2165, 020002 (2019).

[90] M. Baranger, Phys. Rev. 120, 957 (1960); Cargese lectures in theoretical physics, 1962 (W.A. Benjamin,New York, 1963).

[91] M. Baranger and K. Kumar, Nucl. Phys. A 110, 490 (1968).

[92] C. Barbero, F. Krmpotic, A. Mariano and D. Tadic, Nucl. Phys. A650, 485 (1999).

[93] R. K. Bardin, P. J. Gollon, J. D. Ullman and C. S. Wu Nucl. Phys. A 158, 337 (1970).

[94] J. Barea and F. Iachello, Phys. Rev. C 79, 044301 (2009).

[95] J. Barea, J. Kotila, and F. Iachello, Phys. Rev. C 87, 014315 (2013).

[96] J. Barea, J. Kotila, F. Iachello, Phys. Rev. C 91, 034304 (2015).

[97] L. Baudis *et al.,*, Phys. Lett. B 407, 219 (1997).

[98] L. Baudis *et al.,* Phys. Rev. Lett. 83, 41 (1999).

[99] G. Bellini *et al.* (BOREXINO Collaboration), Nature 512, 383 (2014).

[100] E. Bellotti *et al.,* Phys. Lett. B 146, 6, 450-456 (1984).

[101] E. Bellotti, C. Cattadori, O. Cremonesi, E. Fiorini, C. Liguori, A. Pullia, P. P. Sverzellati and L. Zanotti, Euro. Phys. Lett. 3, 889 (1987).

[102] A. C. Benvenuti *et al.,* Phys. Rev. Lett. 32, 800–803 (1974).

[103] J. Beringer *et al.,*, Particle Data Group, Phys. Rev. D 86, 01001 (p. 1266) (2012).

[104] R. Bernabei, P. Belli, F. Cappella, R. Caulli, F. Montecchia, A. Incicchitti, D. Prosperi and C. J. Dai, Phys. Lett. B 546, 23 (2002).

[105] T. Bernatowicz, J. Brannon, R. Brazzle, R. Cowsik, C. Hohenberg, F. Podosek, Phys. Rev. Lett. 69, 2341 (1992); ibid. Phys. Rev. C 47, 806 (1993).

[106] J. Bernabeu, B. Desplanques and J. Navarro, Z. Phys. C 46, 323 (1990).

[107] C. Bloch and A. Messiah, Nucl. Phys. 39, 95 (1962).

[108] J. Blomqvist and S. Wahlborn, Ark. Fys. 16/46, 545 (1960).

[109] A. Bobyk, W. A. Kaminski, P. Zareba, Nucl. Phys. A 669, 221 (2000).

[110] A. Bobyk and W. A. Kaminski, Phys. Rev. C 63, 051301(R) (2001).

[111] F. Boehm and P. Vogel, Physics of Massive Neutrinos, Cambridge University Press, Cambridge (1992).

[112] A. Bohr and B. R. Mottelson, Nuclear Structure Vol. II p. 356 (New York, Benjamin, (1975).

[113] A. Bohr and B. R. Mottelson, Nuclear Structure Vol. I (World Scientific, Singapore, 1998).

[114] D. M. Brink, Int. School of Phys. "Enrico Fermi" course 36 , editor C. Bloch (Academic Press, NY) (1966).

[115] R. L. Brodzinski *et al.,* Nucl. Phys. B 31, 76-79 (1993).

[116] V. B. Brudanin *et al.,*, Phys. Atom. Nucl. 63 1218-1221(2000).

[117] J. Busto, Nucl. Phys. B 48 (Proc. Suppl.), 251 (1996).

[118] D. O. Caldwell *et al.,*, Phys. Rev. D 33, 2737 (1986).

[119] A. Caminata *et al.,* Universe 5, 10 (2019).

[120] L. Cardani *et al.,* J. Phys. G 41, 075204 (2014).

[121] O. Castanos, J.G. Hirsch, O. Civitarese, P.O. Hess, Nucl. Phys. A571, 276 (1994).

[122] E. Caurier, A. Poves, A.P. Zuker, Phys. Lett. B 252, 13 (1990).

[123] E. Caurier, F. Nowacki, A. Poves, J. Retamosa, Phys. Rev. Lett. 77, 1954 (1996).

[124] E. Caurier, F. Nowacki, A. Poves and J. Retamosa, Nucl. Phys. A 654, 973 (1999).

[125] E. Caurier, J. Menéndez, F. Nowacki, and A. Poves, Phys. Rev. Lett. 100, 052503 (2008).

[126] V. E. Ceron, J. G. Hirsch, Phys. Lett. B 471, 1 (1999).

[127] D. Cha, Phys. Rev. C 27, 2269 (1983).

[128] R. Chandra, J. Singh, P. K. Rath, P. K. Raina and J. G. Hirsch, Euro. Phys. J. A 23, 223 (2005).

[129] R. Chandra, K. Chaturvedi, P.K. Rath, P.K. Raina, J.G. Hirsch, Europhys. Lett. 86, 32001 (2009).

[130] K. Chaturvedi, B. M. Dixit, P. K. Rath and P. K. Raina, Phys. Rev. C 67, 064317 (2003).

[131] K. Chaturvedi, R. Chandra, P.K. Rath, P.K. Raina, and J. G. Hirsch, Phys. Rev. C 78, 054302 (2008).

[132] M. K. Cheoun, A. Bobyk, A. Faessler, F. Simkovic and G. Teneva, Nucl. Phys. A 561, 74 (1993); Nucl. Phys. A 564, 329 (1993).

[133] M. K. Cheoun, A. Faessler, F. Simkovic, G. Teneva and A. Bobyk, Nucl. Phys. A 587, 301 (1995).

[134] C. Ching, T. Ho and X. Wu, Phys. Rev. C 40, 304 (1989).

[135] O. Civitarese, A. Faessler and T. Tomoda, Phys. Lett. B 194, 11 (1987).

[136] O. Civitarese *et al.,*, Phys. Lett. B 25, 333 (1990).

[137] O. Civitarese, A. Faessler, J. Suhonen and X. R. Wu, Nucl. Phys. Lett. A 524, 404 (1991); J. Phys. G 17, 943 (1991).

[138] O. Civitarese and J. Suhonen, Phys. Rev. C 47, 2410 (1993).

[139] O. Civitarese and J. Suhonen, Nucl. Phys. A 575, 251 (1994).

[140] O. Civitarese, J. Suhonen and A. Faessler, Nucl. Phys. A591, 195 (1995).

[141] O. Civitarese and J. Suhonen, Phys. Rev. C 58, 1535 (1998).

[142] O. Civitarese and J. Suhonen, Nucl. Phys. A 653, 321 (1999).

[143] O. Civitarese and J. Suhonen, Phys. Lett. B 482, 368 (2000).

[144] O. Civitarese and J. Suhonen, Nucl. Phys. A 729, 867 (2003).

[145] O. Civitarese, J. Phys.: Conference Series 173, 012012 (2009).

[146] C. L. Cowan, F. Reines, F.B. Harrison, H.W. Kruse, A.D. McGuire, Science 124, 103 (1956).

[147] G. Danby, J.M. Gaillard, K. Goulianos, L.M. Lederman, N. Mistry, M. Schwartz, J. Steinberger, Phys.Rev.Lett. 9, 36 (1962).

[148] F. A. Danevich, A. Sh. Georgadze, V. V. Kobyachev, B. N. Kropivyanskey, V. N. Kuts, A. S. Nikolaiko, V. I. Tretyak and Yu. Zdesenko, Phys. Lett. B 344, 72 (1995).

[149] F. A. Danevich *et. al.* Nucl. Phys. B (Proc. Suppl.) 70, 246 (1999).

[150] F. A. Danevich, A. Sh. Georgadze, V. V. Kobychev, B. N. Kropivyansky, A. S. Nikolaiko, O. A. Ponkratenko, V. I. Tretyak, S. Yu. Zdesenko and Yu. G. Zdesenko, Phys. Rev. C 62, 045501 (2000).

[151] F. A. Danevich *et al.,* Phys. Rev. C 68, 035501 (2003).

[152] Dassie *et al.,* (NEMO Collaboration), Phys. Rev. D 51, 2090 (1995).

[153] R. Davis, Phys. Rev. 97, 766 (1955); Bull. Am. Phys. Soc., Series II, 1,219 (1956).

[154] R. Davis, Jr., D. S. Harmer and K. C. Hoffman, Phys. Rev. Lett. 20, 1205 (1968).

[155] S. Dell'Oro *et al.,* 2015 Review. Adv High Energy Phys. 2016:2162659 (2016).

[156] A. De Silva, M. K. Moe, M. A. Nelson and M. A. Vient, Phys. Rev. C 56, 2451 (1997).

[157] B. M. Dixit Ph.D. Thesis, University of Lucknow (2002).

[158] M. Doi, T. Kotani, H. Nishiura, K. Okuda and E. Takasugi, Phys. Lett.B 102, 323 (1981); ibid 103, 219 (1981); ibid 113, 513(E) (1982).

[159] M. Doi, T. Kotani, H. Nishiura, K. Okuda and E. Takasugi, Prog. Theor. Phys. 66, 1739-1765 (1981); ibid 68, 340(E), 347(E) (1982).

[160] M. Doi, M. Kenmoku, T. Kotani, H. Nishiura and E. Takasugi, Prog.Theor. Phys. 70, 1331 (1983).

[161] M. Doi, T. Kotani, H. Nishiura and E. Takasugi, Prog. Theor. Phys. 69, 602 (1983).

[162] M. Doi, T. Kotani, E. Takasugi, Prog. Theor. Phys. Suppl. 83, 1 (1985).

[163] M. Doi and T. Kotani, Prog. Theor. Phys. 87, 1207 (1992).

[164] M. Doi and T. Kotani, Prog. Theor. Phys., 89, 139 (1993).

[165] S. Di Domizio (CUORE collaboration), private communication, December (2016).

[166] C. Dorr, H.V. Klapdor-Kleingrothaus, Nucl. Instr. Meth. A 513, 596 (2003).

[167] K. Eguchi *et al.,*, Phys. Rev. Lett. 90, 021802 (2003).

[168] H. Ejiri *et al.,*, J. Phys. G 17, 155 (1991).

[169] H. Ejiri *et al.,*, J. Phys. Soc. Jpn. 64, 339 (1995).

[170] H. Ejiri *et al.,* Nucl. Phys. A 611, 85 (1996).

[171] H. Ejiri *et al.,*, Phys. Rev. Lett. 85, 245 (2000).

[172] H. Ejiri *et al.,*, Phys. Rev. C 63, 65501 (2001).

[173] H. Ejiri, J. Phys. G: Nucl. Part. Phys. 44, 115201 (2017).

[174] S. R. Elliott, A. A. Hann and M. K. Moe, Phys. Rev. Lett. 59, 2020 (1987); ibid 59, 1649 (1987).

[175] S. R. Elliott, M. K. Moe, M. A. Nelson and M. A. Vient, J. Phys. G 17, S145 (1991).

[176] S. R. Elliott *et al.,*, Phys. Rev. C46, 1535 (1992).

[177] S. R. Elliott, M. K. Moe, M. A. Nelson and M. A. Vient, Nucl. Phys. B (Proc. Suppl.) 31, 68 (1993).

[178] S. R. Elliott and P. Vogel, Annu. Rev. Nucl. Part. Sci. 52 (2002).

[179] J. Engel, P. Vogel and M.R. Zirnbauer, Phys. Rev. C 37, 731 (1988).

[180] J. Engel, W.C. Haxton and P. Vogel, Phys. Rev. C 46, 2153 (1992).

[181] J. Engel, S. Pittel, M. Stoitsov, P. Vogel and J. Dukelsky, Phys. Rev. C 46, 1781 (1997).

[182] F. Englert and R. Brout, Phys. Rev. Lett. 13, 321–322, (1964).

[183] A. Faessler, S. Kovalenko, F. Simkovic, J. Schwieger, Phys. Rev. Lett. 78, 183 (1997); Phys. Atom. Nucl. 61, 1229 (1998).

[184] A. Faessler, S. Kovalenko, F. Simkovic, Phys. Rev. D 58, 115 004 (1998a).

[185] A. Faessler, S. Kovalenko, F. Simkovic, Phys. Rev. D 58, 055 004 (1998b).

[186] A. Faessler and F. Simkovic, J. Phys. G 24, 2139 (1998); hep-ph/9901215.

[187] A. Faessler, F. Simkovic, Phys. Atom. Nucl. 63, 1165 (2000).

[188] A. Faessler and F. Simkovic, Prog. Part. Nucl. Phys. 46, 233 (2001).

[189] A. Faessler, V. Rodin, F. Šimkovic, Phys. Rev. C 82, 051301(R) (2010)

[190] A. Faessler, V. Rodin, F. Šimkovic, J. Phys. G: Nucl. Part. Phys. 39, 124006 (2012).

[191] D. L. Fang, A. Faessler, V. Rodin and F. Šimkovic, Phys. Rev. C 83, 034320 (2011).

[192] D. L. Fang, A. Faessler and F. Šimkovic, Phys. Rev. C 97, 045503 (2018).

[193] E. Fiorini *et al.,* Lett. Nuovo Cimento 3, 149 (1970).

[194] A. Forster *et al.,*, Phys. Lett 138 B, 301 (1984).

[195] S. J. Freeman *et al.,* Phys. Rev. C 96, 054325 (2017).

[196] J. H. Fremlin and M. C. Walters, Proc. phys. Soc. A 65, 911 (1952).

[197] H. Fritzsch and P. Minkoeski, Annals of Physics 93, 1–2, 193-266 (1975).

[198] Y. Fukuda *et al.„* Phys. Lett. B 335, 237 (1994).

[199] Y. Fukuda *et al.* (Super-Kamiokande Collaboration), Phys. Rev. Lett. 81, 1562 (1998), hep-ex/9807003

[200] Y. Fukuda *et al.,*, Phys. Rev. Lett. 82, 1810 (1999); ibid 82, 2430 (1999); ibid 82, 2644 (1999).

[201] W. Furry, Phys. Rev. 56, 1184 (1939).

[202] H. Georgi and S.L. Glashow, Phys. Rev. Lett. 32, 438 (1974).

[203] H. Georgi and A. Pais, Phys. Rev. D 10, 539 (1974).

[204] H. Georgi, AIP Conference Proceedings 23, 575 (1975).

[205] H. Georgi and A. Pais, Phys. Rev. D 12, 508 (1975).

[206] A. Gando *et al.,* Phys. Rev. C 85, 045504 (2012).

[207] A. Gando *et al.,* Phys. Rev. C 86, 021601(R) (2012).

[208] A. Gando *et al.* (KamLAND-Zen collaboration), Phys. Rev. Lett. 110, 062502 (2013).

[209] A. Gando *et al.* (KamLAND-Zen collaboration), Phys. Rev. Lett. 117, 082503 (2016).

[210] Ju, M. Gavriljuk, V. V. Kuzminov, N. Ya. Osetrova and S. S. Ratkevich, Phys. Rev. C 61, 35501 (2000).

[211] S. L. Glashow, Nucl. Phys. 22, 579–588 (1961).

[212] M. Goldhaber, L. Grodzins, and A.W. Sunyar, Phys. Rev. 109, 1015–1017 (1958).

[213] D. Gonzalez *et al.,*, Nucl. Phys. B(Proc. Suppl.), 87, 278 (2000).

[214] A. L. Goodman, "Advances in Nuclear Physics", Ed. J. W. Negele and E. Voget (Plenum, New York, 1979).

[215] V. Gribov and B. Pontecorvo, Phys. Lett. B 28, 493 (1969).

[216] A. Griffiths and P. Vogel, Phys. Rev. C 46, 181 (1992).

[217] K. Grotz, H.V. Klapdor, J. Metzinger, J. Phys. G 9, L169 (1983).

[218] K. Grotz, H.V. Klapdor, Phys. Lett. B 157, 242 (1985); Nucl. Phys. A 460, 395 (1986).

[219] Guersey *et al.,* Phys. Lett., B; (Netherlands) (1976).

[220] M. Gunther *et al.,*, Phys. Rev. D 55, 54 (1997).

[221] M. R. Gunye and C. S. Warke, Phys. Rev. 155, 108 (1967).

[222] G. S. Guralnik, C.R. Hagen and T.W.B. Kibble, Phys. Rev. Lett. 13, 585–587 (1964).

[223] J. A. Halbleib, R.A. Sorensen, Nucl. Phys. A 98, 542 (1967).

[224] F. J. Hasert *et al.,* Phys. Lett. B 46, 138–140 (1973a).

[225] F. J. Hasert *et al.,* Phys. Lett. B 46, 121–124 (1973b).

[226] F. J. Hasert *et al.,* Nucl. Phys. B 73, 1, (1974).

[227] W. C. Haxton, G. J. Stephenson Jr. and D. Strottman, Phys. Rev. Lett. 47, 153 (1981).

[228] W. C. Haxton, G. J. Stephenson Jr. and D. Strottman, Phys. Rev. D 25, 2360 (1982).

[229] W. C. Haxton, G.J. Stephenson Jr., Prog. Part. Nucl. Phys. 12, 409 (1984).

[230] P. W. Higgs, Phys. Rev. Lett. 13, 508–509, (1964a).

[231] P. W. Higgs, Phys. Lett. 12, 132–133, (1964b).

[232] P. W. Higgs, Phys. Rev. 145, 1156–1163, (1966).

[233] J. G. Hirsch, O. Castanos, P. O. Hess and O. Civitarese, Nucl. Phys. A 589, 445 (1995*a*).

[234] J. G. Hirsch, O. Castanos, P. O. Hess and O. Civitarese, Phys. Rev. C 51, 2252 (1995).

[235] J. G. Hirsch, O. Castanos and P. O. Hess, Nucl. Phys. A 582, 124 (1995*b*)

[236] J. G. Hirsch, P.O. Hess and O. Civitarese, Phys. Rev. C 54, 1976 (1996).

[237] J. G. Hirsch, P. O. Hess and O. Civitarese, Phys. Lett. B 390, 36 (1997); Phys. Rev. C 56, 199 (1997).

[238] J. G. Hirsch, O. Castanos, P.O. Hess and O. Civitarese, Phys. Lett. B 534, 57 (2002).

[239] M. Hirsch, X.Wu, H.V. Klapdor, C. Ching, T. Ho, Z. Phys. A 345, 163 (1993).

[240] M. Hirsch *et al.*,, Z. Phys. A 347, 51 (1994).

[241] M. Hirsch, X. R. Wu, H. V. Klapdor-Kleingrothaus, Ching Cheng-rui and Ho Tso-hsiu, Phys. Rep. 242, 403 (1994).

[242] M. Hirsch, H.V. Klapdor-Kleingrothaus and S.G. Kovalenko, Phys. Rev. Lett. 75, 17 (1995).

[243] M. Hirsch, H.V. Klapdor-Kleingrothaus and O. Panella, Phys. Lett. B 374, 7 (1996); Phys. Rev. D 53, 13297 (1996).

[244] M. Hirsch, H.V. Klapdor-Kleingrothaus, S.G. Kovalenko and H. Päs, Phys. Lett. B 372, 8 (1996a).

[245] M. Hirsch, H.V. Klapdor-Kleingrothaus and S.G. Kovalenko, Phys. Lett. B 372, 181 (1996b).

[246] M. Hirsch, H.V. Klapdor-Kleingrothaus and S.G. Kovalenko, Phys. Rev. D 54, R4207 (1996c).

[247] M. Hirsch, H.V. Klapdor-Kleingrothaus and S.G. Kovalenko, Phys. Lett. B 378, 17 (1996); Phys. Rev. D 53, 1329 (1996).

[248] M. Hirsch, H.V. Klapdor-Kleingrothaus, St. Kolb and S.G. Kovalenko, Phys. Lett. B 398, 311 (1997); Phys. Lett. B 403, 291 (1997).

[249] M. Hirsch, H.V. Klapdor-Kleingrothaus, S.G Kovalenko, Phys. Lett. B 398, 311 (1999).

[250] M. Hirsch, J.W.F. Valle, Nucl. Phys. B 557, 355 (2001).

[251] G. 't Hooft, Nucl. Phys. B 35, 167–188 (1971a).

[252] G. 't Hooft, Nucl. Phys. B 33, 173–199 (1971b).

[253] G. 't Hooft and M.J.G. Veltman, Nucl. Phys. B 44, 189–213 (1972).

[254] J. Hyvarinen and J. Suhonen, Phys. Rev. C 91, 024613 (2015).

[255] F. Iachello and J. Barea, Nucl. Phys. B Proc. Suppl. 217, 5 (2011).

[256] F. Iachello, J. Barea, and J. Kotila, AIP Conf. Proc. 1417, 62 (2011)a.

[257] Ni Kaixiang *et al.,* Chinese Phys. C 43, 113001 (2019).

[258] A. Kawashima, K. Takahashi and A. Masuda, Phys. Rev. C 47, 2452 (1993).

[259] B. P. Kay *et al.,* Phys. Rev. C57, 011302 (R)(2013).

[260] S. K. Khosa, P. N. Tripathi and S. K. Sharma, Phys. Lett. B 119, 257(1982).

[261] S. K. Khosa and P. K. Mattu, Phys. Rev. C 43, 634 (1991).

[262] T. W. B. Kibble, Phys. Rev. 155, 1554–1561 (1967).

[263] T. Kirsten *et al.,*, Proc. Int. Symp."Nuclear Beta Decay and Neutrino (Osaka 86)", World Sci., Singapore, 81 (1986).

[264] H. V. Klapdor, K. Grotz, Phys. Lett. B 142, 323 (1984).

[265] H. V. Klapdor-Kleingrothaus, Int. J. Mod. Phys. A 13, 3953 (1998).

[266] H. V. Klapdor-Kleingrothaus, H. Päs and U. Sarkar, Eur. Phys. J. A5 3-6 (1999).

[267] H. V. Klapdor-Kleingrothaus *et al.,*, Mod. Phys. Lett. A 16, 2409 (2001); Eur. Phys. J. A 12 147-154 (2001).

[268] H. V. Klapdor-Kleingrothaus and U. Sarkar, Mod. Phys. Lett. A 16 2469-2482 (2001).

[269] A. A. Klimenko, A. A. Pomansky and A. A. Smolnikov, Nucl. Instrum. Meth. B 17, 445 (1986).

[270] M. Kortelainen and J. Suhonen, Phys. Rev. C 76, 024315 (2007).

[271] S. E. Koonin, D.J. Dean, K. Langanke, Phys. Rep. 278, 1 (1997).

[272] F. Krmpotic, A. Mariano, T. T. S. Kuo and K. Nakayama, Phys. Lett. B 319, 393 (1993).

[273] F. Krmpotic and S. Sharma, Nucl. Phys. A 572, 329 (1994).

[274] F. Krmpotic, T.T.S. Kuo, A. Mariano, E.J.V. de Passos and A.F.R. de Toledo Piza, Physica B 5, 93 (1996).

[275] F. Krmpotic, T.T.S. Kuo, A. Mariano, E.J.V. de Passos and A.F.R. de Toledo Piza, Nucl. Phys. A 612, 223 (1997).

[276] N. Kudomi, H. Ejiri, K. Nagata, K. Okada, T. Shibata, T. Shima, and J. Tanaka, Phys. Rev. C 461 2132 (1992).

[277] N. Kudomi *et al.,* Nucl. Phys. A 629, 1-2, 527-530, (1998).

[278] N. Kudomi *et al,* Nucl. Phys. B (Proc. Suppl.) 87, 301 (2000).

[279] K. Kume *et al.,* Nucl. Phys. A 577, 405 (1994).

[280] D. Lalanne, $hep-ex/0509005$.

[281] F. Leccia *et. al.* Nuovo Cimento 78 A 50 (1983).

[282] C. M. Lederer and V. S. Shirley (ed.), Table of Isotopes, 7^{th} Edition, Wiley (NewYork), (1978).

[283] J. W. Lin *et al.,*, Nucl. Phys. A 481, 484 (1988).

[284] R. Luescher *et. al.* Nucl. Phys. B (Proc. Suppl.) 66, 195 (1998).

[285] E. Majorana, Nuovo Cimento 14, 171 (1937).

[286] O. K. Manuel, J. Phys. G 17, 221 (1991).

[287] M. Goeppert-Mayer, Phys. Rev. 48, 512 (1935).

[288] J. Menéndez *et al.*, arXiv:0801.3760v3 (2008).

[289] J. Menéndez, A. Poves, E. Caurier, F. Nowacki, Nucl. Phys. A 818, 139 (2009).

[290] J. Men´endez *et at.,* J. Phys. G 45, 014003 (2018).

[291] A. P. Meshik *et al.,* Nucl. Phys. A, 809, 3–4, 275-289, (2008).

[292] G. A. Miller and J.E. Spencer, Annals Phys. 100, 562 (1976).

[293] H. S. Miley *et al.,*, Phys. Rev. Lett. 65, 3092 (1991).

[294] M. Moe, S. R. Elliott, A. A. Hahn, Pre-print, Univ. of California Neutrino-88-11 (Irvine, 1988).

[295] M. Moe and P. Vogel, Ann. Rev. Nucl. Part. Sci. 44, 247 (1994).

[296] R. N. Mohapatra and J. C. Pati, Phys. Rev. D 11, 566,2588 (1975).

[297] R. N. Mohapatra and R. E. Marshak, Phys. Lett. B 91, 222 (1980).

[298] R. N. Mohapatra and G. Senjanović, Phys. Rev. D 23, 165 (1981).

[299] R. N. Mohapatra, Phys. Rev. D 34, 909 (1986); ibid 34, 3457 (1986).

[300] R. N. Mohapatra, hep-ph=9808284.

[301] A. Morales, Nucl. Phys. B (Proc. Suppl.) 77, 335 (1999).

[302] K. J. Moody, R. W. Lougheed, E. K. Hulet, Phys. Rev. C 46, 2642 (1992).

[303] A. Morales *et al.,*, Nuovo Cimento A 100, 525 (1998).

[304] A. Morales, Nucl. Phys. B (Proc. Suppl.) 77, 335 (1999).

[305] M. T. Mustonen and J. Engel, Phys. Rev. C. 87, 064302 (2013).

[306] K. Muto, H.V. Klapdor, Phys. Lett. B 201, 420 (1988).

[307] K. Muto, E. Bender and H.V. Klapdor, Z. Phys. A, 334 177 (1989a).

[308] K. Muto, E. Bender and H.V. Klapdor, Z. Phys. A, 334 187 (1989b).

[309] K. Muto, Phys. Rev. C 48, 402 (1993).

[310] H. Nakada, T. Sebe, K. Muto, Nucl. Phys. A 535, 509 (1996).

[311] I. Ogawa *et al.*,, Nucl. Phys. A 730, 215 (2004).

[312] H. Paes, M. Hirsch, H.V. Klapdor-Kleingrothaus, Phys. Lett. B 459, 450 (1999).

[313] G. Pantis, A. Faessler, W.A. Kaminski and J.D. Vergados, J. Phys. G: Nucl. Part. Phys. 18, 605 (1992).

[314] G. Pantis and J.D. Vergados, Phys. Rep. 242, 285 (1994).

[315] G. Pantis, F. Simkovic, J.D. Vergados, A. Faessler, Phys. Rev. C 53, 695 (1996).

[316] J. C. Pati and A. Salam, Phys. Rev. D 10, 275 (1974).

[317] W. Pauli, Letter to the "radioactives" in Tubingen, December 1930, reproduced in Cambridge Monogr. Part. Phys. Nucl. Phys. Cosmol. 14, 1 (2000).

[318] A. Piepke *et al.*,, Nucl. Phys. A577, 493 (1994).

[319] F. Piquemal, Nucl. Phys. B (Proc. Suppl.) 77, 352 (1999).

[320] D. Poda, *et al.,* EPJ Web Conf. 65, 01005 (2014).

[321] B. Pontecorvo, Sov. Phys. JETP 6, 429 (1957); Zh. Eksp. Teor. Fiz. 33, 549 (1957).

[322] B. Pontecorvo, Sov. Phys. JETP 26, 984 (1968); Zh. Eksp. Teor. Fiz. 53, 1717 (1967).

[323] C. R. Praharaj, J. Phys. G14, 843 (1988).

[324] H. Primakoff, Phys. Rev. 85, 888 (1952).

[325] H Primakoff and S P Rosen, Rep. Prog. Phys. 22, 121 (1959).

[326] H. Primakoff, Rev. Mod. Phys. 31, 802 (1959).

[327] H. Primakoff, S.P Rosen, Proc. Roy. Soc. (London) 78, 464 (1961).

[328] H. Primakoff, S.P Rosen, Phys. Rev. 184 1925 (1969); Proc. Roy. Soc. (London) 78, 464 (1961).

[329] H. Primakoff and S. P. Rosen, Ann. Rev, Nucl. Part. Sci. 31, 145 (1981).

[330] G. Racah, Nuovo Cimento 14, 322-328 (1937).

[331] P. B. Radha, D.J. Dean, S.E. Koonin, T.T.S. Kuo, K. Langanke, A. Poves, J. Retamosa, P. Vogel, Phys. Rev. Lett. 76, 2642 (1996).

[332] A. A. Raduta, A. Faessler, S. Stoica, W.A. Kaminski, Phys. Lett. B 254, 7 (1991).

[333] P. Raghavan, Atomic Data and Nuclear Data Table, 42, 189 (1989).

[334] S. Raman, C. W. Nestor Jr. and P. Tikkanen, Atomic Data and Nuclear Data Table, 78, 1 (2001).

[335] P. K. Rath and S. K. Sharma, Phys. Rev. C 38, 2928 (1988).

[336] P. K. Rath, R. Chandra, K. Chaturvedi, P.K. Raina, and J.G. Hirsch, Phys. Rev. C. 82, 064310 (2010).

[337] P. K. Rath, R. Chandra, P.K. Raina, K. Chaturvedi, and J.G. Hirsch, Phys. Rev. C. 85, 014308 (2012).

[338] P. K. Rath, R. Chandra, K. Chaturvedi, P. Lohani, P. K. Raina, and J. G. Hirsch, Phys. Rev. C 88, 064322 (2013).

[339] P. K. Rath, R. Chandra, K. Chaturvedi, P. Lohani, and P. K. Raina, Phys. Rev. C 93, 024314 (2016).

[340] H. Ray, arXiv:hep-ex/0701040v1 (2007).

[341] A. Renshaw *et al.* (Super-Kamiokande Collaboration), Phys.Rev.Lett. 112, 091805 (2014), arXiv:1312.5176 [hep-ex].

[342] J. Retamosa, E. Caurier, F. Nowacki, Phys. Rev. C 51, 371 (1995).

[343] G. Ripka, In Advances in Nuclear Physics, Ed. M. Baranger and E. Vogt, (Plenum, New York) Vol. I, p183 (1968).

[344] T. R. Rodríguez and G. Martínez-Pinedo, Phys. Rev. Lett. 105, 252503 (2010).

[345] O. A. Rumyantsev and M.H. Urin, JETP Lett. 61, 361 (1995).

[346] O. A. Rumyantsev and M. H. Urin, Phys. Lett. B 443, 51 (1998).

[347] M. Sakai, Atomic Data and Nuclear Data Tables 31, 400 (1984).

[348] A. Salam, (1969), Proc. of the 8th Nobel Symposium on 'Elementary Particle Theory, Relativistic Groups and Analyticity', Stockholm, Sweden, 1968, edited by N. Svartholm, p. 367-377.

[349] M. Sambataro and J. Suhonen, Phys. Rev. C 56, 782 (1997).

[350] J. Schechter, J.W.F. Valle, Phys. Rev. D 25, 2951 (1982).

[351] O. Scholten and Z. R. Yu, Phys. Lett. B 161, 13 (1985).

[352] J. Schwieger, F. Simkovic and A. Faessler, Nucl. Phys. A, 600 179 (1996) .

[353] J. Schwieger (1997) Thesis, Tuebingen.

[354] S. V. Semenov, F. Simcovic, V. V. Khruschev and P. Domin, Phys. At. Nucl. 63, 1196 (2000).

[355] G. Senjanovic and R. N. Mohapatra, Phys. Rev. D 12, 1502 (1975).

[356] R. A. Sen'kov and M. Horoi, Phys. Rev. C 90, 051301(R) (2014).

[357] S. K. Sharma, P. N. Tripathi and S. K. Khosa, Phys. Rev. C 38, 2935 (1988).

[358] L. D. Skouras, J.D. Vergados, Phys. Rev. C 28, 2122 (1983).

[359] F. Simkovic, JINR communications 39, 21 (1989).

[360] F. Simkovic, G. Teneva, A. Bobyk, M.K. Cheoun, S.B. Khadkikar and A. Faessler, Prog. Part. Nucl. Phys. 32, 329 (1994).

[361] F. Simkovic, J. Schwieger, G. Pantis and A. Faessler, Found.Phys. 27 1275 (1997).

[362] F. Simkovic and G. Pantis, Czech. J. Phys. B 48, 235 (1998).

[363] F. Simkovic and Veselesky, Proc. Int.WorkshopMEDEX97, Praha, June 1997, Czech. J. Phys. B 48, 245 (1998).

[364] F. Simkovic, G. Pantis, J. D. Vergados and A. Faessler, Phys. Rev. C 60, 055502 (1999).

[365] F. Šimkovic, A. A. Raduta, M. Veselský and A. Faessler, Phys. Rev. C 61, 044319 (2000).

[366] F. Simkovic, M. Nowak, W. A. Kaminski, A. A. Raduta and A. Faessler, Phys. Rev. C 64, 035501 (2001).

[367] F. Šimkovic, A. Faessler, V. Rodin, P. Vogel, and J. Engel, Phys. Rev. C 77, 045503 (2008).

[368] F. Šimkovic, A. Faessler, H. Müther, V. Rodin, and M. Stauf, Phys. Rev. C 79, 055501 (2009).

[369] F. Simkovic, J. Vergados and A. Faessler, Phys. Rev. D 82, 113015 (2010).

[370] F. Šimkovic, V. Rodin, A. Faessler, and P. Vogel, Phys. Rev. C 87, 045501 (2013).

[371] J. J. Simpson et. al, Phys. Rev. Lett. 53, 141 (1984).

[372] J. Singh, R. Chandra, P. K. Raina and P. K. Rath , Pramana Journal of Physics 65, 517 (2005).

[373] S. Singh, R. Chandra, P. K. Rath, P. K. Raina, J. G. Hirsch, Eur. Phys. J. A 33, 375 (2007).

[374] Y. K. Singh *et al.*, Eur. Phys. J A 53, 244 (2017).

[375] Y. K. Singh *et al.*, IJMPE 28, 1-2, 1950001 (2019).

[376] L. S. Song, J.M. Yao, P. Ring and J. Meng, Phys. Rev. C 95, 024305 (2017).

[377] K. H. Speidel, O. Kenn and F. Nowacki Prog. Part. Nucl. Phys. 49, 91 (2002).

[378] A. Staudt, K. Muto and H. V. Klapdor, Euro. Phys. Lett. 13, 31 (1990).

[379] A. Staudt, T. T. S. Kuo and H. V. Klapdor, Phys. Rev. C, 46, 871 (1992).

[380] S. Stoica and W. A. Kaminski, Phys. Rev. C 47, 867 (1993).

[381] S. Stoica, Phys. Rev. C 49, 2240 (1994).

[382] S. Stoica, Phys. Lett. B 350, 152 (1995).

[383] S. Stoica and I. Mihut, Nucl. Phys. A 602, 197 (1996).

[384] S. Stoica and H. V. Klapdor-Kleingrothaus, Eur. Phys. J. A 9, 345 (2000).

[385] S. Stoica and H. V. Klapdor-Kleingrothaus, Phys. Rev. C 63, 064304 (2001); Nucl. Phys. A654, 269 (2001).

[386] S. Stoica, and M. Mirea, Phys. Rev. C 88, 037303 (2013).

[387] J. Suhonen, T. Taigel, A. Faessler, Nucl. Phys. A 486, 91 (1988).

[388] J. Suhonen, S. B. Khadkikar and A. Faessler, Phys. Lett. B 237, 8 (1990).

[389] J. Suhonen, S. B. Khadkikar and A. Faessler, Nucl. Phys. A535, 509 (1991).

[390] J. Suhonen and O. Civitarese, Phys. Lett. B 280, 191 (1992).

[391] J. Suhonen and O. Civitarese, Phys. Lett. B 308, 212 (1993); ibid 312, 367 (1993).

[392] J. Suhonen, O. Civitarese, Phys. Rec. C 49, 3055 (1994).

[393] J. Suhonen, P.C. Divari, L.D. Skouras, I.P. Johnstone, Phys. Rev. C 55, 714 (1997).

[394] J. Suhonen, J. Toivanen, A. S. Barabash, I. A. Vanushin, V. I. Umatov, R. Gurriaran, F. Hubert and Ph. Hubert, Z. Phys. A 358, 297 (1997).

[395] J. Suhonen, O. Civitarese, Phys. Rep. 300, 123 (1998).

[396] J. Suhonen, Phys. Lett. B 477, 99 (2000); Phys. Rev. C 62, 042501 (2000).

[397] J. Suhonen, Nucl. Phys. A700, 649 (2002).

[398] J. Suhonen, Phys. Lett. B 607, 87 (2005).

[399] J. Suhonen, Nucl. Phys. A 864, 63 (2011).

[400] J. Suhonen and O. Civitarese, J. Phys. G 39, 124005 (2012).

[401] N. Takaoka *et al.*,, Phys. Rev. C 53, 1557 (1996).

[402] G. Teneva, F. Simkovic, A. Bobyk , M.K. Cheoun, A. Faessler and S.B. Khadkikar, Nucl. Phys. A 249, 586 (1995).

[403] H. V. Thomas, R.A.D. Pattrick, S.A. Crowther, D.J. Blagburn, J.D. Gilmour, Phys. Rev. C 78, 054606 (2008).

[404] J. Toivanen and J. Suhonen, Phys. Rev. Lett. 75, 410 (1995).

[405] J. Toivanen and J. Suhonen, Phys. Rev. C 55, 2314 (1997).

[406] T. Tomoda and A. Faessler, Phys. Lett. B 157, 4 (1985).

[407] T. Tomoda, A. Faessler, K.W. Schmid and F. Gruemmer, Nucl. Phys. A 452, 591 (1986).

[408] T. Tomoda and A. Faessler, Phys. Lett. B 199, 475 (1987).

[409] T. Tomoda, Rep. Prog. Phys. 54, 53 (1991) .

[410] V. Tretyak, Y. Zdesenko, ADNT 61, 43 (1995) .

[411] V. I. Tretyak and Y. G. Zdesenko, Atomic data and Nuclear data Tables, 61, 43 (1995), ibid 80, 83 (2002).

[412] V. I. Tretyak, F. A. Danevich, S. S. Nagorny and Yu. G. Zdesenko Europhys. Lett. 69, 41 (2005).

[413] P. N. Tripathi, Ph.D. Thesis, I.I.T. Kanpur, (1984).

[414] P. N. Tripathi, S. K. Sharma and S. K. Khosa, Phys. Rev. C 29, 1951 (1984).

[415] D. Troltenier, J.P. Draayer and J.G. Hirsch, Nucl. Phys. A 601, Issue 1, 29, 89-102 (1996)

[416] A. L. Turkevich, T. E. Economou and G. A. Gowan, Phys. Rev. Lett. 67, 3211 (1991).

[417] S. Umehara *et al.,* Phys. Rev. C 78, 058501 (2008).

[418] N. L. Vaquero. T.R. Rodriguez and J.L. Egido, Phys. Rev. Lett. 111, 142501 (2013).

[419] A. A. Vasenko, I. V. Kirpichniaov, V. A. Kuznetsov, A S. Starostin, A. G. Djanyan, V. S. Pogosov, S. P. Shachysisyan and A. G. Tamanyan, Mod. Phys. Lett. A 5, 1299 (1990).

[420] S. I. Vasilev *et al.,* JETP Lett. 51, 622-626 (1990); Pisma Zh.Eksp.Teor.Fiz. 51, 550-553 (1990).

[421] S. I. Vasilev *et al.,*, JETP Lett. 51, 622 (1990); 58, 178 (1993).

[422] J. D. Vergados and T. T. S. Kuo, Phys. Lett. 35 B, 93 (1971).

[423] J. D. Vergados, Phys. Rev. C 13, 865 (1976).

[424] J. D. Vergados, Phys. Rep. 133, 1 (1986).

[425] J. D. Vergados, Phys. Lett. B 184, 55 (1987).

[426] J. D. Vergados, Phys. Rep. 361, 1 (2002).

[427] D. M. Vladimirov and Yu.V. Gaponov, Sov. J. Nucl. Phys. 55, 1010 (1992).

[428] F. Villars, Proceedings of International School of Physics, "Enrico Fermi" Course 36 edited by C. Bloch (Academic, New York) (1966).

[429] P. Vogel, M.R. Zirnbauer, Phys. Rev. Lett. 57, 3148 (1986).

[430] P. Vogel, Double Beta Decay: Theory and Experiment, nucl-th=0005020; nucl-th=9904065.

[431] J. L. Vuilleumier, Proc. 8^{th} Moriond Workshop on 5^{th} Force-Neutrino Physics (Les Arcs), 23-30 January 1988 ed. O. Fackler and J. Tran Thanh Van (Gif-sur-Yvette: Editions Frontieres) p. 25.

[432] J. L. Vuilleumier et. al, Phys. Rev. D 48, 1009 (1993).

[433] A. H. Wapstra and G. Audi, Nucl. Phys. A 432, 55 (1985).

[434] D. Waters (SuperNEMO collaboration), private communication, December (2016).

[435] S. Weinberg, Phys. Rev. Lett. 19, 1264–1266 (1967).

[436] M. E. Wieser and J. R. De Laeter, Phys. Rev. C 64, 024308 (2001).

[437] R. G. Winter, Phys. Rev. 85, 687 (1952).

[438] A. Wodecki, W. Kamivnski, S. Pagerka, Phys. Lett. B 413, 342 (1997).

[439] C. S. Wu, E. Ambler, C. H. Hayward, D. D. Hopper and R. P. Hudson, Phys. Rev. 105, 1413 (1957).

[440] H. F. Wu *et al.,* Phys. Lett. B 162, 4–6, 227-232 (1985).

[441] X. Wu, A. Staudt, H.V. Klapdor, C. Ching and T. Ho, Phys. Lett. B 272, 169 (1991).

[442] X. Wu, A. Staudt, T.T.S. Kuo and H.V. Klapdor, Phys. Lett. B 276, 274 (1992).

[443] J. M. Yao, L. S. Song, K. Hagino, P. Ring and J. Meng, Phys. Rev. C91, 024316 (2015).

[444] Y. R. Yen (EXO collaboration), Talk at Recontres de Moriond, March 15, (2016).

[445] K. You *et al.*,, Phys. Lett. B 265, 53 (1991).

[446] Y. B. Zeldovich, Doklady Akad. Nauk SSSR 97, 421 (1954).

[447] L. Zhao, B.A. Brown, W.A. Richter, Phys. Rev. C 42, 1120 (1990).

[448] L. Zhao, B.A. Brown, Phys. Rev. C 47, 2641 (1993).

I. List of Publications

1. 'Nuclear transition matrix elements of neutrinoless double beta decay including V+A current', Yash Kaur Singh, V. K. Nautiyal, R. Chandra, P. K. Rath and P. K. Raina, DAE-BRNS Symp. on Nucl. Phys. 63, 148 (2018).

2. 'Correlations in the nuclear transition matrix elements of $(\beta\beta)_{0\nu}$ decay within PHFB model', R. Gautam, V. K. Nautiyal, R. Chandra, P. K. Rath and P. K. Raina, DAE-BRNS Symp. on Nucl. Phys. 62, 324 (2017).

3. 'Neutrinoless double beta decay and Physics beyond the Standard Model',Yash Kaur Singh, Pooja Lohani, V. K. Nautiyal, R. Gautam, R.Chandra, K. Chaturvedi, P. K. Rath and P. K. Raina, DAE-BRNS Symp. on Nucl. Phys. 61, 286 (2016).

4. 'Study of squark-neutrino mechanism of neutrinoless doublebeta decay in R-parity violating supersymmetric models', R. Chandra, V. K. Nautiyal, R. Gautam, K. Chaturvedi, P. K. Rath and P. K. Raina, DAE-BRNS Symp. on Nucl. Phys. 60, 300 (2015).

5. 'Two neutrino double beta decay and sub-shell occupation numbers of ^{100}Mo, ^{128,130}Te within PHFB model', V. K. Nautiyal, R. Gautam, R. Chandra, P. K. Rath and P. K. Raina, communicated to Int. J. Mod. Phys. E.

6. 'Re-examining the $0\nu\beta^-\beta^-$ decay nuclear transition matrix elements of ^{100}Mo, ^{128,130}Te in mass mechanisms within PHFB model', V. K. Nautiyal, R. Chandra, P. K. Rath and P. K. Raina, communicated to Phys. Rev. C.

II. Participation in Conference /Workshop/Schools/Symposium

1. Participated in the workshop on Neutrinoless Double Beta Decay (NDBD-2016)' during October 17-21, 2016 at IIT Ropar, Rupnagar (Punjab).

2. Participated in the 2nd DAE-BRNS workshop on 'Evaluation of Nuclear Structure and Decay Data' during February 29-March 04, 2016 at HBCSE, TIFR Mumbai.

3. Participated in the Winter School on 'Beyond the Standard Model Physics' held at Banaras Hindu University, Varanasi during Jan 24-Feb 14, 2016.

4. Presented a poster in the 3^{rd} Lucknow Science Congress and National Conference on 'Science For Society: An Interdisciplinary Apporach' held at Babasaheb Bhimrao Ambedkar University, Lucknow on Oct. 31-Nov. 2, 2015.

5. Presented a poster in the 6th IJAA-JSPS International conference on 'Contemporary Advances of Science and Technology (IC-CAST-2015)'held at Banaras Hindu University on August 7-9, 2015.

6. Participated in the DST-SERC School on 'Nuclear Structure on High Angular Momentum and Isospin' held at HBCSE campus, Tata Institute of Fundamental Research, Mumbai during October 5-24, 2014.

Nuclear transition matrix elements of neutrinoless double beta decay including V+A current

Yash Kaur Singh[1], V. K. Nautiyal[1], R. Chandra[1],* P. K. Rath[2] and P. K. Raina[3]

[1] *Department of Physics, Babasaheb Bhimrao Ambedkar University, Lucknow - 226025, INDIA*
[2]*Department of Physics, University of Lucknow, Lucknow, 226007, INDIA*
[3]*Department of Physics, IIT Ropar, Nangal Road, Rupnagar, Punjab – 140001, INDIA*
* *email: ramesh.luphy@gmail.com*

Introduction

The study of neutrinoless double beta ($0\nu\beta\beta$) decay has far reaching consequences in the panorama of lepton number violating processes. Over the past years, the theoretical studies devoted to the calculation of NTMEs have been excellently reviewed in refs. [1,2,3] and references there in. In $0\nu\beta\beta$ decay, the emission of a neutrino from one nucleon and its absorption by another nucleon implies the Majorana nature of neutrinos with finite mass. The $0\nu\beta\beta$ decay is not necessarily linked with the exchange of neutrino between two nucleons but is also possible with the simultaneous existence of right-handed V+A and left-handed V-A currents. In the present work, we consider the electron emitting $0\nu\beta^-\beta^-$ decay mode.

The $0\nu\beta^-\beta^-$ decay has not been observed so far and present status for the search of this particular mode has been given in refs. [4,5]. The nuclear models predict half-lives $T_{1/2}^{0\nu}$ of $0\nu\beta^-\beta^-$ decay assuming certain value of neutrino mass or conversely, limits on various lepton number violating gauge-theoretical parameters are extracted from the observed experimental half-life limits by calculating the appropriate NTMEs.

In the present work, our aim is to calculate the NTMEs of $0\nu\beta^-\beta^-$ decay of some nuclei in the mass range A=90-150 for the $0^+\rightarrow 0^+$ transition within mechanisms involving the light Majorana neutrino, and right handed V+A current and to extract limits on the effective light Majorana neutrino mass $\langle m_\nu \rangle$, the effective weak coupling of right-handed leptonic current with right-handed hadronic current $\langle\lambda\rangle$ and the effective weak coupling of right-handed leptonic current with left-handed hadronic current $\langle\eta\rangle$ from the observed limit on half-life $T_{1/2}^{0\nu}$.

Theoretical framework

Using approximation of Doi *et al*. [6,7] and Tomoda [8], the inverse half-life of the $0\nu\beta^-\beta^-$ decay for $0^+\rightarrow 0^+$ transition is given by

$$\begin{aligned}[T_{1/2}^{0\nu}]^{-1} &= \left(\frac{<m_\nu>}{m_e}\right)^2 C_{mm} + \left(\frac{<m_\nu>}{m_e}\right) <\lambda> C_{m\lambda} \\ &+ \left(\frac{<m_\nu>}{m_e}\right) <\eta> C_{m\eta} + <\lambda>^2 C_{\lambda\lambda} \\ &+ <\eta>^2 C_{\eta\eta} + <\lambda><\eta> C_{\lambda\eta}\end{aligned} \tag{1}$$

and the nuclear structure factors C_{xy} are given as

$$\begin{aligned}C_{mm} &= G_{01}\left|M^{0\nu}\right|^2 \\ C_{m\lambda} &= M^{0\nu}(G_{04}M_{1+} - G_{03}M_{2-}) \\ C_{m\eta} &= M^{0\nu}(G_{03}M_{2+} - G_{04}M_{1-} - G_{05}M_P + G_{06}M_R) \\ C_{\lambda\lambda} &= G_{02}\left|M_{2-}\right|^2 - \frac{2}{9}G_{03}(M_{1+}M_{2-}) + \frac{1}{9}G_{04}\left|M_{1+}\right|^2 \\ C_{\eta\eta} &= G_{02}\left|M_{2+}\right|^2 - \frac{2}{9}G_{03}(M_{1-}M_{2+}) + \frac{1}{9}G_{04}\left|M_{1-}\right|^2 \\ &- G_{07}(M_P M_R) + G_{08}\left|M_P\right|^2 + G_{09}\left|M_R\right|^2 \\ C_{\lambda\eta} &= -2G_{02}(M_{2+}M_{2-}) \\ &+ \frac{2}{9}G_{03}(M_{2+}M_{1+} + M_{2-}M_{1-}) \\ &- \frac{2}{9}G_{04}(M_{1-}M_{1+})\end{aligned} \tag{2}$$

where the combinations of NTMEs, $M^{0\nu}$ and $M_{i\pm}$ (i=1,2) are defined as

$$\begin{aligned}M^{0\nu} &= M_{GT} - M_F + M_T \\ M_{1\pm} &= M_{qGT} - 6M_{qT} \pm 3M_{qF} \\ M_{2\pm} &= M_{\omega GT} \pm M_{\omega F} - \frac{1}{9}M_{1\mp}\end{aligned} \tag{3}$$

The values of $M^{0\nu}$ have been taken from [9] reevaluated at g_A=1.2701. The phase space

factors are taken from ref. [10] reevaluated at g_A=1.2701.

Results and discussions

The NTMEs M_α have been calculated employing projected Hartree-Fock-Bogoliubov (PHFB) model with four parametrizations of pairing plus multipolar effective two-body interaction, namely PQQ1, PQQHH1, PQQ2 and PQQHH2 and three parametrizations of short range correlations (SRC) due to Miller-Spencer parametrization (SRC1), Argonne NN (SRC2) and CD-Bonn potentials (SRC3) including finite size (F) of nucleons. The details about these parametrizations and method to fix them have been given in ref. [11] and references there in. Due to paucity of space we present the results of only ^{96}Zr and ^{150}Nd nuclei for PQQ1 parametrization in Table 1.

Table 1: Theoretically calculated NTMEs M_α (α= ωF,qF,ωGT,qGT,qT,P,R) of $0\nu\beta^-\beta^-$ decay for the $0^+\rightarrow0^+$ transition in PQQ1 parametrization.

Nuclei	NTME	F+SRC		
		SRC1	SRC2	SRC3
^{96}Zr	$M_{\omega F}$	0.425	0.496	0.517
	M_{qF}	0.496	0.542	0.547
	$M_{\omega GT}$	-2.054	-2.429	-2.553
	M_{qGT}	-2.651	-2.957	-3.005
	M_{qT}	0.074	0.073	0.073
	M_P	2.169	2.325	2.341
	M_R	-1.211	-1.967	-2.472
^{150}Nd	$M_{\omega F}$	0.475	0.537	0.554
	M_{qF}	0.632	0.674	0.678
	$M_{\omega GT}$	-2.164	-2.496	-2.602
	M_{qGT}	-3.013	-3.293	-3.334
	M_{qT}	0.043	0.043	0.043
	M_P	0.319	0.380	0.387
	M_R	-1.309	-2.103	-2.620

Subsequently, nuclear structure factors C_{xy} are calculated using appropriate NTMEs M_α and phase space factors. Using the average nuclear structure factors, on-axis limits on $\langle m_\nu \rangle$, $\langle\lambda\rangle$ and $\langle\eta\rangle$ are extracted from the observed limits on half-lives $T_{1/2}^{0\nu}$ =9.2×10^{21} [12] and 2.0×10^{22} [13] for ^{96}Zr and ^{150}Nd, respectively. The extracted limits on $\langle m_\nu \rangle$, $\langle\lambda\rangle$ and $\langle\eta\rangle$ for ^{96}Zr (^{150}Nd) are 10.92 eV (3.88 eV), 8.26×10^{-6} (2.94×10^{-6}) and 9.68×10^{-8} (4.61×10^{-8}), respectively.

Conclusions

Using HFB wave functions generated with PQQ1 parametrization of pairing plus multipolar type of effective two body interaction, and three different parametrizations of SRC, the NTMEs $M_{\omega F,qF}$, $M_{\omega GT,qGT}$, M_{qT}, M_P, and M_R of $0\nu\beta^-\beta^-$ decay for the $0^+\rightarrow0^+$ transition have been calculated for ^{96}Zr and ^{150}Nd nuclei. Limits obtained for the case of ^{150}Nd nuclei are more stringent.

References

[1] J. Suhonen, O. Civitarese, Phys. Rep. **300**, 123 (1998).
[2] A. Faessler and F. Simkovic, J. Phys. G **24**, 2139 (1998).
[3] J. Engel and J. Menéndez, Rep. Prog. Phys. **80**, 046301 (2017).
[4] Reyco Henning, Reviews in Physics 1, **29**, (2016).
[5] I. Ostrovskiy, Modern Physics Letters A, **31**, 1630017 (2016).
[6] M. Doi, T. Kotoni and E. Takasugi, Prog. Theor. Phys. Suppl. **83**, 1 (1985).
[7] M. Doi and T. Kotani, Prog. Theor. Phys., **89**, 139 (1993).
[8] T. Tomoda, Rep. Prog. Phys. 54, 53 (1991).
[9] P. K. Rath, R. Chandra, K. Chaturvedi, P. Lohani, P. K. Raina, and J. G. Hirsch, Phys. Rev. C **88**, 064322 (2013).
[10] D. Štefánik, R. Dvornický, F. Šimkovic, and P. Vogel, Phys. Rev. C **92**, 055502 (2015).
[11] P. K. Rath, R. Chandra, K. Chaturvedi, P. K. Raina, and J. G. Hirsch, Phys. Rev. C. **82**, 064310 (2010).
[12] J. Argyriades et al. Nucl. Phys. A **847**, 168,(2010).
[13] R. Arnold et al. Phys. Rev. D **94**, 072003 (2016).

Correlations in the nuclear transition matrix elements of $(\beta\beta)_{0\nu}$ decay within PHFB model

R. Gautam[1], V. K. Nautiyal[1], R. Chandra[1],* P. K. Rath[2] and P. K. Raina[3]
[1] *Department of Applied Physics, Babasaheb Bhimrao Ambedkar University, Lucknow - 226025, INDIA*
[2]*Department of Physics, University of Lucknow, Lucknow, 226007, INDIA*
[3]*Department of Physics, IIT Ropar, Nangal Road, Rupnagar, Punjab – 140001, INDIA*
* *email: ramesh.luphy@gmail.com*

Introduction

The neturinoless double beta $(\beta\beta)_{0\nu}$ decay is one of the potential keys to open the window for physics beyond standard model of electroweak unification (SM) as it violates the lepton number conservation. In order to get the absolute mass and unfold the nature of neutrinos i.e. Dirac or Majorana, the $(\beta\beta)_{0\nu}$ decay is the natural choice theoretically as well as experimentally [1,2]. The $(\beta\beta)_{0\nu}$ has not been observed experimentally and only limits on half-lives are available. The neutrino mass and other gauge theoretical parameters can be extracted from the available half-life limits using appropriate nuclear transition matrix elements (NTMEs) and accurately calculable phase space factors of $(\beta\beta)_{0\nu}$ decay. The accuracy of these extracted gauge theoretical parameters highly depends on the reliability of NTMEs of $(\beta\beta)_{0\nu}$ decay. The NTME $M^{0\nu}$ is a model dependent quantity and in the absence of experimental data the calculation of the $M^{0\nu}$ of $(\beta\beta)_{0\nu}$ decay is a formidable task. The two-neutrino double beta $(\beta\beta)_{2\nu}$ decay has been observed experimentally for twelve nuclei [3] and experimental NTMEs $M_{2\nu}$ for this mode are available. In practice, the reliability of $M^{0\nu}$ for $(\beta\beta)_{0\nu}$ decay is tested by reproducing the experimentally extracted $M_{2\nu}$ of $(\beta\beta)_{2\nu}$ decay as both the modes involve same set of wave functions.

The NTMEs $M^{0\nu}$ are mainly calculated in three types of models namely, shell-model, quasiparticle random phase approximation (QRPA) and alternative models along with their several variants and extensions [4,5]. It is found that there is a large uncertainty in the values of $M^{0\nu}$ calculated in these models. Even the NTMEs calculated in the same type of generic model have noticeable uncertainty. There are several reasons for the observed uncertainty in NTMEs. There is no specific prescription in practice to fix the two basic ingredients of any nuclear model i.e. the model space and appropriate effective two-body interaction. Generally, different model space and different effective interactions are used in models. Further, even for the same model space the basic approach to fix the parameters of effective two-body interactions is different. Moreover, the choice of axial vector coupling constant g_A and short range correlations also contribute to uncertainty in the NTMEs. Faessler et al. [6] has shown the importance of correlated nuclear matrix elements uncertainties within QRPA model in comparing the decay rates of $(\beta\beta)_{0\nu}$ decay for different nuclei.

The projected Hartree-Fock Bogoliubov (PHFB) model has been successfully employed to study the $(\beta\beta)_{0\nu}$ decay (see [7] and references therein). In the present work we establish correlations between NTMEs $M^{0\nu}$ of ^{96}Zr, ^{100}Mo, ^{110}Pd, ^{128,130}Te and ^{150}Nd calculated within PHFB model.

Theoretical framework

In the approximation of light Majorona neutrinos, the inverse half-life of $(\beta\beta)_{0\nu}$ decay for $0^+ \rightarrow 0^+$ transition is given by [8],

$$\left[T_{1/2}^{0\nu}\right]^{-1} = \left(\frac{\langle m_\nu \rangle}{m_e}\right)^2 G_{01} \left|\left(M_{GT}^{0\nu} - M_F^{0\nu}\right)\right|^2 \quad (1)$$

where G_{01} is the phase space factor which can be calculated exactly and the NTMEs are given by

$$M_k = \Sigma \left\langle 0_F^+ \left\| O_{k,nm} \tau_n^+ \tau_m^+ \right\| 0_I^+ \right\rangle \quad (2)$$

with

$$O_F = \left(\frac{g_V}{g_A}\right)^2 H(r_{12}), \qquad O_{GT} = \sigma_1.\sigma_2 H(r_{12}) \quad (3)$$

Results and discussions

The model space, single particle energies (SPE's), parameters of the pairing plus multipole (PQQHH) type of effective two-body interaction have been already given in Ref. [9]. The effective Hamiltonian used in the present work is given as

$$H = H_{s.p.} + V(P) + V(QQ) + V(HH) \quad (4)$$

where $H_{s.p.}$, $V(P)$, $V(QQ)$ and $V(HH)$ denote the single particle Hamiltonian, pairing, quadrupole-quadrupole and hexadecapole-hexadecapole parts of the effective two-body interaction. We use four parametrizations of effective two-body interaction namely, PQQ1, PQQHH1, PQQ2 and PQQHH2. The details about these parametrizations and method to fix them have been provided in our earlier work [10]. Further, the NTMEs have been calculated by considering the finite size of nucleon and Jastrow type of short range correlations with Miller-Spencer, Argonne V18 and CD-Bonn NN potentials. Hence, with four parametrizations and three short range correlations we have a set of twelve NTMEs for each nucleus.

Following Faessler et al. [6], the associated covariance matrx is given as

$$\mathrm{cov}(n_i,n_j) = \rho_{ij}\sigma_i\sigma_j$$

where diagonal elements coincide with the variances σ_i^2, n_i is matrix element, σ_I is the error and ρ_{ij} is the correlation. Here, we analyze the correlation between NTMEs of ^{96}Zr, ^{100}Mo, ^{110}Pd, ^{128,130}Te and ^{150}Nd nuclei calculated within PHFB model. The results are given in Table 1.

Table 1: Correlation matrix ρ_{ij} between NTMEs $M^{0\nu}$ of $(\beta\beta)_{0\nu}$ decay of ^{96}Zr, ^{100}Mo, ^{110}Pd, ^{128,130}Te and ^{150}Nd nuclei calculated within PHFB model.

	Correlation matrix ρ_{ij}					
	^{96}Zr	**^{100}Mo**	**^{110}Pd**	**^{128}Te**	**^{130}Te**	**^{150}Nd**
^{96}Zr	1.00					
^{100}Mo	0.86	1.00				
^{110}Pd	0.74	0.82	1.00			
^{128}Te	0.52	0.44	0.40	1.00		
^{130}Te	0.70	0.90	0.96	0.34	1.00	
^{150}Nd	0.53	0.80	0.92	0.20	0.97	1.00

It is observed from Table 1 that there is a positive correlation between NTMEs of $(\beta\beta)_{0\nu}$ decay of two or more nuclei within PHFB model. The detailed results will be presented in the symposium.

References

[1] J. Engel and J. Menéndez, Rep. Prog. Phys. **80**, 046301 (2017).

[2] I. Ostrovskiy, Modern Physics Letters A, **31**, 1630017 (2016).

[3] R. Saakyan, Annu. Rev. Nucl. Part. Sci. **63**, 503 (2013).

[4] J. Suhonen, O. Civitarese, Phys. Rep. **300**, 123 (1998).

[5] A. Faessler and F. Simkovic, J. Phys. G **24**, 2139 (1998).

[6] A. Faessler, G. L. Fogli, E. Lisi, V. Rodin, A. M. Rotunno and F. Simkovic, Phys. Rev. D **79**, 053001 (2009).

[7] P. K. Rath, R. Chandra, K. Chaturvedi, P. Lohani, P. K. Raina, and J. G. Hirsch, Phys. Rev. C **88**, 064322 (2013**)**.

[8] W. C. Haxton and G. J. Stephenson Jr., Prog. Part. Nucl. Phys. **12**, 409 (1984).

[9] R. Chandra, K. Chaturvedi, P. K. Rath, P. K. Raina and J. G. Hirsch, Europhys. Lett. **86**, 32001 (2009).

[10] P. K. Rath, R. Chandra, K. Chaturvedi, P. K. Raina and J. G. Hirsch, Phys. Rev. C. **82**, 064310 (2010).

Acknowledgment

One of the authors RC thanks DST-SERB, India for financial support vides Dy. No. SERB/F/6190/2015-16.

Neutrinoless double beta decay and Physics beyond the Standard Model

Yash Kaur Singh[1], Pooja Lohani[2], V. K. Nautiyal[1], R. Gautam[1], R. Chandra[1],* K. Chaturvedi[3], P. K. Rath[2] and P. K. Raina[4]

[1] *Department of Applied Physics, Babasaheb Bhimrao Ambedkar University, Lucknow - 226025, INDIA*
[2]*Department of Physics, University of Lucknow, Lucknow, 226007, INDIA*
[3] *Department of Physics, Bundelkhand University, Jhansi – 284128, INDIA*
[4]*Department of Physics, IIT Ropar, Nangal Road, Rupnagar, Punjab – 140001, INDIA*
* *email: ramesh.luphy@gmail.com*

Introduction

The nuclear ββ decay, in which the charge *Z* of an even *Z*-even *N* nucleus is changed by two units while the mass number *A* remains the same, is a rare and spontaneous process of weak interaction in nature. The ββ decay can be categorized in mainly two modes, namely two neutrino double beta $(\beta\beta)_{2\nu}$ decay and neutrinoless double beta $(\beta\beta)_{0\nu}$ decay. The $(\beta\beta)_{2\nu}$ decay establishes the validity of different nuclear models employed for nuclear structure calculations by calculating the nuclear transition matrix elements (NTMEs) $M_{2\nu}$. The $(\beta\beta)_{0\nu}$ decay violates the lepton number conservation by two units and can be studied in any theory in which lepton number conservation is not exact. Hence $(\beta\beta)_{0\nu}$ decay is an excellent process to probe the new physics beyond the standard model (SM) of electroweak unification. Apart from the well studied left-right symmetric model, the $(\beta\beta)_{0\nu}$ decay can also be studied in Majoron models, R-parity violating as well as conserving supersymmetric (SUSY) models. Further, the $(\beta\beta)_{0\nu}$ decay can verify issues like compositeness, leptoquarks, sterile neutrinos and violation of weak equivalence principle. The detailed progress of experimental as well as theoretical studies on ββ decay in general and $(\beta\beta)_{0\nu}$ decay in particular can be found in references [1,2] and references there in.

The PHFB model in conjunction with pairing plus multipole type of two-body effective interaction has been successfully applied to study the $(\beta\beta)_{0\nu}$ decay [3-7]. In present work the same PHFB model has been applied to study the $(\beta\beta)_{0\nu}$ decay in various theories beyond the SM.

Theoretical framework

The details about the model space, single particle energies, *PQQ* type of effective two-body interaction and the procedure to fix its parameters have been given in Refs. [3,4]. The Hamiltonian of the effective two-body interaction used in the present work is given as

$$H = H_{s.p.} + V(P) + V(QQ) + V(HH) \quad (1)$$

where $H_{s.p.}$, $V(P)$, $V(QQ)$ and $V(HH)$ denote the single particle Hamiltonian, pairing, quadrupole-quadrupole and hexadecapole-hexadecapole parts of the effective two-body interaction. We use four different parametrizations of the interaction Hamiltonian, namely *PQQ*1, *PQQ*2, *PQQHH*1 and *PQQHH*2 [5]. Further, we use the Jastrow type of short range correlations with Miller-Spencer, Argonne V18 and CD-Bonn NN potentials [5,8]. The detailed theoretical formalism to study the $(\beta\beta)_{0\nu}$ decay in Majoron and SUSY models are given in refs. [9,10,11]. Further, the theory of compositeness and leptoquark in connection with $(\beta\beta)_{0\nu}$ decay is given in refs. [12,13].

Results and discussions

The NTMEs involved in $(\beta\beta)_{0\nu}$ decay in various theories stated above are calculated within PHFB model using pairing plus multipole type of two-body interaction. The NTMEs have been calculated by considering the finite size of nucleon (F) and Jastrow type of short range correlations (SRC) with Miller-Spencer, Argonne V18 and CD-Bonn NN potentials for $(\beta\beta)_{0\nu}$ decay of ^{94,96}Zr, ^{100}Mo, ^{128,130}Te and ^{150}Nd isotopes for the $0^+ \rightarrow 0^+$ transition. At present, some results are presented for the case of ^{100}Mo

with *PQQ1* parametrization. The detailed results will be presented in the symposium.

Table 1: NTMEs for the Majoron accompanied $(\beta\beta)_{0\nu}$ decay of ^{100}Mo for the *PQQ1* parametrization.

NTME	F	F+S		
		SRC1	SRC2	SRC3
$M^{(\chi)}_{Fm_\nu}$	2.15	1.89	2.15	2.22
$M^{(\chi)}_{GTm_\nu}$	-5.52	-4.72	-5.43	-5.66
$M^{(\chi)}_{Tm_\nu}$	0.05	0.05	0.05	0.05
$M^{(\chi)}_{CR}$	-0.26	-0.23	-0.26	-0.27
$M^{(\chi)}_{F\omega^2}$ $\times 10^3$	1.18	1.14	1.19	1.20
$M^{(\chi)}_{GT\omega^2}$ $\times 10^3$	-5.79	-5.60	-5.86	-5.91

Table 2: NTMEs of $(\beta\beta)_{0\nu}$ decay in SUSY models via exchange of gluinos for ^{100}Mo with in PHFB model using *PQQ1* interaction.

NTME	F	F+S		
		SRC1	SRC2	SRC3
M^N_F	0.716	0.037	0.056	0.067
M^P_F	0.007	0.003	-0.002	0.002
M^N_{GT}	-0.210	-0.108	-0.164	-0.196
M^P_{GT}	-0.023	0.009	0.004	-0.007
$M^{1\pi}_{GT}$	5.422	2.169	3.80	4.831
$M^{2\pi}_{GT}$	2.613	1.856	2.45	2.661
M^P_T	0.001	0.001	0.001	0.001
$M^{1\pi}_T$	0.285	0.285	0.302	0.302
$M^{2\pi}_T$	0.130	0.132	0.134	0.134

Table 3: NTMEs of $(\beta\beta)_{0\nu}$ decay in SUSY models via exchange of squark for ^{100}Mo with in PHFB model using *PQQ1* interaction.

NTME	F	F+S		
		SRC1	SRC2	SRC3
M_F	-258.7	-131.7	-201.4	-241.1
$M_{GT\text{-}MT}$	412.4	207.4	318.8	382.1
$M_{GT\text{-}AP}$	-25.77	-20.00	-24.92	-26.57
$M_{GT\text{-}\pi}$	506.4	441.8	511.2	528.9
$M_{T\text{-}MT}$	-10.33	-10.36	-10.85	-10.83
$M_{T\text{-}AP}$	-1.13	-1.14	-1.15	-1.15
$M_{T\text{-}\pi}$	17.90	18.06	18.09	18.07

In Table 1, 2 and 3, SRC1, SRC2 and SRC3 denote the Jastrow type of short range correlations (SRC) with Miller-Spencer, Argonne V18 and CD-Bonn NN potentials, respectively.

References

[1] F. T. Avignone III, S. R. Elliott, and J. Engel, Rev. Mod. Phys.**80**, 481 (2008).

[2] J. D. Vergados, H. Ejiri, and F. Simkovic, Rep. Prog. Phys. **75**,106301 (2012).

[3] R. Chandra, J. Singh, P. K. Rath, P. K. Raina, and J. G. Hirsch, Eur. Phys. J. A **23**, 223 (2005).

[4] S. Singh, R. Chandra, P. K. Rath, P. K. Raina, and J. G. Hirsch, Eur. Phys. J. A **33**, 375 (2007).

[5] P. K. Rath, R. Chandra, K. Chaturvedi, P. K. Raina, and J. G. Hirsch, Phys. Rev. C. **82**, 064310 (2010).

[6] P. K. Rath, R. Chandra, K. Chaturvedi, P. Lohani, P. K. Raina, and J. G. Hirsch, Phys. Rev. C **88**, 064322 (2013).

[7] P. K. Rath, R. Chandra, K. Chaturvedi, P. Lohani, and P. K. Raina, Phys. Rev. C **93**, 024314 (2016).

[8] F. Simkovic, A. Faessler, H. Muther, V. Rodin, and M. Stauf, Phys. Rev. C **79**, 055501 (2009).

[9] M. Hirsch, H. V. Klapdor-Kleingrothaus, S. G. Kovalenko and H. Pas, Phys. Lett. B **372**, 8 (1996).

[10] M. Hirsch, H. V. Klapdor-Kleingrothaus and S. G. Kovalenko, Phys. Lett. B **372**, 181 (1996).

[11] A. Faessler, T. Gutsche, S. Kovalenko and F. Simkovic, Phys. Rev. D **77**, 113012 (2008).

[12] O. Panella, C. Carimalo, Y.N. Srivastava and A. Widom, Phys. Rev. D **56**, 5766 (1997).

[13] M. Hirsch, H.V. Klapdor-Kleingrothaus and S.G. Kovalenko, Phys. Rev. D **54**, R4207 (1996).

Acknowledgment

One of the authors RC thanks DST-SERB, India for financial support vide Dy. No. SERB/F/6190/2015-16.

Study of squark-neutrino mechanism of neutrinoless double beta decay in R-parity violating supersymmetric models

R. Chandra[1],* V. K. Nautiyal[1], R. Gautam[1], K. Chaturvedi[2], P. K. Rath[3] and P. K. Raina[4]

[1] *Department of Applied Physics, Babasaheb Bhimrao Ambedkar University, Lucknow - 226025, INDIA*
[2]*Department of Physics, Bundelkhand University, Jhansi – 284128, INDIA*
[3]*Department of Physics, University of Lucknow, Lucknow, 226007, INDIA*
[4]*Department of Physics, IIT Ropar, Nangal Road, Rupnagar, Punjab – 140001, INDIA*
* *email: ramesh.luphy@gmail.com*

Introduction

The non-observation of $(\beta^-\beta^-)_{0\nu}$ decay is usually interpreted in terms of an upper limit on the Majorana mass of the neutrino. However, in principle in any kind of extension of the standard model (SM) of electroweak unification, which allows lepton number violation at some level, one can expect contributions to $(\beta^-\beta^-)_{0\nu}$ decay, not necessarily related to the mass of the neutrino. Supersymmetric (SUSY) theories with R-parity violation are the most prominent examples of this class of models. In SUSY models, the new SUSY partner differ from the SM field content in a discrete multiplicative quantum number R-parity (R_p) defined as $R_p=(-1)^{3B+L+2S}$ where B, L and S denote the baryon number, lepton number and spin of a particle leading to $R_p=+1$ for the SM particles and $R_p=-1$ for superpartners.

The quark-level lepton number violating interactions and nuclear structure aspects relevant for the R_p-violating SUSY mechanism have been widely studied in the literature [1]. The two types of R_p-violating SUSY mechanism at quark level are (i) the short range mechanism with the exchange of heavy superpartners [2] and (ii) the long range mechanism involving the exchange of heavy squark and the light neutrino [3] known as squark-neutrino mechanism [4].

Faessler et al. [4] has shown that R_p-violating SUSY contributes to the $(\beta^-\beta^-)_{0\nu}$ decay dominantly via exchange of charged pion between the decaying nucleons by employing QRPA model for the calculation of relevant nuclear transition matrix elements (NTMEs).

In reference [5] and references there in, the PHFB model has been successfully applied to study the $(\beta\beta)_{0\nu}$ decay in left-right symmetric models and majoron models. This motivates us to calculate the relevant NTMEs of $(\beta^-\beta^-)_{0\nu}$ decay of nuclei in the mass range 94–150 within R_p-violating SUSY models involving squark-neutrino mechanism using PHFB model in conjunction with pairing plus multi pole type of two body interaction. Finally the constraints on the lepton number violating SUSY parameters are extracted from the available half-life limits of $(\beta^-\beta^-)_{0\nu}$ decay.

Theoretical framework

The inverse half life of $(\beta^-\beta^-)_{0\nu}$ decay in Rp-violating SUSY model is given by [4]

$$T_{1/2}^{-1} = G_{01}\left|M_h^{\bar{q}}\right|^2\left|\eta^{11}_{(q)LR}\right|^2 \tag{1}$$

where G_{01} is phase space factor. The nuclear matrix elements $M_h^{\bar{q}}$ are denoted as $M_{2N}^{\bar{q}}$ and $M_\pi^{\bar{q}}$ for the 2N and pion mode, respectively and expressed as

$$M_{2N}^{\bar{q}} = M_{AP}^{\bar{q}} + M_{MT}^{\bar{q}} + M_{VT}^{\bar{q}} \tag{2}$$

with

$$M_{AP}^{\bar{q}} = \left\langle H_{AP-GT}^{\bar{q}}(r_{12})\sigma_{12} + H_{AP-T}^{\bar{q}}(r_{12})S_{12}\right\rangle \tag{3}$$

$$M_{MT}^{\bar{q}} = \left\langle H_{MT-GT}^{\bar{q}}(r_{12})\sigma_{12} + H_{MT-T}^{\bar{q}}(r_{12})S_{12}\right\rangle \tag{4}$$

$$M_{VT}^{\bar{q}} = \left\langle H_{VT-F}^{\bar{q}}(r_{12})\right\rangle \tag{5}$$

and

$$M_\pi^{\bar{q}} = \left\langle H_{\pi NN-GT}^{\bar{q}}(r_{12})\sigma_{12} + H_{\pi NN-T}^{\bar{q}}(r_{12})S_{12}\right\rangle \tag{6}$$

In PHFB model using closure approximation the NTMEs M_α are calculated as

$$M_\alpha = \sum_{n,m}\left\langle 0_F^+\left\|O_{\alpha,nm}\tau_n^+\tau_m^+\right\|0_I^+\right\rangle \tag{7}$$

Results and discussions

The NTMEs involved in $(\beta^-\beta^-)_{0\nu}$ decay in Rp-violating SUSY model calculated within PHFB model using pairing plus quadrupole-quadrupole (PQQ) interaction are presented in Table 1. Further, the NTMEs have been calculated by considering the finite size of nucleon (F) and Jastrow type of short range correlations (SRC) with Miller-Spencer, Argonne V18 and CD-Bonn NN potentials for the SUSY accompanied $(\beta^-\beta^-)_{0\nu}$ decay of ^{94,96}Zr, ^{98,100}Mo, ^{104}Ru, ^{110}Pd, ^{128,130}Te and ^{150}Nd isotopes for the $0^+ \rightarrow 0^+$ transition. At present, the results are presented for the case of ^{100}Mo and ^{150}Nd.

Table 1: The NTMEs M_α of squark-neutrino R_p-violating SUSY mechanism of $(\beta^-\beta^-)_{0\nu}$ decay of ^{100}Mo and ^{150}Nd in the PHFB model using PQQ interaction.

Nuclei	M_α	F+SRC		
		SRC1	SRC2	SRC3
^{100}Mo	$M_{2N}^{\bar{q}}$	44.16	80.48	103.35
	$M_{\pi}^{\bar{q}}$	459.81	529.26	547.01
^{150}Nd	$M_{2N}^{\bar{q}}$	21.02	37.55	47.67
	$M_{\pi}^{\bar{q}}$	219.22	249.90	257.56

In Table 1, SRC1, SRC2 and SRC3 denote the Jastrow type of short range correlations (SRC) with Miller-Spencer, Argonne V18 and CD-Bonn NN potentials, respectively. The calculation of NTMEs for rest of the nuclei stated above along with the extracted limits on SUSY parameters will be presented in the symposium.

Conclusions

To summarize, we study the $(\beta^-\beta^-)_{0\nu}$ decay of ^{94,96}Zr, ^{98,100}Mo, ^{104}Ru, ^{110}Pd, ^{128,130}Te and ^{150}Nd isotopes for the $0^+ \rightarrow 0^+$ transition within R_p-violating SUSY models involving squark-neutrino mechanism using PHFB model. The lepton number violating parameters of R_p-violating SUSY model using calculated NTMEs and experimental data will be extracted and presented in the symposium.

References

[1] J.D. Vergados, Phys. Rep. **361**, 1 (2002).
[2] R.N. Mohapatra, Phys. Rev. D **34**, 909 (1986); ibid **34**, 3457 (1986).
[3] M. Hirsch, H.V. Klapdor-Kleingrothaus and S.G. Kovalenko, Phys. Lett. B **372**, 181 (1996).
[4] A. Faessler, T. Gutsche, S. Kovalenko and F. Simkovic, Phys. Rev. D **77**, 113012 (2008).
[5] P. K. Rath, R. Chandra, K. Chaturvedi, P. Lohani, P. K. Raina and J. G. Hirsch, Phys. Rev. C **88**, 064322 (2013).

Acknowledgment

One of the authors RC thanks DST-SERB, India for financial support vide Dy. No. SERB/F/5139/2013-14.